ไฮโดรจิโนไลซิสของกลีเซอรอลเป็นโพรเพนไดออลโดยใช้ตัวเร่งปฏิกิริยาฐานโคบอลต์

นางสาวสุพัตรา รักษาพรต

วิทยานิพนธ์นี้เป็นส่วนหนึ่งของการศึกษาตามหลักสูตรปริญญาวิทยาศาสตรดุษฎีบัณฑิต
สาขาวิชาเคมีเทคนิค ภาควิชาเคมีเทคนิค
คณะวิทยาศาสตร์ จุฬาลงกรณ์มหาวิทยาลัย
ปีการศึกษา 2556
ลิขสิทธิ์ของจุฬาลงกรณ์มหาวิทยาลัย

HYDROGENOLYSIS OF GLYCEROL TO PROPANEDIOL USING Co-BASED
CATALYSTS

Miss Supattra Raksaphort

A Dissertation Submitted in Partial Fulfillment of the Requirements
for the Degree of Doctor of Philosophy Program in Chemical Technology
Department of Chemical Technology
Faculty of Science
Chulalongkorn University
Academic Year 2013

Thesis Title   HYDROGENOLYSIS   OF   GLYCEROL   TO
                      PROPANEDIOL USING Co-BASED CATALYSTS
By   Miss Supattra Raksaphort
Field of Study   Chemical Technology
Thesis Advisor   Associate Professor Mali Hunsom, Ph.D., Dr. de L'INPT
Thesis Co-advisor   Assistant Professor Sitthiphong Pengpanich, Ph.D.

Accepted by the Faculty of Science, Chulalongkorn University in Partial Fulfillment of the Requirements for the Doctoral Degree

....Dean of the Faculty of Science

(Professor Supot Hannongbua, Dr. rer. nat.)

THESIS COMMITTEE

....Chairman

 (Associate Professor Kejvalee Pruksathorn, Dr. de L'INPT)

....Thesis Advisor

(Associate Professor Mali Hunsom, Ph.D., Dr. de L'INPT)

....Thesis Co-advisor

(Assistant Professor Sitthiphong Pengpanich, Ph.D.)

....Examiner

(Professor Pattarapan Prasassarakich, Ph.D.)

....Examiner

(Assistant Professor Siriporn Jongpatiwut, Ph.D.)

....External Examiner

(Assistant Professor Soipatta Soisuwan, Ph.D.)

สุพัตรา รักษาพรต : ไฮโดรจิโนไลซิสของกลีเซอรอลเป็นโพรเพนไดออลโดยใช้ตัวเร่ง
ปฏิกิริยาฐานโคบอลต์. (HYDROGENOLYSIS OF GLYCEROL TO PROPANEDIOL
USING Co-BASED CATALYSTS) อ.ที่ปรึกษาวิทยานิพนธ์หลัก : รศ.ดร.มะลิ หุ่นสม, อ.
ที่ปรึกษาวิทยานิพนธ์ร่วม : ผศ.ดร.สิทธิพงษ์ เพ็งพานิช, 130 หน้า.

งานวิจัยนี้ศึกษาการเตรียมตัวเร่งปฏิกิริยาฐานโคบอลต์บนตัวรองรับด้วยวิธีอิมเพรกเนชัน
เพื่อใช้ในการเร่งปฏิกิริยาไฮโดรจิโนไลซิสของกลีเซอรอลในวัฏภาคของเหลว ตัวแปรที่ศึกษาคือ
ชนิดของโลหะ (Co Mo และ CoMo) ชนิดของตัวรองรับ (Al_2O_3, HZSM5 และ AlMCM-41)
อัตราส่วนน้ำหนักของตัวเร่งปฏิกิริยาต่อสารละลายกลีเซอรอล (15-30 มิลลิกรัมต่อกรัมกลีเซอรอล)
ปริมาณโลหะที่ใส่ลงบนตัวรองรับ (ร้อยละ 2.5-20 โดยน้ำหนัก) และภาวะในการทำปฏิกิริยาไฮโดร
จิโนไลซิส ได้แก่ อุณหภูมิ (100-220 องศาเซลเซียส) ความดันไฮโดรเจน (3-9 เมกะปาสกาล) และ
เวลาที่ใช้ในการทำปฏิกิริยา (3-9 ชั่วโมง) พบว่าความสามารถในการเร่งปฏิกิริยาขึ้นอยู่กับความเป็น
กรด พื้นที่ผิว และปริมาณรูพรุน โดยตัวเร่งปฏิกิริยาที่มีความแรงของกรดสูงจะมีกัมมันตภาพสูงใน
การเปลี่ยนกลีเซอรอลเป็นผลิตภัณฑ์ และมีผลต่อสภาพการเลือกผลิตภัณฑ์อื่นอย่างมีนัยสำคัญ โดย
ตัวเร่งปฏิกิริยา Co/HZSM5 ที่มีปริมาณโลหะบนตัวรองรับร้อยละ 5 โดยมวล ให้ร้อยละการเปลี่ยน
ของกลีเซอรอลสูงสุดถึงร้อยละ 42 และร้อยละผลได้ของผลิตภัณฑ์ที่ต้องการ ได้แก่ อะโครลีน 1,2-
โพรเพนไดออล และ 1,3-โพรเพนไดออล สูงสุดถึงร้อยละ 1, 8 และ 5 ตามลำดับ โดยใช้อัตราส่วน
น้ำหนักของตัวเร่งปฏิกิริยาต่อสารละลายกลีเซอรอล 20 มิลลิกรัม/กรัม ภายใต้ภาวะของการทำ
ปฏิกิริยาที่อุณหภูมิ 180 องศาเซลเซียส ความดัน 7 เมกะปาสกาล และเวลา 6 ชั่วโมง

ภาควิชา   เคมีเทคนิค   ลายมือชื่อนิสิต

สาขาวิชา   เคมีเทคนิค   ลายมือชื่อ อ.ที่ปรึกษาวิทยานิพนธ์หลัก

ปีการศึกษา   2556   ลายมือชื่อ อ.ที่ปรึกษาวิทยานิพนธ์ร่วม

5273881123: MAJOR CHEMICAL TECHNOLOGY

KEYWORDS : GLYCEROL / HYDROGENOLYSIS / Co-BASED CATALYST / PROPANEDIOLS / ACROLEIN

SUPATTRA RAKSAPHORT : HYDROGENOLYSIS OF GLYCEROL TO PROPANEDIOL USING Co-BASED CATALYSTS. ADVISOR : ASSOC. PROF. MALI HUNSOM, Ph.D., Dr. de L'INPT, CO-ADVISOR : ASST. PROF. SITTHIPHONG PENGPANICH, Ph.D., 130 pp.

This work was carried out to prepare the supported Co-based catalysts by the impregnation method for glycerol hydrogenolysis in aqueous phase. The investigated parameters were types of support (Al_2O_3, HZSM5 and AlMCM-41), types of metal (Co, Mo and CoMo), weight ratio of catalyst to glycerol (15-30 mg/g glycerol), metal loading (2.5-20 wt.%) and the reaction conditions including temperature (100-220 ^{o}C), H_2-pressure (3-9 MPa) and reaction time (3-9 h). The results demonstrated that the catalytic activity of catalysts depended on the acidity of the utilized catalyst, specific surface area and pore volume. Strong-strength acid sites exhibited a better activity for glycerol conversion and effected significantly on the product selectivity. Among as-prepared catalysts, the 5 wt.% Co/HZSM5 catalysts exhibited the highest activity of glycerol hydrogenolysis. It gave the maximum conversion of glycerol of 42% and the maximum yield of the desired products including acrolein, 1,2-PDO and 1,3-PDO of 1, 8 and 5%, respectively, in the presence of the weight ratio of supported Co/HZSM5 catalysts to glycerol of 20 mg/g under the reaction condition of 180 ^{o}C, 7 MPa H_2-pressure and 6 h reaction time.

Department : Chemical Technology   Student's Signature

Field of Study : Chemical Technology   Advisor's Signature

Academic Year : 2013   Co-advisor's Signature

ACKNOWLEDGEMENTS

CONTENTS

LIST OF TABLES

LIST OF FIGURES

LIST OF ABBREVATIONS

AlMCM-41	Aluminum Mobile Crystalline Material 41
BET	Brunauer-Emmett-Teller technique for the measurement of the specific surface area of a material
GC-MS	Gas Chromatograph and Mass Spectrometry technique
HPLC	High Performance Liquid Chromatography technique
HZSM5	The alumination of highly siliceous Zeolite Socony Mobil-5
S	Product selectivity
SEM-EDX	Scanning Electron Microscopy with Energy Dispersive X-ray technique
TEM	Transmission Electron Microscopy technique
TPD	Temperature Programmed Desorption technique
TPR	Temperature Programmed Reduction technique
X_G	Glycerol conversion
XRD	X-ray Diffraction technique
Y	Product yield
1,2-PDO	1,2-propanediol
1,3-PDO	1,3-propanediol

CHAPTER I

INTRODUCTION

1.1 Background

Glycerol is the principal by-product of biodiesel production. Approximately 100 kg of glycerol is generated when a ton of biodiesel is produced. Any further increase in biodiesel production rates will significantly raise the quantity and surplus of crude glycerol and partially waste in the environment. High-purity glycerol is an important industrial feedstock for applications in the food, cosmetic and pharmaceutical industries, as well as other more minor uses. In addition, it can be converted to various valuable compounds such as acrylaldehyde (or acrolein) by dehydration reaction, acrylic acid by oxydehydration reaction [1-3], ethers by etherification reaction [4], glyceric acid by oxidation reaction [5] and propanediols or ethylene glycol by hydrogenolysis reaction [6-13].

In particular, glycerol hydrogenolysis has been studied to achieve mechanistic and kinetic understandings and to produce value-added compounds such as acrolein, 1,2-propanediol and 1,3-propanediol which can be used as raw material in the synthesis of pharmaceuticals, polymers, agricultural adjuvant, plastics and transportation fuel [14]. Currently, acrolein and propanediols are produced from petroleum-derived propylene via oxidation to propylene oxide and subsequent hydrolysis. These methods are restricted by the supply of olefins due to the decreasing and unstable supply of petroleum. Another common method that can be converted glycerol to propanediols is fermentation method by using bacteria [15]. However, the fermentation process provided low productivity, long fermentation time and short life span of bacterial strains. In addition, the present industrial process to obtain acrolein, an important intermediate in order to produce the chemical products including propanediols, is gas phase oxidation of propanediol with a Bi/Mo-mixed oxide catalyst and liquid phase or supercritical phase dehydration of glycerol over solid acid catlysts [2, 3]. Although many different processes have been studied, the catalytic hydrogenolysis of glycerol to produce value-added compounds seems to be a highly promising alternative route.

Hydrogenolysis is a chemical reaction whereby a carbon-carbon or carbon-heteroatom single bond is cleaved or undergoes "lysis" by hydrogen. Several elements can be heteroatom, but it usually is oxygen, nitrogen, or sulfur. A related reaction is hydrogenation, where hydrogen is added to the molecule, without cleaving bonds. Usually hydrogenolysis is conducted catalytically using hydrogen gas [16]. For the common mechanism of glycerol hydrogenolysis to propanediols, preliminary reactions were conducted in two steps. The first step, dehydration of a glycerol molecule to form hydroxyacetone (acetol), 3-hydroxypropanal and/or acrolein is occurred and they are possibly an intermediate of an alternative path for forming propanediol. In the second step, hydrogenation of an intermediate, acetol, 3-hydroxypropanal and/or acrolein, further react to form propanediol by catalytic hydrogenation with 1 mol of water by-product [8].

Two types of catalysts have been reported in the literatures for glycerol hydrogenolysis. The first one is the transition metal oxides, such as Raney-nickel, copper chromite or copper-zinc oxide (Cu-ZnO) catalysts and the second one is the catalysts consisting of supported noble metal catalysts [17]. Several metal-based catalysts such as platinum (Pt), ruthenium (Ru), palladium (Pd), nickel (Ni) or rhodium (Rh), are usually more active than cobalt (Co) based catalysts for glycerol hydrogenolysis. However, due to their high cost, the cheaper catalyst such as Co is required to enhance the sustainability and economics of glycerol hydrogenolysis. From volcano plot, the trend in activity of Co is at a fixed set of these catalysts. In addition, Co catalyst is quite promising for oxidation–reduction processes. Several studies have shown that Co supported mainly on aluminosilicates displayed high activity for the selective catalytic hydrogenation of alkenes, aldehydes and ketones [18]. Therefore, Co is one of the promising candidate metal-based catalyst for improving the conversion and selectivity of glycerol hydrogenolysis.

1.2 Objectives

1. To investigate the effect of parameters and the optimum operating conditions for glycerol hydrogenolysis to product distribution by Co-based catalyst in an aqueous phase.

2. To study and propose mechanism of glycerol hydrogenolysis to product distribution by catalytic conversion.

1.3 Scope of dissertation

1. Investigate effect of parameters on glycerol conversion and product yield from glycerol hydrogenolysis over supported Co-based catalyst in an aqueous phase.

2. Propose the mechanism of glycerol hydrogenolysis over supported Co-based catalyst.

1.4 Outputs of dissertation

1. The high activity supported Co-based catalyst for glycerol hydrogenolysis in an aqueous phase.

2. The optimum operating condition for glycerol hydrogenolysis over supported Co-based catalyst in an aqueous phase.

3. The mechanism of glycerol hydrogenolysis over supported Co-based catalyst.

CHAPTER II
THEORY AND LITERATURE REVIEWS

2.1 Glycerol [19]

Glycerol is a simple alcohol having an IUPAC name of propane-1,2,3-triol. Glycerol is also commonly known as glycerin (more than 95% of purified commercial glycerol), 1,2,3-propanetriol, 1,2,3-trihydroxypropane, glyceritol or glycyl alcohol. It is biodegradable, green refinery process and recyclable liquid manufactured from renewable sources and is a material of outstanding utility in various applications. Glycerol is generally low oral toxicity in humans and low irritant potential to human skin and eyes. However, glycerol with high concentrations has caused kidney and red blood cell damage after oral and intravenous administration [20].

2.1.1 Physical properties

Glycerol is a colorless, odorless, sweet-tasting, viscous, non-toxic and non-irritating liquid. It is highly stable under typical storage conditions and widely used in pharmaceutical formulations. Glycerol molecule contains three hydrophilic hydroxyl groups (-OH), which are responsible for its solubility in water and alcohol, and its hygroscopic nature. Furthermore, glycerol has useful solvent properties similar to those of water and simple aliphatic alcohol. It is slightly soluble in ether, ethyl acetate, and dioxane and insoluble in hydrocarbon [21, 22]. Its melting point and boiling point are 17.9 $^{\circ}$C and 290 $^{\circ}$C, respectively.

2.1.2 Chemical properties

The chemical formula of glycerol is $C_3H_8O_3$ or $HO-CH_2-CHOH-CH_2-OH$ as shown in Figure 2.1. Glycerol is a trihydric alcohol, capable of reacting as an alcohol. Its backbone is central to all lipids known as triglycerides [23]. Two terminal primary hydroxyl groups are more reactive than the internal secondary hydroxyl group. Under neutral or alkaline conditions, glycerol can decompose to acrolein via dehydration reaction at 280 $^{\circ}$C [24]. Alkaline glycerol begins to dehydrate at 180 $^{\circ}$C

forming an ether-linked polyglycerols [25]. At room temperature, glycerol rapidly absorbs water. The dilute glycerol can be degraded by microorganism.

On oxidation, glycerol yields to variety of product depending on the reaction conditions. The use of mild oxidizing agent is possible to oxidize only one hydroxyl group to yield glyceraldehyde. These compounds may be considered very simple aldose and simplest ketoses. The mixture of these two compounds obtained from glycerol or glyceraldehyde has been called glycerose. Glycerol can be converted to glyceric acid ($CH_2CHCHOHCOOH$) in the presence of nitric acid. Some industrial important reaction products of glycerol include [26]:

1. Mono-, di- and tri-esters of inorganic and organic acids
2. Mono- and di- glyceride of fatty acids formed by transesterification of triglycerides
3. Aliphatic and aromatic esters formed by reactions with alkylating agents
4. Polyglycerols formed by the intermolecular disaffection of water with alkaline catalyst
5. Cyclic 1,2 or 1,3-acetals or ketals formed by the reaction with aldehyde or ketons, respectively
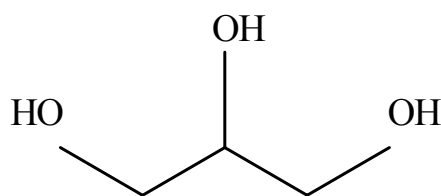
Figure 2.1. Structure of glycerol.

The basic physico-chemical properties of glycerol which are important for its applications are shown in Table 2.1.

Table 2.1 Basic physico-chemical properties of glycerol [21].

Properties	Values
Chemical formula	HO-CH$_2$-CHOH-CH$_2$-OH
Formula weight	92.09
Form and colour	Colourless and liquid
Specific gravity	1.260$^{50/4}$
Melting point	17.9 ^{o}C
Boiling point	290 ^{o}C
Solubility in 100 parts	
Water or alcohol	Infinitely
Ether	Insoluble
Vapor pressure in 760 mmHg	290 ^{o}C
Heat of fusion at 18.07 ^{o}C	47.49 cal/g
Viscosity liquid glycerol	
At 100% purity	10 cP
At 50% purity	25 cP
Diffusivity in	(DL x 10^5 cm^2/s)
i-Amyl alcohol	0.12
Ethanol	0.56
Water	0.94
Food energy	4.32 kcal/g
Flash point	160 ^{o}C
Surface tension	64.00 mN/m

Specific heat glycerol in aqueous solution (mol%)	15 ^{o}C (cal/g ^{o}C)	30 ^{o}C (cal/g ^{o}C)
2.12	0.961	0.960
4.66	0.929	0.924
11.5	0.851	0.841
22.7	0.765	0.758
43.9	0.670	0.672
100	0.555	0.576

2.1.3 Characteristics of glycerol

Glycerol can be categorized into three main types as crude glycerol, purified glycerol and refined/commercial glycerol. The major different properties between these three types of glycerol from biodiesel industry can be illustrated in Table 2.2. The purity of crude glycerol is 60-80% which is lowered than that of purified or commercial glycerol, which is generally close to 100%. In addition, the moisture, ash and soap contents of crude glycerol are higher than other types of glycerol. The acidity value is slightly higher than the others, and the color is also dark in crude glycerol which might be due to the presence of such impurities.

Table 2.2. Quality parameters of different categories of glycerol [27].

Parameters	Crude glycerol	Purified glycerol	Refined/commercial glycerol
Glycerol content (%)	60-80	99.1-99.8	99.2-99.98
Moisture content (%)	1.5-6.5	0.11-0.8	0.14-0.29
Ash (%)	1.5-2.5	0.054	<0.002
Soap (%)	3.0-5.0	0.56	N/A
Acidity (pH)	0.7-1.3	0.10-0.16	0.04-0.07
Chloride (ppm)	ND	1.0	0.6-9.5
Color (APHA)[a]	Dark	34-45	1.8-10.3

a: APHA color is a color standard named for the American Public Health Association and defined by ASTM D1209.

2.2 Source of glycerol [19]

2.2.1 Triglyceride sources

Glycerol is generated in almost every industries that use triglyceride from animal fats or vegetable oils as raw material, especially the soap and biodiesel industries. As demonstrated in Figure 2.2, glycerol is a by-product of fats and oils hydrolysis and transesterification to produce biodiesel and also saponification to produce soap.
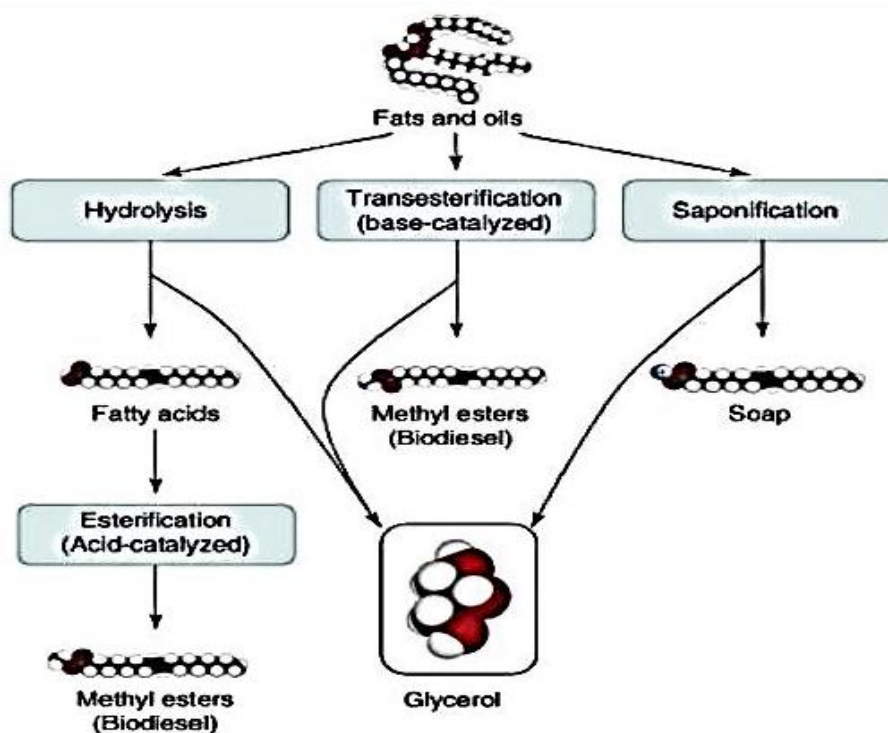
Figure 2.2. Glycerol production from fats and oils [28].

a. Hydrolysis and esterification

Esterification is the chemical reaction between alcohol and acid to form alkyl ester as the reaction product. In biodiesel production process, if the feedstock oil has high acid value and water content, acid-catalyzed esterification is generally used to accelerate the reaction between fatty acids and alcohol to produce biodiesel. Acid-catalyzed hydrolysis can break down fats or oils and release the free fatty acids. After that, free fatty acids are treated with an alcohol in the presence of acid catalyst to give methyl esters and glycerol as by-product as shown in Figure 2.3. However, biodiesel production in the presence of acid catalyst is much slower than that in base.
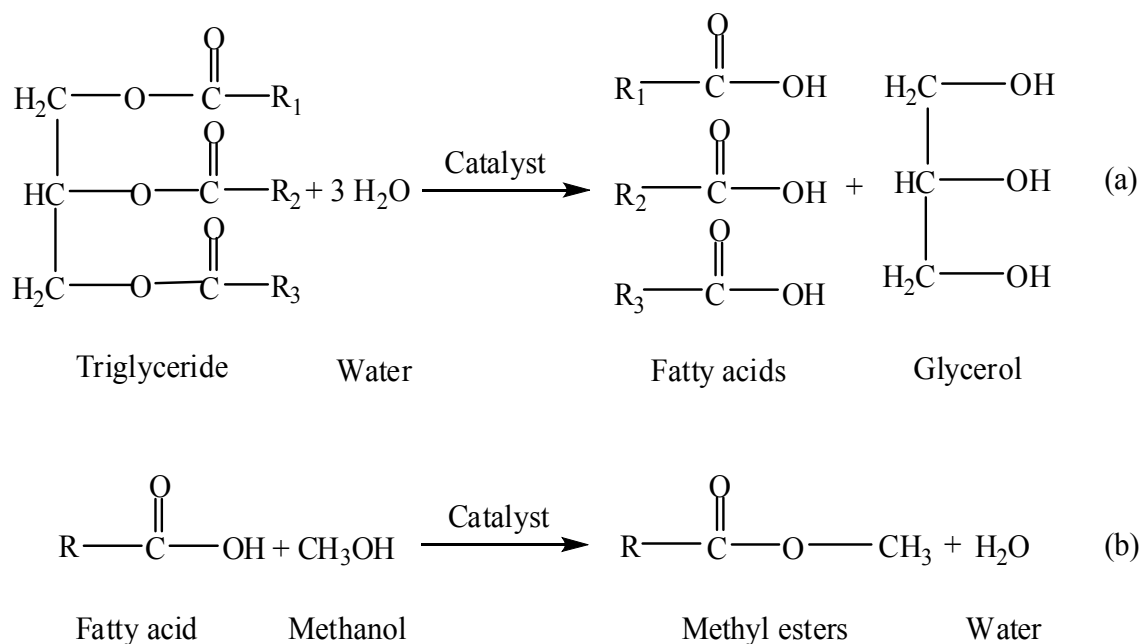
Where R, R_1, R_2, and R_3 are long chains of carbons and hydrogen atoms, sometimes called fatty acid chains.

Figure 2.3. Hydrolysis (a) and esterification (b) reaction of triglyceride from vegetable oil and animal fat [29].

b. Transesterification

Transesterification is the chemical reaction between triglyceride of vegetable oil and animal fat and alcohol in the presence of either acid or base catalysts to form alkyl ester as the main product and glycerol as the by-product. Practically, the transesterification of biodiesel industry uses the base-catalyzed technique because it is the most economical process for treating fats and oils, requiring only low temperature and pressure and the yield of conversion is greater than 98%. The transesterification reaction of triglyceride from vegetable oil and animal fat is shown in Figure 2.4.
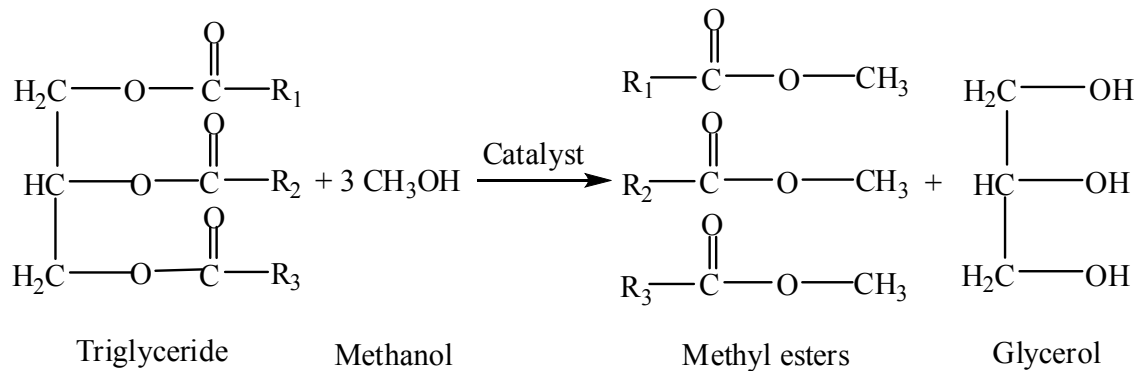
$$H_2C-O-\overset{\displaystyle O}{\overset{\|}{C}}-R_1$$
$$HC-O-\overset{\displaystyle O}{\overset{\|}{C}}-R_2 + 3\ CH_3OH \xrightarrow{\text{Catalyst}}$$
$$H_2C-O-\overset{\displaystyle O}{\overset{\|}{C}}-R_3$$

$$R_1-\overset{\displaystyle O}{\overset{\|}{C}}-O-CH_3 \qquad H_2C-OH$$
$$R_2-\overset{\displaystyle O}{\overset{\|}{C}}-O-CH_3 + HC-OH$$
$$R_3-\overset{\displaystyle O}{\overset{\|}{C}}-O-CH_3 \qquad H_2C-OH$$

| Triglyceride | Methanol | Methyl esters | Glycerol |

Where R_1, R_2, and R_3 are long chains of carbons and hydrogen atoms, sometimes called fatty acid chains.

Figure 2.4. Transesterification reaction of triglyceride from vegetable oil and animal fat [30].

c. Saponification

The saponification reaction is the alkaline hydrolysis of the fatty acid esters linkages in the presence of either strong acid or base catalysts. In soap industries, animal fats or vegetable oils is heated with alkali chemical such as sodium hydroxide (NaOH) or potassium hydroxide (KOH) to produce fatty acid salts (soap) and glycerol as by-product as shown in Figure 2.5. Once the saponification reaction is complete, sodium chloride (NaCl) is added to precipitate the soap. The water layer is drawn off the top of the mixture and the glycerol is recovered using vacuum distillation.
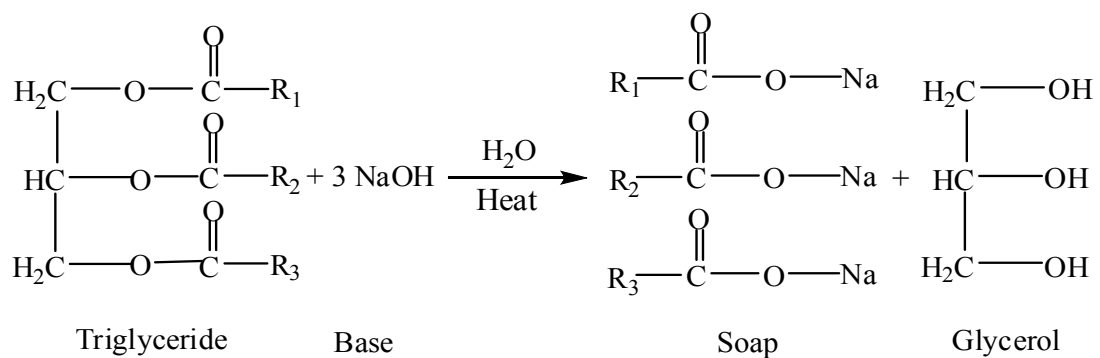
$$H_2C-O-\overset{\displaystyle O}{\overset{\|}{C}}-R_1$$
$$HC-O-\overset{\displaystyle O}{\overset{\|}{C}}-R_2 + 3\ NaOH \xrightarrow[\text{Heat}]{H_2O}$$
$$H_2C-O-\overset{\displaystyle O}{\overset{\|}{C}}-R_3$$

$$R_1-\overset{\displaystyle O}{\overset{\|}{C}}-O-Na \qquad H_2C-OH$$
$$R_2-\overset{\displaystyle O}{\overset{\|}{C}}-O-Na + HC-OH$$
$$R_3-\overset{\displaystyle O}{\overset{\|}{C}}-O-Na \qquad H_2C-OH$$

| Triglyceride | Base | Soap | Glycerol |

Where R_1, R_2, and R_3 are long chains of carbons and hydrogen atoms, sometimes called fatty acid chains.

Figure 2.5. Saponification reaction of triglyceride from vegetable oil and animal fat [19].

d. Fatty alcohol production

Besides, crude glycerol can be produced as a by-product of fatty alcohol production according to the acid route, ester route and wax ester route as demonstrated in Figure 2.6. For the acid route, the free fatty acids from oil are pretreated and splitting to glycerol. The obtained glycerol is derivered to the glycerine recovery process. The acid route uses the slurry hydrogenation process, which the catalyst is suspended in a loop type reactor. This reactor contains an excess of fatty alcohol, and then the fatty acids are separated. The advantage of this process is the constant catalyst activity. For the ester route, the fatty acids are de-acidified after oil pretreatment and fed to the transesterification process to produce methyl ester. This process generated glycerol as by-product. The methyl ester is fed to a fixed bed hydrogenation reactor, where methanol is generated and separated from fatty alcohol. For the wax ester route, the glycerol is splitted from the free fatty acids obtaining from oil purification. Afterward, the fatty acids are pre-esterified and fed to a fixed bed hydrogenation reactor. It is shown that, the combination of the pre-esterification with the slurry process allows the reduction of the catalyst consumption compared with the original slurry by two thirds. The advantage of this process is that the catalyst costs are lowered.
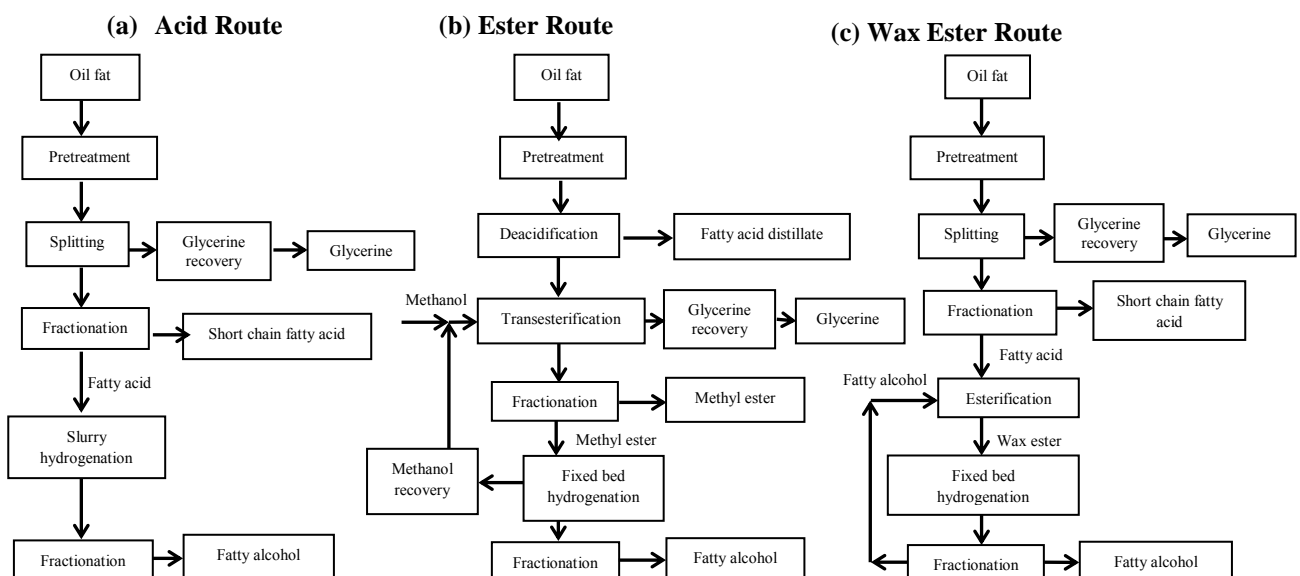
Figure 2.6. Fatty alcohol processes based on renewable feed stocks (a) acid route, (b) ester route and (c) wax ester route [30].

The crude glycerol obtained from these industries has low economic value due to the presence of various impurities such as moisture, ash, soap and chloride as listed in Table 2.2. Crude glycerol generally consists of about 65-80% glycerol. However, some biodiesel production can be produced more than 80% glycerol, depending on the specific manufacturing processes. Refined glycerol is about 99.5% purity resulting from the refining process [27]. Therefore, if glycerol is used for the formation of consumer products like food, cosmetic and pharmaceutic, it must be purified prior to use.

2.2.2 Non-triglyceride sources

Besides the production from triglyceride sources, glycerol can be produced from non-triglyceride sources by various chemical routes from petrochemical feedstocks, microbial fermentation, hydrogenation of carbohydrates and others. This type of glycerol is so-called synthetic glycerol.

a. Chemical processes from propylene [19,31]

Glycerol can be produced from the reaction of propylene ($CH_2=CHCH_3$) as demonstrated in Figure 2.7. For the first route, allyl chloride ($CH_2=CHCH_2Cl$) obtained from the chlorination process of propylene is oxidized with hypochlorite (ClO^-) to dichlorohydrin ($ClCH_2CH(OH)CH_2Cl$), and then reacts without isolation to epichlorohydrin (CH_2CHOCH_2Cl) by ring closure in the presence of a strong base as sodium or calcium hydroxide. Epichlorohydrin can further hydrolyze with 10-15 wt.% sodium hydroxide or sodium carbonate (Na_2CO_3) at 80-200ºC and atmospheric or overpressure to form glycerol. The yield of dilute glycerol solution is more than 98%. The solution contains 5-10% sodium chloride (NaCl) and less than 2% of other impurities. For the second route, propylene is epoxidized to propylene oxide (CH_3CHCH_2O) or oxidized to acrolein ($CH_2=CHCHO$). Both generated intermediates can further isomerize to form allyl alcohol ($CH_2=CHCH_2OH$), the epoxidization of allyl alcohol with peracetic acid (CH_3CO_3H) produces glycidol (CH_2CHOCH_2OH), which can be hydrolyzed to glycerol.
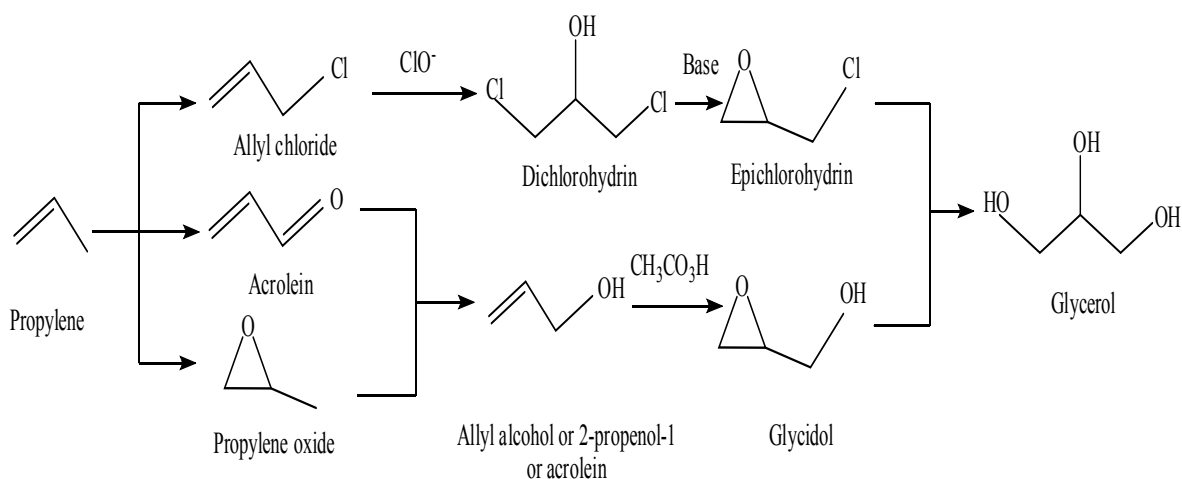
Figure 2.7. Synthesis of glycerol processes from propylene [19].

b. Microbial fermentation [31, 32]

As the cost of propylene has increased and glycerol is used for feedstock of various chemical productions, glycerol production by fermentation has become more attractive as an alternative route. The production of glycerol from monosaccharides by yeast fermentation can be achieved by forming a complex between acetaldehyde and bisulfite ions, growing the yeast cultures at pH values around 7 or above or using osmotolerant yeasts without a need for a steering agent. In recent years, significant developments have been made in the glycerol process based on osmotolerant yeasts on a commercial scale in China. The novel osmotolerant yeast strains can produce glycerol up to 58%, 30 g/L-day and 110–120 g/L for glycerol yields, productivities and concentrations in broth, respectively, which have been attained on a commercial scale in an optimized aerobic fermentation process. While glycerol metabolism has become better understood in yeasts, opportunities to construct novel glycerol overproducing microorganisms by metabolic engineering will arise. Nevertheless, the formation of glycerol by microbial fermentation consequently declined since it was unable to compete with chemical synthesis from petrochemical feedstocks because the glycerol yields were low and the recovery of glycerol from broth expensive and inefficient.

c. Hydrogenation of carbohydrates

Hydrogenation of natural polyalcohols such as cellulose, starch, or sugar leads to the formation of mixture solution of glycols and glycerol, which can be further separated by distillation [32]. Catalysts used for this reaction are nickel (Ni), cobalt (Co), copper (Cu), chromium (Cr) and tungsten (W) as well as oxides of lanthanides. The crude glycerol obtained from this process is poor in quality and requires severe and expensive refining methods.

d. Glycerol photoproduction

Glycerol photoproduction with other biomass is possible in the presence of solar energy and algae [33]. For saving energy and raw materials required in glycerol production, an immobilized cell system was prepared and worked in a continuous bubble column bioreactor. Cells of the freshwater green alga *Chlamydomonas reinhardtii*, that can excrete glycerol into the medium in a response to an osmotic shock (200‑250 mM NaCl), were immobilized over supports. This process can produce 7 g/L of a glycerol within 27 days with the productivity of 2 g/L-day and corresponding to 23 mg per mg chlorophyll per day.

2.3 Global status and market of glycerol production

From the late 1990s to 2003, the glycerol production worldwide remained relatively stable and very low level. Afterwards, biodiesel production slightly increased and further severely increased with corresponding the numerous production of crude glycerol and partially waste in the environment during the period of 2004–2006 as shown in Figure 2.8 [34]. According to Figure 2.8, it was found that approximately four times of glycerol production from 62 million lbs to 213 million lbs increased in only one year from 2005 to 2006. It was due to the high production of biodiesel from 75 gallons to 250 gallons during 2005–2006. Earlier, glycerol was produced mainly using synthetic processes but due to the evolution of biodiesel industry, synthetic processes were replaced by transesterification process which

resulted in 66.2% of the total glycerol being obtained from the biodiesel industry in 2011[35].
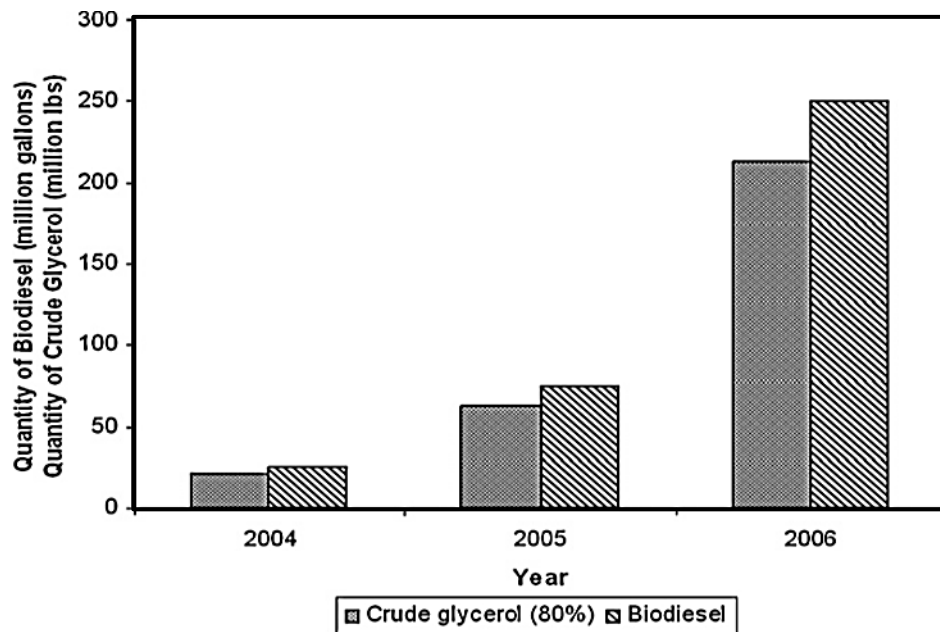
Figure 2.8. Production of biodiesel and crude glycerol during 2004–2006 [34].

The National Biodiesel Board [36] reported that the production of biodiesel in 2005 was increased sharply from less than 100 million gallons to 450 million gallons in 2007 with corresponded to the production of crude glycerol. Basically, glycerol was produced at under 0.5 billion pounds by European Nations only before 2006. After that, the production of biodiesel of some other countries like USA, Malaysia, Indonesia, India and China during 2006–2007 sharply increased the production of crude glycerol. After 2007, the production of crude glycerol rapidly increased due to the numerous production of biodiesel by all these countries. According to the BBI International's Engineering and Consulting team [37], biodiesel manufacturers created 187,000 tons of crude glycerol in 2007. In addition, there was a great depress in imports of the United State crude glycerol during the years of 2008 and 2009 resulting to the depress of overall crude glycerol market in the United State. This was a direct effect of an increase in the biodiesel production in Southeast Asia and Europe, which were exporting glycerol to the United States in large volume and at low cost,

and also experienced a drop in its demand in Asian glycerol market due to a new Argentine biodiesel market that was established in this zone.

The main regions having the numerous production of crude glycerol are the European Union, the United States and South East Asian countries. The estimated production of crude glycerol resulting from biodiesel production in different countries is shown in Figure 2.9.
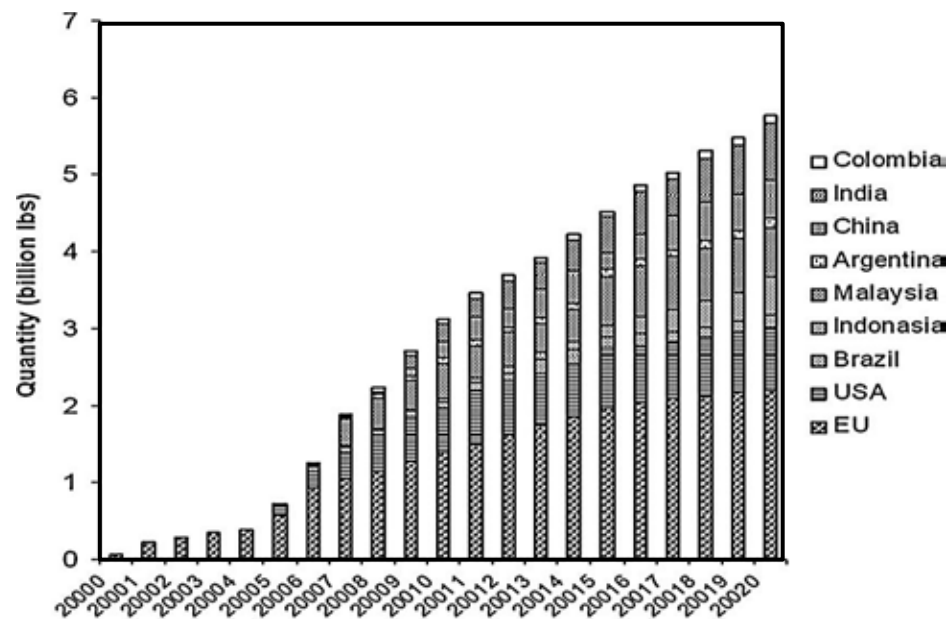
Figure 2.9. Estimated production of crude glycerol in different countries [38].

In 2020, the estimated production of glycerol would reach 5.8 billion pounds. This is due to demand of biodiesel that is projected at 8 billion gallons in 2020. Before 2006, the glycerol production was very low which less than one billion lbs and mostly produced by the European Union. After that, the glycerol production was so rapidly increased and many other countries like USA, Indonesia, Malaysia, China and India started to produce glycerol and continued so that its production reached above 2 billion lbs in 2009. The projected data estimates that the glycerol production will attain 4 billion lbs in 2015 and touch to 6 billion lbs after 2020 if its production increases at the same pace. In 2020, the major portion of projected glycerol quantity belongs to EU and then USA. The other countries those will encourage glycerol

production in future are Malaysia, India, China, Indonesia, Brazil, Argentina and Colombia. Eventually, it can be concluded that the production of crude glycerol resulting from biodiesel is rapidly increasing in different religions of the world.

2.4 Glycerol utilization

Glycerol can be directly used as an additive or raw material for various industries as shown in Figure 2.10. The top category belongs to the usage in drugs and pharmaceuticals industries for around 18%, inferior to personal care 16% and polyether and polyols industries 14%, respectively. Currently, the amount of glycerol going annually into chemical applications is around 160,000 tonnes, and is expected to grow at an annual rate of 2.8% [26].
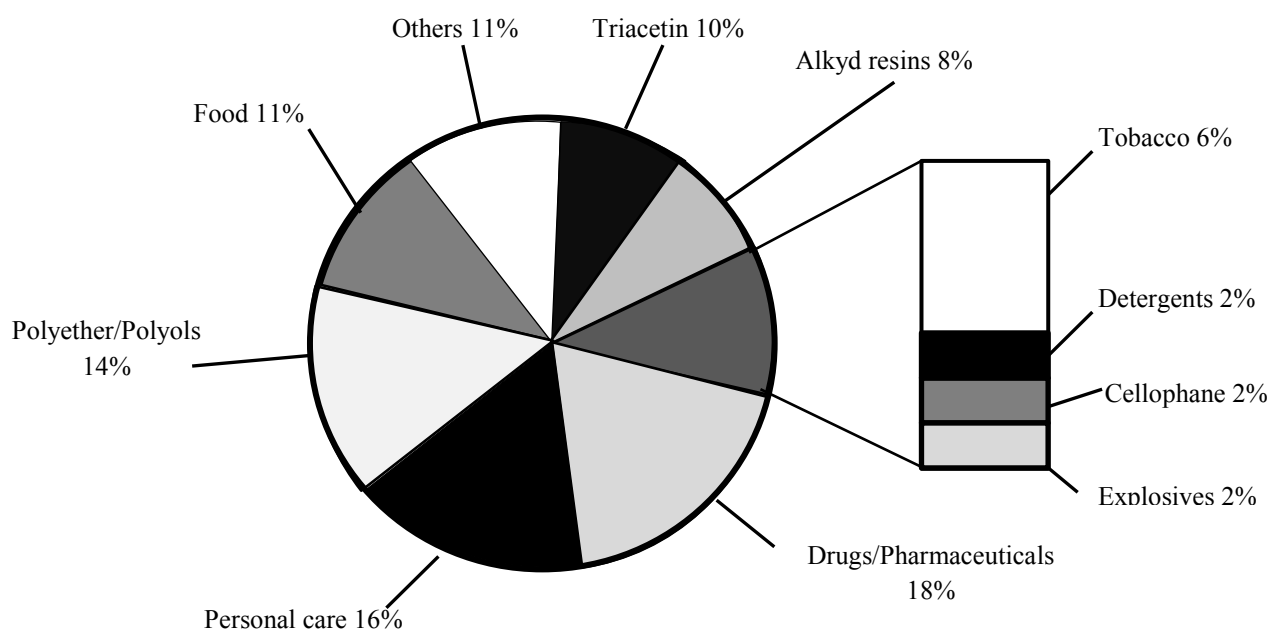
Figure 2.10. Market for glycerol [26].

2.4.1 Raw materials in various industries [19, 26, 27]

Glycerol also is employed as a raw material in different chemical syntheses. It can be used as a humectant, plasticizer, emollient, thickener, dispersing medium, lubricant, sweetener, bodying agent, detergents and antifreeze. Thus, it is

used as an ingredient or processing aid in cosmetics, toiletries, personal care, drugs and food products.

a. Drug and pharmaceuticals industries

As one of major raw materials for the manufacture of medical and pharmaceutical preparations, about 18% of overall glycerol usage [26]. Glycerol is widely used as a laxative and, based on the same induced hyperosmotic effect, cough syrups, elixirs and expectorants and also found in allergen immunotherapies.

b. Personal care application

Glycerol is an ideal ingredient in many personal care products of about 16% [26], commonly found in toothpaste, mouthwashes, skin care products, shaving cream, hair care products, water-based personal lubricants and soaps. Glycerol is a component of glycerine soap. Essential oils are added for fragrance. This kind of soap is used by people with sensitive, easily-irritated skin because it prevents skin dryness with its moisturizing properties. It draws moisture up through skin layers and slows or prevents excessive drying and evaporation. For sugar free gum, it is giving a sweet taste without contributing to tooth decay. In solid dosage forms like tablets, glycerol is used as a tablet holding agent and glycerol can be used as a laxative.

c. Polymer industry

The application of glycerol as polyether or alcoholic hydroxyl group polyol was about 14% [26]. Basically, it provides for flexible foams, the construction of rigid polyurethane foams. Polyols are used mostly on a large scale as sugar-free sweeteners or sorbital, which is facing particularly stiff competition from glycerol. Glycerol contains approximately 27 calories per tea-spoonful and is 60% as sweet as sucrose. However, it does neither raise blood sugar levels, nor does it feed the bacteria that cause plaque and dental cavities. Glycerol is the inhibitor to which propylene oxide and ethylene oxide are added. Another application of glycerol is ester

or triacetin about of 10% [26]. Glycerol is widely used as a formulation of some alkyd resins and regenerated cellulose of about 8% [26]. These materials are used as productive surface coating and paints, and components of plastics as softener and plasticizer to impart flexibility, pliability and toughness of regenerated cellulose films, meat casing and special quality papers or cellophane.

d. Food industry

According to the statistics on glycerol usages, 11% of overall glycerol is used in food industries [26]. In foods and beverages, glycerol serves as a humectant, solvent, and sweetener, and may help preserve foods. It is also used as filler in commercially prepared low-fat foods (e.g., cookies), and as a thickening agent in liqueurs. As used in foods, glycerol has a caloric density similar to table sugar, but a lower glycemic index and different metabolic pathway within the body, so some dietary advocates accept glycerol as a sweetener compatible with low carbohydrate diets.

e. Botanical extracts

Glycerol prevents tannins from precipitating in ethanol extracts of plants. It is also used as an 'alcohol-free' alternative to ethanol as a solvent in preparing herbal extractions. Glycerol is a stable preserving agent for botanical extracts that does not allow inverting or reduction-oxidation of a finished extract's constituents. Both glycerol and ethanol are viable preserving agents. Glycerol is bacteriostatic in its action, and ethanol is bactericidal in its action.

f. Antifreeze

Glycerol is a non-ionic kosmotrope that forms strong hydrogen bonds with water molecules, competing with water-water hydrogen bonds. This disrupts the crystal lattice formation of ice unless the temperature is significantly lowered. The minimum freezing point temperature is at about −36 °F / −37.8 °C corresponding to 70% glycerol in water. In the laboratory, glycerol is a common component of solvents for enzymatic reagents stored at temperatures below 0 °C due

to the depression of the freezing temperature of solutions with high concentrations of glycerol. It is also used as a cryoprotectant where the glycerol is dissolved in water to reduce damage by ice crystals to laboratory organisms that are stored in frozen solutions, such as bacteria, nematodes, and mammalian embryos.

g. Chemical intermediate

Glycerol is used to produce nitroglycerin, which is an essential ingredient of various explosives such as dynamite, gelignite, and propellants like cordite. Nitroglycerin, also known as glyceryl trinitrate (GTN) is commonly used to relieve *angina pectoris*, taken in the form of sub-lingual tablets, or as an aerosol spray.

Although above-mentioned applications consumes large quantity of glycerol as a reactant or as an additive, more and more crude glycerol is continuously generated from the biodiesel industry. If the biodiesel production rates will significantly raise as the prediction in Figure 2.8, the surplus of crude glycerol and partially waste in the environment will be observed. In addition, high supply of crude glycerol will affect the glycerol price. As demonstrated in Table 2.3. There is a decreasing trend in refined and crude glycerol prices during 2001 to 2006 which is dropped from 15 cents/lb to 2 cents/lb since the United State demand for glycerol was not large enough for all of this excess glycerol and the global economic recession [39]. During the middle of 2007 to the start of 2008, the increasing price of glycerol was due to an imbalance between supply and demand of glycerol in global market. Afterward, it started to decline again in the end of 2008 and significant decreased in the following years which was due to oversupply of glycerol [40].

Table 2.3 Annual glycerol price from 2001 to 2009 [39].

Type of glycerol	Glycerol price (cent per pound)								
	2001	2002	2003	2004	2005	2006	2007	2008	2009
Synthetic	72	73	90	85	85	-	-	-	-
Refined	60	58	65	55	45	35	70.5	55	41
Crude	15	12	12	10	5	2	10	5	6

2.4.2 Glycerol value-added products [23, 41]

Due to the oversupply of glycerol from the numerous growth of biodiesel industry, using the growing supply of glycerol for the production of other in-demand reagents is a logical step in moving towards a more sustainable economy and improving the economic viability of processes. A great deal of research efforts to find new applications of glycerol for commercially value-added products such as hydrogen and synthesis gas [44-58], ethanol and butanol [58-61], acrolein [1-3, 62-65], acrylic acid [65, 66], succinic acid [75-77], dihydroxyacetone [67-69], polyglycerols [72-74], poly(hydroxyalkanoates) [78] and propanediol both 1,2-propanediol (1,2-PDO) and 1,3-propanediol (1,3-PDO) [6-13, 15-17, 59, 60], etc.

a. Hydrogen and synthesis gas

Hydrogen is an attractive alternative energy direction for the next generation, especially if it is produced from renewable resources. In addition, synthesis gas (H_2 and CO) can be used as fuel to generate electrical power or as a source of hydrogen. Thus, a great deal of research efforts is being done in the production of hydrogen from glycerol using catalytic reforming [44-49], pyrolysis [50-53], and steam gasification reaction [54-57].

H_2 production can be obtained through various reforming processes such as steam reforming, partial oxidation, aqueous phase reforming, autothermal reforming, and supercritical water reforming. Catalytic reforming is a chemical process used to convert petroleum refinery naphthas into high-octane liquid products which are components of high-octane gasoline. Supercritical water reforming can improve space-time yield, reduce mass transfer limitations and be more favourable

towards endothermic reforming reactions, as compared with steam and liquid water reforming. Glycerol reforming under catalytic supercritical water using Co catalyst deposited on various supports including ZrO_2, yttria-stabilized zirconia (YSZ), La_2O_3, γ-Al_2O_3, and α-Al_2O_3 was investigated. It was found that an increase in operating temperature could increase in glycerol conversion and carbon formation caused system operation failure at high operating temperatures (i.e. 748-798 K). Co supported on YSZ provided the most efficient performance for hydrogen production [45].

Pyrolysis is a thermal decomposition which occurs in the absence (fully or partially) of oxygen, the oxidation occurring effects in decreasing product quality. Pyrolysis becomes of the promises alternative technology to give value added of glycerol, which can be chemicals such as organic acids, sugars, aldehydes, ketones, hydroxyaldehydes, and hydroxyketones, phenols and hydrocarbons for substitute fuel such as hydrogen and syngas (feedstock used in synthetic fuels production via Fisher-Tropsch reaction) and avoid its accumulation in the environment. The products were mostly gas, essentially consisting of CO, H_2, CO_2, CH_4 and C_2H_4. The advantages of pyrolysis process are low production cost, high thermal efficiency, short residence time, and low CO_2 emission. Lower process temperature and longer vapor residence times favor the production of charcoal. Higher temperature and longer residence time increase the gas production, while moderate temperature and short vapor residence time are desired conditions for producing liquids. As other pyrolysis processes, syngas production from glycerol pyrolysis depends on different process conditions and process technologies adopted. The parameters as temperature, carrier flow rates and types and sizes of packing material had effected on the conversion of glycerol as well as product distribution [50]. The pyrolysis of glycerol over activated carbon under microwave heating increased gas fraction with a higher H_2 - CO composition, even low temperatures [51]. Earlier work showed that the swine manure effectively to be treated as a liquid biofuel and glycerol can be used as bio-based reagent to improve the performance of liquefaction for liquid fuel production. Thus, cohydrothermal pyrolysis of manure with crude glycerol or free fatty acid makes it possible to obtain a relatively high yield of bio-oil at a moderate high temperature [52]. The efficiency of the pyrolysis process can be improved by co-pyrolysis of crude glycerol with biomass

such as olive kernel method which concerned the maximum concentration of H_2 in the produced gas at high temperature (T = 720 ◦C) [53]. Moreover, the thermochemical treatment of crude glycerol–biomass mixtures may offer several economic and environmental advantages in biodiesel industry and reduce the cost of biodiesel production. If a limited amount of oxygen is available during the processing of the feedstock, gasification occurs rather than pyrolysis.

Gasification is a well-known thermochemical process, whereby organic matter is transformed into a combustible gas with low calorific power in the presence of a gasifying agent. Gasification of glycerol for the production of hydrogen and syngas is the main application that has been explored for energy purposes. Hydrothermal gasification in supercritical water of biomass substrates, such as glucose, cellulose and lignin, produced H_2, CH_4 and syngas. Supercritical water (SCW) provides a highly reactive and homogeneous medium for the conversion of organic molecules. SCW has low dielectric constant and weaker hydrogen bonds than liquid water resulting to miscible with organic compounds and gases, but simultaneously facilitates the occurrence of ionic chemistry due to its relatively high ion product. Mass transfer limitations and coke formation on catalyst surfaces are also reduced due to a low viscosity and high diffusivity. For high-temperature SCW, gasification at reaction temperatures ranging from 550 to 800 ^{o}C is carried out with non-metallic catalyst and low-temperature catalytic SCW gasification using a metal-based catalyst at reaction temperatures below 550 ^{o}C. Solid catalysts have been studied to promote gas formation at lower temperature, maximum hydrogen selectivity. The Ru/ZrO_2 catalyst was tested on the SCW gasification with glycerol concentration of 5 wt% in a continuous isothermal fixed-bed reactor. This catalyst presented good stability and overall activity but in the intermediate temperature range has been studied, its selectivity towards reforming reactions was not high enough [54]. The alkali catalysts in SCW can significantly increase the gasification efficiency and hydrogen yield by promoting water-gas shift reaction. The hydrogen yield with respect to catalysts was in the following order of $NaOH > Na_2CO_3 > KOH > K_2CO_3$. The glycerol concentration affected the gasification efficiency and hydrogen yield, which decreased rapidly at first and then remained steady when the glycerol concentration was increased from 10 to 50 wt.%. Because of the gas-water two phase

flow of cooled reactor effluent, the irregular impact on the back pressure regulator and pipeline system was observed when the gas yield was high [55].

For the in-situ gasification/reforming of waste glycerol, Ni/olivine displayed excellent properties to convert waste material to gas product with high product heating values and good cold-gas efficiency at low temperature. This study showed that the calcination temperature effect to the performance of this catalyst [56]. A co-gasification of hardwood chips blending with crude glycerol in various loading levels applies to converting liquid crude glycerol into a gas phase mixture involving a pilot scale fixed-bed downdraft gasifier. The crude glycerol loading levels affected the performance of gasifier and the quality of syngas produced. When crude glycerol loading level increased, the concentration of CO, CH_4, and tar in the syngas also increased but the particle concentration decreased. Thus, concluded that downdraft gasifiers suitable for co-gasification of hardwood chips blending with liquid crude glycerol up to 20 wt.% [57].

b. Ethanol and butanol

Ethanol was produced by glycerol fermentation using microbial [58, 59]. It is largely used as fuel and fuel additive, also a fuel for bipropellant rocket, chemical feedstock for organic compounds such as ethyl halides, ethyl ester, or acetic acid. Commonly, it also used as antiseptic and antidote for poisonous and toxic chemicals in medical application. The bioconversion of raw glycerol using a *Klebsiella* sp. HE1 strain via anaerobic fermentation was used to simultaneously produce H_2, ethanol, 1,3-PDO, and 2,3-butanediol biofuels. The production of biofuels depends on the operation temperature, pH, and glycerol concentration. The highest yields for H_2, ethanol, 1,3-PDO, and 2,3-butanediol were obtained at 0.35, 0.80, 0.37, and 0.08 mol/mol glycerol, respectively [58]. The production of 1,3-PDO, 2,3-butanediol and ethanol during cultivations of strain *Klebsiella oxytoca* FMCC-197 on biodiesel-derived glycerol based media was investigated. Different kinds of glycerol feedstocks and experimental conditions had an important impact on the distribution of metabolic products. The production of 1,3-PDO was positively influenced by stable pH conditions and by the absence of N_2 gas infusions throughout

the fermentation. The yield of 1,3-PDO of about 47 wt.% and also ethanol of about 20 wt.% were formed [59]. Butanol is considered as a potential biofuel or biobutanol. Butanol at 85 percent strength can be used for gasoline or petroleum engine without any change to the engine design (unlike 85% ethanol). It contains more energy for a given volume than ethanol and almost as much as gasoline, so a vehicle using butanol would return fuel consumption more comparable to gasoline than ethanol. Butanol can also be used as a blended additive to diesel fuel to reduce soot emissions, a solvent for chemical and textile processes, in organic synthesis, a chemical intermediate, and as well as a solvent in coating applications and a paint thinner. It discovers other uses such as a component of hydraulic and brake fluids, and a perfumes base. Crude glycerol, generated from biodiesel manufacturing waste, is used as cheaper carbon sources for the dual substrate biobutanol production to reduce the production cost of butanol by biological processes [60, 61].

c. **Dihydroxyacetone**

Dihydroxyacetone or DHA, also known as glycerone with the formula $HOCH_2COCH_2OH$, is a simple three-carbon sugar and non-toxic in nature. DHA is a versatile compound extensively used as a cosmetic ingredient mainly in sunless tanning formulations, as precursor of pharmaceuticals and as a chemical intermediate in organic synthesis. A large number of products can be obtained by the selective oxidation of glycerol using inexpensive and clean oxidizing agents such as air, oxygen or hydrogen peroxide. The oxidation of the secondary hydroxyl group of glycerol to produce high-value chemical dihydroxyacetone (DHA) and hydroxypyruvic acid ($HOCH_2COCOOH$) seems to be preferred only under acidic conditions [62, 63]. The use of multi-walled carbon nanotubes as support for gold nanoparticles, Au/MWCNT, makes a catalytic glycerol oxidation possible competitive alternative to the cumbersome biotechnological process presently used in industry. The selectivity of dihydroxyacetone of 60% was obtained in combination with a high activity [62]. The other method is the production of dihydroxyacetone from glycerol by *Gluconobacter oxydans* in a low-cost way [64].

d. Glyceric acid

Glyceric acid or 2,3-dihydoxypropionic acid (HOCH$_2$CH(OH)COOH) is one of the useful chemicals with pharmacy and industries which can be obtained from glycerol oxidation. Glyceric acid is naturally found as a phytochemical constituent in a variety of plants, such as peanuts, artichokes, tomatoes, apples, bananas, and grapes. The gold catalyst supported on activated carbon (support with micropores and small mesopores), prepared and used under the same conditions, with similar metal loading and average particle size, promotes the formation of glyceric acid [63]. The influence of the operating condition on the catalytic activity and products selectivity of liquid-phase oxidation of glycerol was studied by using catalytic systems based on gold nanoparticles supported on different carbon materials including activated carbon (AC), graphite (G) and ribbon-type carbon nanofibers (CNF-R). The influence of the oxygen pressure on the reaction rates was very small. The selectivity to glyceric acid was significantly enhanced by an increase both of oxygen pressure and reaction temperature, leading simultaneously to a decrease both of glycolic and tartronic acid selectivity. Glycerol conversion and glyceric acid selectivity increased when the NaOH/glycerol molar ratio was increased from 1 to 2 and it remained practically unchanged at higher values. A linear correlation was observed between the glycerol conversion and the amount of catalyst (up to 0.5 g), indicating that the reaction was reaction-rate controlled. Furthermore, it was also observed that an increase in the catalyst amount led to a substantial decrease in the selectivity to glyceric acid [65]. Selective oxidation of glycerol with molecular oxygen was studied over different functionalized MWNTs supported Pt catalysts in base-free aqueous solution. It found that Pt/S-MWNTs catalyst with small Pt particles was more active than Pt/MWNTs, Pt/HNO$_3$-MWNTs and Pt/H$_2$O$_2$-MWNTs for glycerol oxidation in base-free aqueous solution. Free glyceric acid formed (with 68.3% selectivity and 90.4% conversion of glycerol) on Pt/S-MWNTs in base-free solution while dihydroxyacetone formed firstly in an aqueous solution of NaOH/glycerol = 2:1 and the cleavage C–C bonds (catalyzed by alkali) arise severely [66].

e. Polyglycerols and their derivatives

Polyglycerols and their derivatives, mainly polyglycerol ester, are biodegradable products. They are non-ionic surfactants that have been used as emulsifiers in food and personal care products and also used in various industrial applications including polymer additives, lubricants, agrochemical formulations, and antifoaming agents in the paper industry or in wastewater, etc. Glycerol etherification [67-69] is the most popular process used for polyglycerol and their derivatives productions. The various selective etherifications of glycerol to obtain polyglycerols were investigated. First, the reaction of MgAl mixed oxides derived from hydrotalcite without solvents. The MgAl mixed oxides catalyst exhibit basic properties and excellent textural properties, making them suitable for base catalysed reaction especially the etherification of glycerol. It was found that the selectivity to desired products such as diglycerols and triglycerol was mainly influenced by the specific surface area and average pore diameter. [68]. Second, the effects of various parameters to the activity of novel $Ca_{1+x} Al_{1-x} La_xO_3$ composite catalysts without solvent was studied. It was found that increasing catalyst amount from 2 wt.% to 4 wt.% resulted in decreasing trends observed in both glycerol conversion and diglycerol selectivity. This observation could be attributed to the back-scission of diglycerol to glycerol. Furthermore, the prolonged etherification reaction resulted in the dehydration of more glycerol molecules, which in turn increased the conversion of glycerol. The cleavage of glycerol molecules during the conversion might not have exactly produced polyglycerols. Instead, it could lead to the double dehydration of glycerol to form other by-products such as acrolein. These by-products are not desirable in the polymerization etherification reaction and can result in the formation of inauspicious products [69]. Using combustion method with hydrotalcite catalysts prepared was investigated by the type of fuel used as different sugars (glucose, fructose and saccharose) and calcination temperatures (450 to 850 °C). It was found that glucose was the most suitable fuel to be used due to suitable molecular size and enthalpy and calcination temperatures had affected to the catalytic activity [67]. The transesterification of glycerol with fatty methyl esters or with triglycerides or by the direct esterification of glycerol with fatty acids can produced monoglycerides,

polyglycerol esters and their derivatives. However, the three hydroxyl groups in glycerol are not very different in reactivity, thus the product of the direct esterification or transesterification of glycerol with acid and/or base catalysts is a mixture of mono-, di-, and some triglyceride, plus glycerol that has not reacted [42]. The direct esterification of the polyol with a free organic acid are most simply produced esters. The reaction can also be carried out by transesterification of a polyol with a triglyceride or a fatty acid alkyl ester. In addition, partial esters of polyglycerol are obtained by acid-catalyzed polycondensation of monoglyceride or monoglyceride and glycerol. Finally, the polymerization of glycidol to a fatty acid or to a fatty acid monoglyceride, catalyzed by acids, also renders polyglycerol esters [42].

f. Succinic acid

Succinic acid is a dicarboxylic acid with the formula $HOOCCH_2CH_2COOH$. It used as an intermediate of the tricarboxylic acid cycle. It can be used for the manufacture of synthetic resins and biodegradable polymers and as an intermediate for chemical synthesis. Recently, the formation of succinic acids by microbial fermentations as *Actinobacillus succinogenes* and *Actinobacillus succinogenes* CH4 was investigated [70-72].

g. Poly(hydroxyalkanoates)

Poly(hydroxyalkanoates) or PHAs are linear polyesters of various hydroxyalkanoates that can be accumulated by numerous bacteria [73] as carbon and energy reserves. It represents a complex class of naturally occurring bacterial polyesters and can be used as good substitutes for non-biodegradable petrochemically produced polymers and as chiral starting materials in fine chemical, pharmaceutical and medical industries.

h. Acrolein and acrylic acid

Acrolein, also known as 2-propenal, acrylaldehyde or acrylic aldehyde, is the simplest unsaturated aldehyde with the formula $CH_2=CHCHO$ as

shown in Figure 2.11. It is used as intermediate for the synthesis of many useful compounds as acrylic acid, acrylic acid esters, super absorber polymers and detergents. Acrolein is produced from gas-phase dehydration of glycerol with acid catalysts or dehydration of glycerol solution to acrolein [74-77] and further oxidation with an oxide catalyst into acrylic acid [77, 78]. Acrylic acid is an unsaturated carboxylic compound with the formula $CH_2=CHCOOH$. Acrylic acid and its esters readily combine with themselves to form polyacrylic acid or other monomers e.g. acrylamides, acrylonitrile, vinyl, styrene, and butadiene by reacting at their double bond, forming homopolymers or copolymers which are used in the manufacture of various plastics, coatings, adhesives, elastomers, as well as floor polishes, and paints.
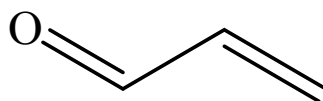
Figure 2.11. Chemical formula of acrolein.

Catalytic dehydration of glycerol to acrolein has the potential to valorize the oversupply of crude glycerol resulting from biodiesel production. This reaction requires catalysts with appropriate acidity including zeolites, heteropolyacids, mixed metal oxides and (oxo)-pyrophosphates. Glycerol conversion and acrolein selectivity depended on the total acidity and on the textural properties. The glycerol dehydration in the gas phase has been catalyzed by sulfated zirconia for high-temperature acid-catalysed reactions, it was found that the reaction parameters affected glycerol conversion and selectivity to acrolein [1]. The Al_2O_3 and TiO_2 supports modified by impregnation with PO_4-ions and SAPO-11 and SAPO-34 samples were acid-catalysts. The mesoporous Al_2O_3–PO_4 and TiO_2–PO_4 catalysts with large pores exhibited high activity but limited selectivity towards acrolein and the SAPO samples with small micropores showed less activity but high selectivity at low reaction times in the presence of water [2]. Dehydration of glycerol solution and further oxidation of glycerol or oxydehydration was studied with mixed oxide catalysts. Iron phosphate catalysts ($FePO_4$), weak solid acid, were active and selective to obtain acrolein. The yield in acrolein or stability was obtained with 100% conversion of glycerol and 92% selectivity in acrolein. However, their deactivation by

coking remains the main obstacle in the way of large-scale industrial applications, the catalyst was deactivated after 25 h. Distribution of products changes during the deactivation of the catalyst, leading to by-products such as acetol, propanal and coke deposited on the surface of the catalyst. Use of oxygen in the feed could decrease the amount of carbon deposit and hydroxyacetone, but oxidation products appeared such as acetic acid or Co_x. The $FePO_4$ catalysts could not oxidize acrolein in acrylic acid. Molybdenum (tungsten) vanadium based catalysts showed interesting results in the one-step oxydehydration of glycerol, leading to the highest yield (28.4%) in acrylic acid obtained. However, yields in acetic acid were always high (23%) and deactivation was unfortunately also observed. New tungsten vanadium catalyst was hydrothermally synthesised and produced less by-products [2].

i. 1,2-Propanediol

Propylene glycol, also called 1,2-propanediol (1,2-PDO) or propane-1,2-diol, is an organic compound with formula $C_3H_8O_2$ or $HO-CH_2-CHOH-CH_3$ as shown in Figure 2.12. It is a colorless, nearly odorless, clear, viscous liquid with a faintly sweet taste, hygroscopic and miscible with water, acetone, and chloroform. The compound is sometimes called α-propylene glycol to distinguish it from the isomer: propane-1,3-diol $HO-(CH_2)_3-OH$, or β-propylene glycol.
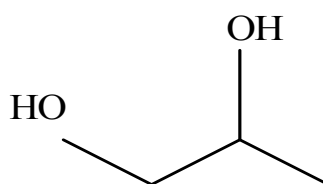
Figure 2.12. Chemical formula of 1,2-PDO.

The common method used to convert glycerol to 1,2-PDO is the hydrogenolysis reaction in the presence of metal-based catalytics [7-10, 12-13, 16-17]. It is widely used as a component in newer automotive antifreezes and de-icers used at airports. Like ethylene glycol, the freezing point of water is depressed when

mixed with 1,2-PDO owing to the effects of dissolution of a solute in a solvent (freezing-point depression); glycols are good for this purpose as they are cheap, non-corrosive and have very low volatity. About 45 % of 1,2-PDO produced is used as chemical feedstock for the production of unsaturated polyester resins. In this regard, 1,2-PDO reacts with a mixture of unsaturated maleic anhydride and isophthalic acid to give a copolymer. This partially unsaturated polymer undergoes further crosslinking to yield thermoset plastics. Related to this application, 1,2-PDO reacts with propylene oxide to give oligomers and polymers that are used to produce polyurethanes.

1,2-PDO is considered Generally Recognized As Safe (GRAS) by the U.S. Food and Drug Administration (FDA), and it is used as an humectant (E1520), solvent, and preservative in food and for tobacco products, as well as being the major ingredient in the liquid used in electronic cigarettes (along with vegetable glycerine and, more rarely, PEG 400). It is also used in pharmaceutical and personal care products. 1,2-PDO is a solvent in many pharmaceuticals, including oral, injectable and topical formulations, such as for diazepam and lorazepam that are insoluble in water, use 1,2-PDO as a solvent in their clinical, injectable forms.

j. 1,3-Propanediol

1,3-Propanediol (1,3-PDO) is the organic compound with the formula $HO-(CH_2)_3-OH$ as shown in Figure 2.13. This three-carbon diol is a colorless viscous liquid that is miscible in water. 1,3-PDO may be chemically synthesized by the hydration of acrolein, or by the hydroformylation of ethylene oxide to 3-hydroxypropionaldehyde, which consequently hydrogenated to 1,3-PDO.
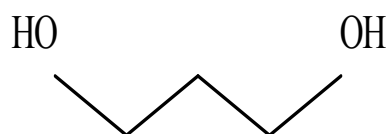
Figure 2.13. Chemical formula of 1,3-PDO.

1,3-PDO can be formulated into a variety of industrial products including composites, adhesives, laminates, powder and UV-cured coatings, moldings, novel aliphatic polyesters, co-polyesters. It is also a solvent and used as an antifreeze and in wood paint. Propanediol-based polymers exhibit better properties than those produced from 1,2-PDO, butanediol or ethylene glycol. Nevertheless, the production is limited due to its high production cost, which restrict the commercial use. Thus, the production of 1,3-PDO from glycerol by the hydrogenolysis reaction [6-7, 9, 11-12, 15-17] and fermentation method [59, 60] have more attractive interest.

2.5 Glycerol conversion to product distribution.

Various previous works have focused on transforming crude glycerol into more valuable chemicals since it is a molecule rich in functionalities with three -OH groups, especially the glycerol conversion to propanediol both 1,2-PDO and 1,3-PDO, and an important intermediate for chemical industry as acrolein has appeared as one of the important processes because of the numerous growth of biodiesel industries.

a. Biological process

The common method that can be converted glycerol to 1,3-PDO is the fermentation method using bacteria. The production of 1,3-PDO by fermentation takes place in a two-step enzymatic reaction sequence. The first step is the conversion of glycerol to 3-hydroxypropionaldehyde (3-HPA) and water by a glycerol dehydratase catalyzes. The second step is the reduction of 3-HPA to 1,3-PDO by a NADH dependent 1,3-PDO dehydrogenase. The 1,3-PDO is not metabolized further and accumulates in the media. Thus, the selective sorbents such as activated carbons and zeolites have been proposed for 1,3-PDO separation [42]. However, the fermentation process provided low productivity, long fermentation time and short life span of bacterial strains. Another method is the hydrogenolysis reaction in the presence of catalytic, which is widely used in the converting glycerol into propanediols [6-13, 15-17, 79-90].

b. Hydrogenolysis

Theoretically, the hydrogenolysis reaction is consisted of the two elementary reactions: dehydration and hydrogenation. This reaction requires catalysts for both dehydration and hydrogenation simultaneously, known as the bifunctional catalysts. The hydrogenolysis of glycerol in the presence of a catalyst and hydrogen produces several products such as 1,2-PDO, 1,3-PDO, ethylene glycol and acrolein, which are an important chemical for various industries. The 1,2-PDO is used for the manufacture of polyester resins, pharmaceuticals, liquid detergents, cosmetics, paints, animal feed, antifreeze, flavours and fragrances, etc. Nowadays, it is produced by the hydration of propylene oxide derived from propylene. The 1,3-PDO is used in polyester, fibbers, films and coatings. Ethylene glycol is used for the production of synthetic fibbers and explosives. Acrolein is used to produce acrylic acid esters, methionins, fragrances, polymers and detergents. Thus, there is an increasing interest for developing new processes for the synthesis of various products by the use of raw materials as glycerol.

Hydrogenolysis is a chemical reaction whereby a carbon-carbon or carbon-heteroatom single bond is cleaved or undergoes "lysis" by hydrogen. The heteroatom may vary, but it usually is oxygen, nitrogen, or sulfur. A related reaction is hydrogenation, where hydrogen is added to the molecule, without cleaving bonds. Usually hydrogenolysis is conducted catalytically using hydrogen gas. For the common mechanism of glycerol hydrogenolysis to propanediols, preliminary reactions were conducted in two steps. First step, hydroxyacetone (acetol), 3-hydroxypropanal and acrolein are formed by dehydration of a glycerol molecule and are possibly an intermediate of an alternative path for forming propanediol. Then, acetol, 3-hydroxypropanal and acrolein are further reacted with hydrogen to form propanediol by catalytic hydrogenation with a mol of water as by-product. The hydrogenolysis mechanism is shown in Figure 2.14.
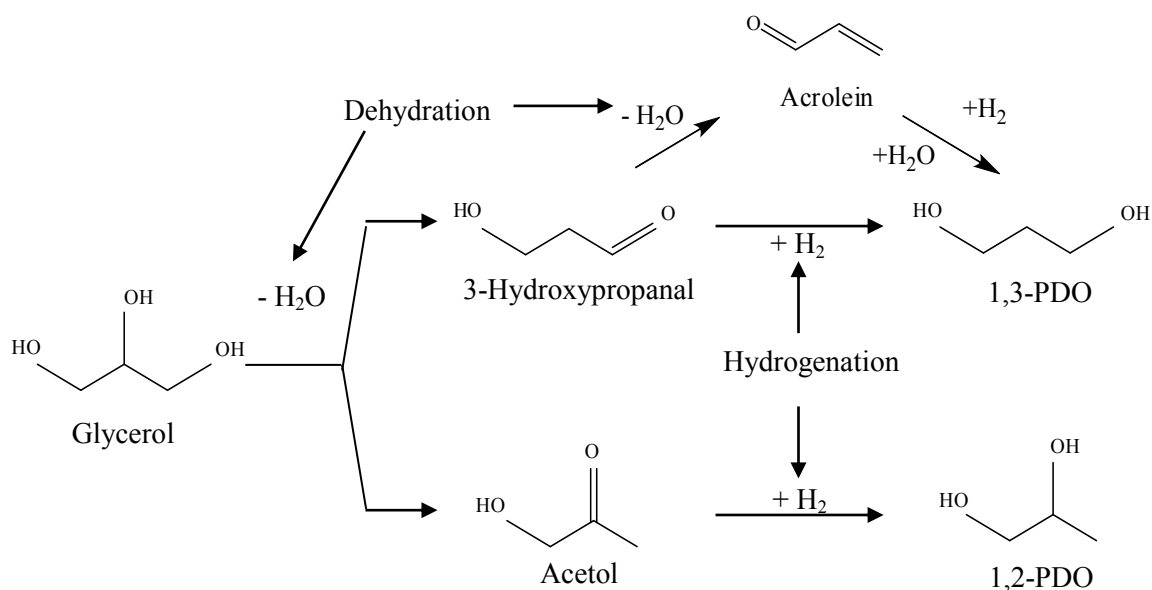
Figure 2.14. Hydrogenolysis of glycerol to 1,2-PDO and 1,3-PDO [89].

Two types of catalysts have previously been reported for glycerol hydrogenolysis. The first are transition metal oxides, such as Raney-nickel, copper chromite or copper-zinc oxide catalysts, etc. The second are the supported noble metal catalysts, such as platinum (Pt), ruthenium (Ru), palladium (Pd) and iridium (Ir). The parameters such as type of catalysts, loading of metal, initial glycerol concentration, reaction temperature, reaction time and reaction pressure, etc., affected the glycerol hydrogenolysis. However, due to the high cost of noble catalysts, cheaper catalysts are required to enhance the sustainability and economics of glycerol hydrogenolysis. From the volcano plot as shown in Figure 2.15 [91], the trend in activity of Co is at a fixed set of these catalysts, whilst Co is quite promising as a catalyst for oxidation–reduction reaction (ORR) processes. Several studies have shown that supported Co catalysts (mainly supported on aluminosilicates) displayed a high activity for the selective catalytic hydrogenation of alkenes, aldehydes and ketenes. Co is a non-noble metal which is widely used with a variety of metal oxide supports. Co-based catalyst was found to provide the similar activity to noble metal catalysts in the C-C bond cleavage, even at low operating temperatures [92-94]. Llorca et al. [92] conducted ethanol steam reforming process at 673 K by varying different transition metal

catalysts supported on γ-Al_2O_3. It was found that the reaction selectivity increased in the order of Co >> Ni > Rh > Pt, Ru, Cu. Therefore, Co is one of the promising candidate metal-based catalysts for glycerol hydrogenolysis.
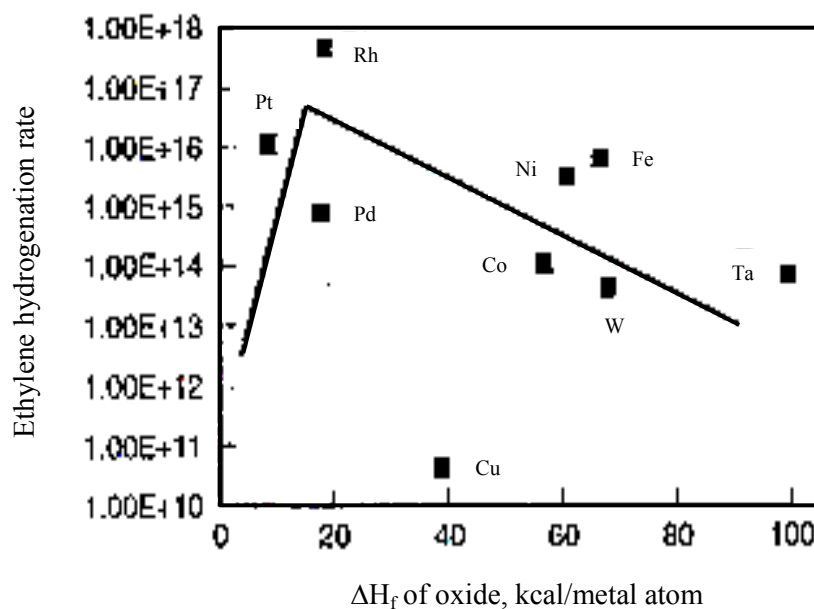
Figure 2.15. A volcano plot for the variations in the rate of ethylene hydrogenation over a subset of the transition metals [91].

It is clear that glycerol can be used as raw material for the synthesis of value-added chemicals. Table 2.4 summarizes the main processes that used glycerol as raw material to produce value-added chemicals.

Table 2.4. Main processes that use glycerol as raw material

Process	Catalysts	Main product	References
Pyrolysis	-	H_2, syngas	[50, 53]
	Carbonaceous catalysts	Syngas	[51]
	-	Bio oil	[52]
Gasification	Ru/ZrO_2	Acetic acid , acetaldehyde	[54]
	NaOH, Na_2CO_3, KOH, K_2CO_3	H_2	[55]
	Olivine, Ni/olivin	Syngas	[56]
	-	Syngas	[57]
Dehydration	Sulfated zirconia	Acrolein	[1]
	$FePO_4$, Mo, V	Acrolein, acrylic acid	[2]
	Al_2O_3–PO_4, TiO_2–PO_4, SAPO-11, SAPO-34	Acrolein, 1-hydroxyacetone, 3-HPA	[3]
Oxidation	Au nanoparticles on carbon nanotubes	DHA	[62]
	Au/AC, Au/G, Au/CNF-R	Glyceric acid	[63]
	Au/C, Pt/MWNTs	DHA, glyceric acid	[65, 66]
Biological process	*Klebsiella* sp. HE1	H_2, ethanol, diols	[58]
	Klebsiella oxytoca	1,3-PDO, 2,3-BDO, ethanol	[59]
	Gluconobacter oxydans	DHA	[64]
	Actinobacillus succinogenes	Succinic acid	[70]
	Zirconia supported heteropolyacids	Bioadditives	[95]
Esterification and transesterification	niobium	Polyglycerol	[96]
Acetylation	Amberlyst-15	Diacetin, triacetin	[97]
	Sulfonic modified catalysts	Ethyl ether	[98]
Etherification	Hydrotalcite catalyst, MgAl mixed oxides	Polyglycerols	[67, 68]

Process	Catalysts	Main product	References
Hydrogenolysis	Pt/WO$_3$/ZrO$_2$, Ir‑ReO$_x$/SiO$_2$, Ru/TiO$_2$ Pt/H$_4$SiW$_{12}$O$_{40}$ (HSiW), Pt/H$_3$PW$_{12}$O$_{40}$ (HPW), Pt/H$_3$PMo$_{12}$O$_{40}$ (HPMo), Pt/WO$_3$	1,3-PDO	[6, 11, 79, 82, 85, 87]
	Ni, Pd, Pt, Cu, copper-chromite, Co/MgO, Ru/Al$_2$O$_3$ + Pt/Al$_2$O$_3$, Ru/TiO$_2$, bentinite/TiO$_2$, Ru-CaZnMg/Al, Ni‑Cu/Al$_2$O$_3$, Cu/SiO$_2$	1,2-PDO	[8, 13, 81, 86, 88, 89, 90]
	Ru/C, Amberlyst 15, Ru/Al$_2$O$_3$, Ru/C, Ru/ZrO$_2$, Cu/Al$_2$O$_3$, Ru: Polyoxometalate	Propanediol	[7, 9, 17, 83, 99]

2.6 Literature reviews

Kurosaka et al. [6] investigated the hydrogenolysis of glycerol by Pt/WO$_3$/ZrO$_2$ catalyst to give 1,3-PDO in the yields up to 24%. The catalytic activities and the selectivity toward 1,3-PDO were effected by the type of support, noble metal loading and the preparation of impregnation method. Controlled experiments showed that the active site of catalyst for the formation of 1,3-PDO may be the Pt over WO$_3$ supported on ZrO$_2$.

Kusunoki et al. [7] reported that the combination of active carbon supported Ru catalyst with a cation exchange resin (Amberlyst 15) exhibited much higher activity in glycerol hydrogenolysis under mild reaction conditions (393 K, 4 MPa H$_2$) than the other metal–acid bifunctional catalyst systems using various zeolites, sulfated zirconia, H$_2$WO$_4$, and liquid H$_2$SO$_4$.

Dasari et al. [8] attempted to develop the glycerol hydrogenolysis at lower temperatures and pressures in order to achieve a high selectivity towards propylene glycol. The hydrogenolysis of glycerol to propylene glycol was performed using Ni, Pd, Pt, Cu and copper-chromite catalysts in the presence of concentrated glycerol. Effects of temperature, H_2-pressure, initial water content, choice of catalyst, catalyst reduction temperature, and the amount of catalyst were evaluated. At temperatures above 200^oC and H_2-pressure of 200 psi, the selectivity to propylene glycol decreased as the increase of temperature due to excessive hydrogenolysis of the propylene glycol. At $200\ ^oC$ and 200 psi, high selectivity to propylene glycol and good glycerol conversion was obtained. The yield of propylene glycol increased with decreasing water content. A new reaction pathway for converting glycerol to propylene glycol via an intermediate was validated by isolating the acetol intermediate.

Ma et al. [9] applied the Ru/Al_2O_3, Ru/C and Ru/ZrO_2 catalysts to the hydrogenolysis of glycerol to propanediol, and examined the effect of Re as an additive on the catalytic performance of Ru catalysts. The glycerol hydrogenolysis was carried out under the conditions of $120–180\ ^oC$, 4–10 MPa H_2-pressure and 4–8 h using 40 wt.% glycerol aqueous solution. The glycerol conversion increased from 18.7% to 29.7% over Ru/Al_2O_3, Ru/C and Ru/ZrO_2 catalysts but the activity and selectivity to propanediol were low when only Ru catalysts was used in the reaction systems. The reaction results indicate that Re possesses high promoting effect on the catalytic performance of Ru catalysts in glycerol hydrogenolysis. The appropriate reaction conditions of the glycerol hydrogenolysis over $Ru/Al_2O_3+Re_2(CO)_{10}$ catalyst were $160\ ^oC$, 8.0 MPa H_2-pressure and 8 h.

Balaraju et al. [10] investigated the influence of acidity of the catalysts on glycerol conversion and selectivity to propylene glycol at different reaction parameters. The reaction was carried out over Ru/C catalysts using different solid acids as co-catalysts, such as niobia, 12-tungstophosphoric acid supported on zirconia (TPA/ZrO_2), cesium salt of TPA (CsTPA) and cesium salt of TPA supported on ZrO_2 (Cs/TPA ZrO_2). For the results, it was found that an increase of Ru/C and solid acid quantity led to a substantial increase in both glycerol conversion and selectivity to propylene glycol. A synergistic effect was observed between solid acid and Ru/C catalyst toward the glycerol conversion and selectivity to 1,2-PDO. The glycerol

conversion and selectivity to 1,2-PDO were also depended on the reaction temperature, H_2-pressure, reaction time and glycerol concentration.

Nakagawa et al. [11] used the rhenium-oxide (ReO_x)-modified supported iridium nanoparticles on silica to catalyze the direct glycerol hydrogenolysis to 1,3-PDO in an aqueous media. The selectivity and yield of 1,3-PDO at an initial stage reached 67 % and 38% at 81 % glycerol conversion. The characterization of catalyst and the reactivity of alcohols suggested that the 1,3-PDO was produced by the attack of active hydrogen species on iridium metal to 1-glyceride species formed on the oxidized rhenium cluster. That is, glycerol was adsorbed on the surface of ReO_x cluster at the terminal position to form 2,3-dihydroxypropoxide. The larger formation constants of metal alkoxides of primary alcohols than that of secondary alcohols have been reported for niobium- or vanadium-containing tungsten oxide clusters and explained by the steric crowding between the cluster framework and the groups bonded with the C-OH carbon of secondary alcohols. Then, hydrogen activated on the Ir metal attacked the 2-position of the 2,3-dihydroxypropoxide to produce 3-hydroxypropoxide which was consequently hydrolyzed to 1,3-PDO.

Chaminand et al. [12] studied the glycerol hydrogenolysis on heterogeneous catalysts at 180 ^{o}C under 80 bar H_2-pressure in order to minimize the carbon-carbon bond rupture and to improve the rate and the selectivity towards 1,2- and 1,3-PDO. The investigated parameters were types of catalyst (Cu, Pd and Rh), types of support (ZnO, C, Al_2O_3), types of solvent (water, sulfolane, dioxane) and additive as tungstic acid (H_2WO_4). The best selectivity (100%) to 1,2-PDO was obtained by hydrogenolysis of water solution of glycerol in the presence of CuO/ZnO catalysts. To improve the selectivity to 1,3-PDO, the reaction was conducted with Rh catalysts with H_2WO_4 added to the reaction medium. The best result in terms of conversion and selectivity to 1,3-PDO (1,3-PDO/1,2-PDO = 2) was obtained by operating in sulfolane. The presence of iron (Fe) dissolved in the reaction medium was also beneficial for the selectivity to 1,3-PDO.

Guo et al. [13] studied the effect of interaction between solid catalyst (Co) and its support (MgO) on the selectivity to propanediols by glycerol hydrogenolysis. The interaction between cobalt species and MgO was adjusted by varying the temperature of calcination. Higher temperature treatment cannot enhance the interaction between

Co_3O_4 and MgO and it promoted the formation of $MgCo_2O_4$ spinel and Mg-Co-O solid solution. Although the reducibility of cobalt oxides was greatly decreased in the Co_3O_4/MgO precursor, this strong interaction prevented the aggregation of Co particles in the resulting Co/MgO catalyst under the harsh reaction conditions, giving a much higher activity and stability. MgO was hydrated to $Mg(OH)_2$ during the reaction and the sizes of $Mg(OH)_2$ and Co particles increased considerably, especially during the initial stage of the reaction. With regards the influence of reaction temperature, H_2-pressure and glycerol concentration on the production of 1,2-PDO, they reported that higher reaction temperature favored the conversion of glycerol but lowered the selectivity of 1,2-PDO due to the formation of significant amounts of lower alcohols and hydrocarbons. On the other hand, both glycerol conversion and selectivity to 1,2-PDO increased gradually with increasing the hydrogen pressure. The glycerol conversion decreased with increasing the glycerol concentration in the reaction media, but the selectivity to 1,2-PDO was almost unchanged, implying that the glycerol conversion was simply associated with the number of active sites.

Guo et al. [17] synthesized supported Cu catalysts and applied to convert glycerol to value-added propanediols. Among all utilized catalysts, the γ-Al_2O_3 supported Cu catalysts showed superior performance. Unlike most supported precious metal catalysts, the scission of C–C bonds was successfully suppressed on the Cu/Al_2O_3 catalysts without a lose of glycerol conversion. The experimental results combined with the characterization studies using TPD and XRD techniques revealed that the optimal Cu loading was 2.7 mmol of Cu metal/g of γ-Al_2O_3 and that the suitable pre-reduction temperature was 300 °C. The Cu/Al_2O_3 catalyst with the optimized amount of Cu showed the selectivity to propanediols about 96.8% with a glycerol conversion about 49.6% under mild reaction conditions (220 °C, 1.5 MPa initial H_2-pressure, 10 h, Cu to glycerol molar ratio 3:100). Compared with a commonly used commercial copper chromite catalyst, the Cu/Al_2O_3 presented much higher activity, selectivity, Cu usage efficiency and non-toxicity.

Besson et al. [79] designed active and long-term stable catalysts for the hydrogenation reaction conducted in a continuous fixed-bed reactor. A Ru-based catalyst was chosen for its stability in aqueous reaction medium compared to Ni and for its high hydrogenation activity for carbonyl compounds. The oxide supports were

SiO_2 and TiO_2. The catalytic hydrogenation of aqueous solutions of 3-hydroxypropanal (3-HPA) to 1,3-PDO was conducted at 40–60 ^{o}C and 40 bar hydrogen with heterogeneous Ru catalysts in a trickle-bed reactor. Catalysts were optimized to obtain stable activity and selectivity as a function of time on stream. Catalyst deactivation was attributed to the deposit of heavy organic impurities on the catalyst surface, blocking the reactant access to the active Ru particles. The pore structure of the catalyst had a significant influence on the catalytic results. The most stable catalysts were supported on low surface area macroporous titania (rutile, ca. 1 m^2/g), whereas mesoporous TiO_2, and particularly microporous SiO_2 supports deactivated because of surface blockage by organic impurities.

Roy et al. [81] demonstrated that the admixture catalyst, 5 wt.% Ru/Al_2O_3 and 5 wt.% Pt/Al_2O_3 catalysts, outperformed the individual catalysts with respect to 1,2-PDO selectivity and yield under without added hydrogen condition. The hydrogen generated in-situ by aqueous phase reforming of glycerol was used for the conversion of glycerol to 1,2-PDO and other products. The hydrogenolysis reaction may thus be carried out at moderate inert gas pressure and without a need for external hydrogen addition. During 6 h batch runs, it was observed that the 1:1 admixture (w/w) of the Ru and Pt catalysts showed better performance at 493 K [glycerol conversion (X) = 50.1%, 1,2-PDO selectivity (S) = 47.2%] compared to the individual catalysts [X = 19.3%, S = 50% with 5 wt.% Ru/Al_2O_3; X = 18.1%, S = 37% with 5 wt.% Pt/Al_2O_3]. A run for glycerol hydrogenolysis with the admixture catalyst in the presence of added hydrogen (41 bar), at otherwise identical operating conditions, showed lower selectivity to 1,2-PDO (31.9%) compared to the run without added hydrogen (47.2%). With external hydrogen addition, the availability of excess hydrogen (in addition to the in situ hydrogen generation) promotes the transformation of CO and CO_2 to methane and other alkanes, adversely affecting the 1,2-PDO selectivity. Finally, the admixture catalyst showed excellent stability as evidenced by several repeatable runs with the recycled catalyst.

Gong et al. [82] loaded metal–acid bi-functional catalyst $Pt/WO_3/TiO_2$ on SiO_2 for glycerol hydrogenolysis. They demonstrated that glycerol can be more effectively and selectively converted to 1,3-PDO in water medium than the $Pt/WO_3/TiO_2$ catalyst in a slurry batch reactor. The existence of TiO_2 species improves the dispersion of Pt

metal in the metal–acid bi-functional $Pt/WO_3/TiO_2/SiO_2$ catalyst based on the results from XRD, TEM characterization. NH_3-TPD and IR results showed that WO_3 species regulated the acidity of the $Pt/WO_3/TiO_2/SiO_2$ catalyst by producing Brønsted acid sites, which played a key role during 1,3-PDO formation. The nature of the solvent also showed distinct influence on glycerol conversion; water was more suitable than ethanol, sulfane and NMI for using as solvent of the reaction.

Ma and He [83] prepared bimetallic $Ru–Re/SiO_2$ and monometallic Ru/SiO_2 catalysts by impregnation method for glycerol hydrogenolysis to propanediols (1,2-PDO and 1,3-PDO) with a batch type reactor (autoclave). Bimetallic $Ru–Re/SiO_2$ showed higher activity (51.7% conversion) than monometallic Ru/SiO_2 catalyst (16.8% conversion) in the glycerol hydrogenolysis under the reaction conditions of 160 ^{o}C, 8.0 MPa and 8 h. Re/SiO_2 alone had almost no activity (1.7% conversion), but adding Re component into Ru/SiO_2 could obviously promote the activity of the catalysts. The different pretreatment of the catalyst precursors had great influence on the catalytic performance of both $Ru–Re/SiO_2$ and Ru/SiO_2 catalysts. High pre-reduction temperature (450 ^{o}C) in H_2 flow accelerated the aggregation of particles and decreased the dispersion of metal components on SiO_2, which in turn decreased the catalytic performance of $Ru–Re/SiO_2$ and Ru/SiO_2. It is suggested that Ru species might be in Ru^0 metal state, while Re species might mostly be in rhenium oxide state during the hydrogenolysis of glycerol. Low temperature reduction (<300 ^{o}C) or in-situ reduction could prevent the over-reduction of Ru species and the growth of Ru^0 particles, and would be favor the interaction of rhenium oxide and ruthenium metal.

Hamzah et al. [84] used a combination of bentonite-TiO_2 as a support material of Ru catalyst to improve the conversion and selectivity to 1,2-PDO for glycerol hydrogenolysis under a mild reaction condition. A series of bentonite, TiO_2, SiO_2 and Al_2O_3 supported Ru catalyst were tested in glycerol hydrogenolysis reaction and were found that the order of glycerol conversion as follow: Ru/SiO_2 < Ru/TiO_2 ≈ Ru/Al_2O_3 < Ru/bentonite. In particular, the reaction of Ru/bentonite catalyst gave the highest glycerol conversion (62.8%) of 20 wt.% glycerol concentration with 80.1% selectivity to 1,2-pronediol at 150 ^{o}C, 20–30 bar H_2-pressure for 7 h. The reaction of Ru/TiO_2 catalyst gave the highest selectivity (83.7%) for glycerol hydrogenolysis to 1,2-PDO but glycerol conversion was low as 38.8%. The combination of support materials

between bentonite and TiO_2 at 1:2 ratio provided a good dispersion of nano size Ru particles which could contribute to high activity of Ru/TiO_2 catalyst for glycerol hydrogenolysis. The glycerol conversion of $Ru/bentonite-TiO_2$ catalyst increased in 80% from 38.8% to 69.8% under the same optimum condition for Ru/TiO2 while maintained 80.6% selectivity to 1,2-PDO. $TPD-NH_3$ analysis found that mixed support could increase catalyst acidity which indicated that the acidity of support played a very important role in the activity of the catalyst.

Zhu et al. [85] investigated several zirconia supported bi-functional catalysts containing Pt and heteropolyacids using $H_4SiW_{12}O_{40}$ (HSiW), $H_3PW_{12}O_{40}$ (HPW) and $H_3PMo_{12}O_{40}$ (HPMo) as active compounds for glycerol hydrogenolysis and also compared with Pt/ZrO_2. It was found that the heteropolyacids modified Pt/ZrO_2 catalysts ($Pt-HPW/ZrO_2$, $Pt-HPMo/ZrO_2$, and $Pt-HSiW/ZrO_2$) showed higher acidity and better catalytic performance of glycerol hydrogenolysis to 1,3-PDO, which was probably related to the high Brønsted acid sites and good thermal stability. In particular, the concentration of Brønsted acid sites was a key to the selective formation of 1,3-PDO, whereas the concentration of Lewis acid sites was related to the formation of 1,2-PDO.

Vasiliadue et al. [88] prepared the highly dispersed copper catalysts on silica gel, SBA and SBA by a simple impregnation and drying preparation method. By varying the calcination conditions, the calcination in stagnant air, in a flow of NO/N_2 or a flow of air gave the Cu catalysts with large crystals, small monodisperse crystallites or a highly dispersed XRD amorphous copper phase, respectively. The different dispersion characteristics for the selective glycerol hydrogenolysis showed different activities (20–50% glycerol conversion), while all the catalysts provided highly selective towards propylene glycol (92–97%) with no any activity in C-C bond cleavage for the formation of ethylene glycol and gaseous degradation products under the condition of 240 °C, 8 MPa H_2-pressure and 5 h reaction time. It was shown that the presence of a solvent greatly influences the intrinsic reaction rate and the nature of structure sensitivity. The deactivation behaviour of all catalysts was studied, the air-calcined catalysts were more deactivation resistant than the NO/N_2 samples. The Cu catalyst supported on SBA-15 calcined at 900 °C (Cu/SBA900C (air)) proved to be the most stable catalyst with negligible deactivation after three reaction cycles.

Lee and Moon [90] investigated the effects of support in Ru-supported catalyst on the glycerol conversion and selectivity to 1,2-PDO in the glycerol hydrogenolysis. The Ca and Zn modified Ru-based hydrotalcite-like catalyst (Ru–CaZnMg/Al) prepared by solid phase crystallization and impregnation methods showed higher catalytic activity and selectivity to 1,2-PDO than the other catalysts under the condition of glycerol hydrogenolysis at 453 K, 2.5 MPa initial H_2-pressure and 20 wt.% glycerol aqueous solution for 18 h. The glycerol conversion and selectivity to 1,2-PDO were obtained about 50% and 85%, respectively. The Ru supported hydrotalcite-based catalysts were showed higher acidity and Ru dispersion than Ru/γ-Al_2O_3 catalyst. It was found that the glycerol conversion and the selectivity to 1,2-PDO in glycerol hydrogenolysis were mainly corresponded to Ru dispersion and the acidity of the catalyst. The results can be interpreted that the acidity of the catalyst plays an important role in improving selectivity to 1,2-PDO and Ru dispersion might be associated with activity, respectively.

Ferrari et al. [100] investigated the influence of the impregnation order of molybdenum (Mo) and cobalt (Co) in carbon-supported catalysts for hydrodeoxygenation reactions of a model compound solution selected on the basis of an in-depth chemical characterization of bio-oils. Four activated carbons were used as supports and the effect of the impregnation order (either Co or Mo first) was considered and tested in hydrodeoxygenation reactions. Both series of samples exhibited a preferential impregnation of the metal oxides at the exterior of the carbon grains, but CoMo (Mo first) was more uniformly distributed than MoCo (Co first). When Mo was added after Co (MoCo), the Mo-Co interactions cause a thick layer of metal oxide crystals to be formed; it covered the external grain surface and it was only in partial physical contact with the carrier. When Co was added after Mo (CoMo), it seemed to bring about the remobilization and migration of Mo to the external part of the grains. Finally, it was shown that inorganic impurities, like calcium (Ca) and iron (Fe), which were presented in low amounts in the activated carbon, can interact with Mo and form mixed oxides. Concerning the catalytic activity, MoCo catalysts showed lower hydrogenation properties for the conversion of ketonic groups and lower decarboxylation selectivity in the conversion of the ester.

CHAPTER III
RESEARCH METHODOLOGY

This chapter shows the research methodology for the glycerol hydrogenolysis over supported Co-based catalysts in an aqueous phase. The catalyst preparation and the activity test for glycerol hydrogenolysis were described. Also, the instruments used to analyze the samples and characterize the characteristic of catalysts were presented here.

3.1 Chemical substances

All the chemical substances used in this study were prepared from the following reagents:

- Acetone (C_3H_6O) ($\geq$ 99.5% purity, Sigma-Aldrich)
- Ammonium molybdate tetrahydrate ($(NH_4)_6 \cdot Mo_7O_{24} \cdot 4H_2O$) (81.4% purity, Mallinckrodt Chemicals)
- Aluminum nitrate nonahydrate ($Al(NO_3)_3 \cdot 9H_2O$) (98.0% purity, Ajex Finechem)
- Aluminum Oxide (γ-Al_2O_3) (Sumitomo Chemical Co., Ltd.)
- Cobalt Chloride hexahydrate ($CoCl_2 \cdot 6H_2O$) (98.0% purity, Carlo Erba reagent)
- Ethanol (C_2H_5OH) (99.9% purity, Merck)
- Ethylene glycol ($C_2H_6O_2$) (99.5% purity, Fisher Scientific)
- Glycerol ($C_3H_8O_3$) (100% purity, Fisher Scientific)
- Hydrogen gas (H_2) (99.99% purity, Praxair (Thailand) Company, Ltd.)
- HZSM-5 zeolite (SiO_2/Al_2O_3=25, Zibo Xinhong Chemical Trade Co., Ltd.)
- Methanol (CH_3OH) (HPLC grade, Fisher Scientific)
- Mobile Crystalline Material 41 (MCM-41) [79-81]
- Sulphuric acid (H_2SO_4) (98% purity, Mallinckrodt Chemicals)
- 1,2-Propanediol ($C_3H_8O_2$) (98.0% purity, Fluka)
- 1,3-Propanediol ($C_3H_8O_2$) (99.0% purity, Fluka)

3.2 Experimental

    3.2.1 Synthesis of AlMCM-41[101]

The AlMCM-41 with $SiO_2/Al_2O_3 = 25$ was prepared by the following steps as summarized in Figure 3.1.

1. 0.50 g of MCM-41 powders was dried at 105 ^{o}C in hot air oven overnight.
2. 0.225 g of $Al(NO_3)_3 \cdot 9H_2O$ was dissolved in 50 ml ethanol, followed by stirring until a clear solution was obtained.
3. The dried MCM-41 powder (1st step) was mixed with the solution obtained from 2nd step and stirred for 30 min.
4. The mixture was filtered and dried at 105 ^{o}C in hot air oven overnight.
5. Finally, the product was calcined at 300 ^{o}C in air for 2 h.

Dried MCM-41 powders at 105 ^{o}C in hot air oven overnight	+	Dissolved $Al(NO_3)_3 \cdot 9H_2O$ in 50 ml ethanol and stirred until clear

↓

Stirred the mixture solution for 30 min

↓

Filtered and dried at 105 ^{o}C in hot air oven overnight

↓

Calcined at 300 ^{o}C in air for 2 h

↓

AlMCM-41
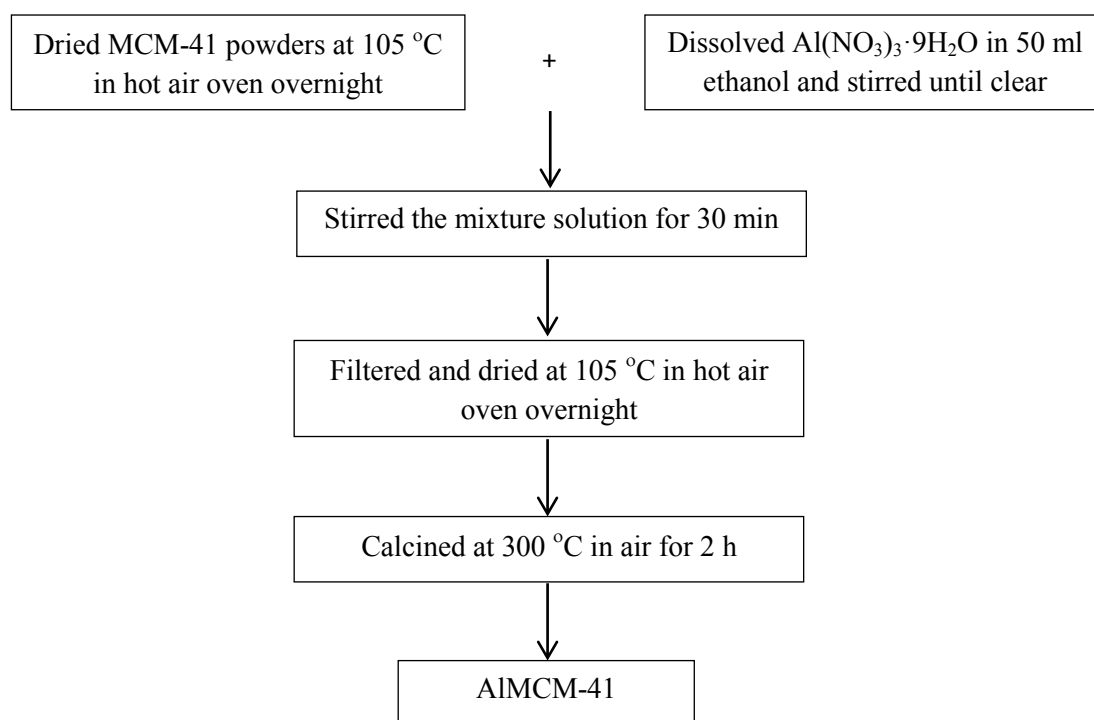
Figure 3.1 Schematic diagram of the synthesis of AlMCM-41.

3.2.2 Catalysts preparation

Supported Co, Mo and CoMo catalysts were prepared by incipient wetness impregnation method on the three different types of support including γ-Al_2O_3, HZSM-5, denoted as Al_2O_3 and HZSM5, respectively, and an as-prepared AlMCM-41. These catalysts were prepared by the following steps as shown in Figures 3.2 and 3.3 for single and bimetallic catalysts, respectively.

3.2.2.1 Preparation of Co/Al$_2$O$_3$ and Mo/Al$_2$O$_3$ catalyst

1. 1.00 g of Al_2O_3 powders was dried at 105 ^{o}C in hot air oven overnight.
2. 4.034 g of $CoCl_2 \cdot 6H_2O$ was dissolved in 10.00 ml de-ionized water.
3. 0.50 ml of the solution obtained from the 2nd step was dropped slowly on the dried Al_2O_3 support (1st step).
4. The obtained product was dried at 105 ^{o}C in hot air oven overnight.
5. Finally, this catalyst was calcined at 400 ^{o}C in air for 2 h [102] and the ready-to-use 5 wt.% Co/Al$_2$O$_3$ catalyst was obtained.
6. For Mo/Al$_2$O$_3$ catalyst, all above steps were repeated, except for the 2nd step. 12.875 g of $(NH_4)_6 \cdot Mo_7O_{24} \cdot 4H_2O$ was dissolved in 10.00 ml de-ionized water instead of $CoCl_2 \cdot 6H_2O$ and the ready-to-use 5 wt.% Mo/Al$_2$O$_3$ catalyst was obtained.

3.2.2.2 Preparation of Co/HZSM5 and Mo/HZSM5 catalyst

1. 1.00 g of HZSM5 powders was dried at 105 ^{o}C in hot air oven overnight.
2. 1.008 g of $CoCl_2 \cdot 6H_2O$ was dissolved in 10.00 ml de-ionized water.
3. 1.00 ml of the solution obtained from the 2nd step was dropped slowly on the dried HZSM5 support (1st step).
4. The obtained product was dried at 105 ^{o}C in hot air oven overnight.
5. Finally, this catalyst was calcined at 400 ^{o}C in air for 2 h [102] and the ready-to-use 2.5wt.% Co/HZSM5 catalyst was obtained.

6. For Mo/HZSM5 catalyst, all above steps were repeated, except the 2nd step. 3.219 g of $(NH_4)_6 \cdot Mo_7O_{24} \cdot 4H_2O$ was dissolved in 10.00 ml de-ionized water instead of $CoCl_2 \cdot 6H_2O$ and the ready-to-use 2.5 wt.% Mo/HZSM5 catalyst was obtained.

7. For 5, 10, 15 and 20 wt.% Co/HZSM5 catalyst, the procedure of the 1st to 5th steps was repeated, except for the 2nd step. 2.017, 4.034, 6.051 and 8.068 g of $CoCl_2 \cdot 6H_2O$ was dissolved in 10.00 ml de-ionized water instead of 1.008 g, respectively. For 5, 10, 15 and 20 wt.% Mo/HZSM5 catalyst, the procedure of the 1st to 5th steps was repeated, except for the 2nd step. 6.438, 12.875, 19.313 and 25.750 g of $(NH_4)_6 \cdot Mo_7O_{24} \cdot 4H_2O$ was dissolved in 10.00 ml de-ionized water instead of $CoCl_2 \cdot 6H_2O$, respectively.

3.2.2.3 Preparation of Co/AlMCM-41 and Mo/AlMCM-41 catalyst

1. 0.50 g of AlMCM-41 powders was dried at 105 ^{o}C in hot air oven overnight.

2. 0.504 g of $CoCl_2 \cdot 6H_2O$ was dissolved in 10.00 ml de-ionized water.

3. 2.00 ml of the solution obtained from the 2nd step was dropped slowly on the dried AlMCM-41 support (1st step).

4. The obtained product was dried at 105 ^{o}C in hot air oven overnight.

5. Finally, this catalyst was calcined at 400 ^{o}C in air for 2 h [102] and the ready-to-use 5 wt.% Co/AlMCM-41 catalyst was obtained.

6. For Mo/AlMCM-41 catalyst, all above steps were repeated, except the 2nd step. 1.609 g of $(NH_4)_6 \cdot Mo_7O_{24} \cdot 4H_2O$ was dissolved in 10.00 ml de-ionized water instead of $CoCl_2 \cdot 6H_2O$ and the ready-to-use 5 wt.% Mo/AlMCM-41 catalyst was obtained.

3.2.2.4 Preparation of CoMo/Al$_2$O$_3$, CoMo/HZSM5 and CoMo/AlMCM-41 catalyst [100]

1. 1.00 g of Al$_2$O$_3$ powders was dried at 105 ^{o}C in hot air oven overnight.

2. 12.875 g of (NH$_4$)$_6$·Mo$_7$O$_{24}$·4H$_2$O was dissolved in 10.00 ml de-ionized water.

3. 4.034 g of CoCl$_2$·6H$_2$O was dissolved in 10.00 ml de-ionized water.

4. 0.50 ml of the solution obtained from the 2nd step was dropped slowly on the dried Al$_2$O$_3$ support (1st step).

5. The product was dried at 105 ^{o}C in hot air oven for 15-20 min.

6. 0.50 ml of the solution obtained from the 3rd step was dropped slowly on the dried product obtained from the 5th step.

7. The product was dried at 105 ^{o}C in hot air oven overnight.

8. Finally, this catalyst was calcined at 400 ^{o}C in air for 2 h and the ready-to-use 10 wt.% CoMo/Al$_2$O$_3$ catalyst was obtained.

9. For CoMo/HZSM5 catalyst, all above steps were repeated and the 1.00 g of HZSM5 powders was used instead of the Al$_2$O$_3$ powders. In the 2nd and 3rd step, 6.438 g of (NH$_4$)$_6$·Mo$_7$O$_{24}$·4H$_2$O and 2.017 g of CoCl$_2$·6H$_2$O was dissolved in 10.00 ml de-ionized water, respectively. For the 4th and 6th step, 1.00 ml of the solution was dropped on the support. The ready-to-use 10 wt.% CoMo/HZSM5 catalyst was obtained, after calcination at 400 °C for 2 h.

10. For 10 wt.% CoMo/AlMCM-41 catalyst, all above steps were repeated and the 0.50 g of AlMCM-41 powders was used instead of the Al$_2$O$_3$ powders. In the 2nd and 3rd step, 0.504 g of (NH$_4$)$_6$·Mo$_7$O$_{24}$·4H$_2$O and 1.609 g of CoCl$_2$·6H$_2$O was dissolved in 10.00 ml de-ionized water, respectively. For the 4th and 6th step, 2.00 ml of the solution was dropped on the support. The ready-to-use 10 wt.% CoMo/AlMCM-41 catalyst was obtained after calcination at 400 ^{o}C for 2 h.

Dried support powders at 105 °C in hot air oven overnight	+	Dissolved the precursor in de-ionized water

Dropped the precursor solution slowly on the dried support

Dried at 105 °C in hot air oven overnight

Calcined at 400 °C in air for 2 h

Co/Al$_2$O$_3$, Mo/Al$_2$O$_3$, Co/HZSM5, Mo/HZSM5, Co/AlMCM-41 and Mo/AlMCM-41 catalysts

Figure 3.2 Schematic diagram of the preparation of single metal catalysts.

Dried support powders at 105 °C in hot air oven overnight	+	Dissolved the Co and Mo precursors in de-ionized water

Dropped the Mo precursor solution slowly on the dried support

Dried at 105 °C in hot air oven for 15-20 min

Dropped the Co precursor solution slowly on the dried supported Mo

Dried at 105 °C in hot air oven overnight

Calcined at 400 °C in air for 2 h

CoMo/Al$_2$O$_3$, CoMo/HZSM5 and CoMo/AlMCM-41 catalysts

Figure 3.3 Schematic diagram of the preparation of bimetallic catalysts.

3.2.3 Catalysts characterization

3.2.3.1 Textural properties of catalysts

The specific surface area, pore volume and average pore diameter of the support or supported Co-based catalysts were measured by N_2 adsorption/desorption and degassing at 300 °C for 15 h on a surface area analyzer (Quantachrome, Autosorb-1). The surface area was calculated from BET method and the pore size distribution was calculated by BJH analysis for Al_2O_3 and AlMCM-41 and by NL-DFT method for HZSM5.

3.2.3.2 Catalyst structure

The phase structures of the catalysts were determined by X-ray diffraction (XRD) with a Bruker AXS D8 Discover X-Ray Diffractometer using Cu Kα radiation at 40 kV and 40 mA at an angle of 0-10$^{°}$2θ for low angle and with a Bruker AXS D8 Advance X-Ray Diffractometer using Cu Kα radiation (λ = 0.15406 nm) at 40 kV and 30 mA at an angle of 5-80$^{°}$2θ for wide angle.

3.2.3.3 Morphology of catalyst

All catalysts were analyzed for their micro-structure and elemental compositions by scanning electron microscopy with energy dispersive X-ray analysis (SEM-EDX) on a JEOL JSM-5800 LV instrument.

The morphology and micro-structure images of these catalysts were characterized by transmission electron microscopy (TEM) with a JEOL, JEM-2100 (200 kV) instrument.

3.2.3.4 Acidity

The acidities of these catalysts were estimated by NH_3-temperature programmed desorption (NH_3-TPD) on a TPDRO/MS 1100 instrument. Prior to monitoring the NH_3-TPD profiles, the catalyst (0.3 g) was pretreated in N_2 at 500 °C for 1 h, then cooled to 30 °C and was saturated with 10% NH_3 in He for 30 min. After

being purged with N_2 for 30 min, the sample was heated to 800 °C with a heating rate of 10°C/min under flowing He of 20 ml/min for 4 h.

3.2.3.5 Reducibility

The reducibility and reduction behavior of these catalysts were characterized by H_2-temperature programmed reduction (H_2-TPR) in an in-house fixed-bed continuous flow microreactor at atmospheric pressure equipped with TCD detector. Typically, the catalyst (0.03 g) was pretreated at 200 °C for 1 h and cool down to room temperature under Ar flow, then heated under 5% H_2 in Ar flow of 30 ml/min up to 900 °C with heating rate of 10 °C/min. The amount of H_2 consumption during the increasing temperature period was determined by using a TCD signal.

3.2.4 Catalytic activity for glycerol hydrogenolysis

The catalytic reaction of glycerol hydrogenolysis was carried out in a 250-ml high pressure and high temperature reactor supplied by Parr Instrument Co., Model 4843. The autoclave reactor is equipped with a thermowell, pressure transducer, gas inlet, gas outlet and a rupture disc. In this research, the glycerol hydrogenolysis to product distribution over supported Co-based catalysts in an aqueous phase was investigated and the glycerol hydrogenolysis experiments were run by these following steps as shown in Figure 3.4.

1. Prior to evaluate the catalytic activity, an as-prepared supported catalyst was reduced under a H_2 atmosphere at constant flow rate of 50 ml/min in a fixed-bed reactor at desired reduced temperature for 4 h.

2. 150 mg supported Co-based catalyst (5 wt.%) was mixed with 10 g glycerol solution (20 wt.%) in a 250-ml pressure reactor (PARR reactor).

3. Pure H_2 was purged several times at a constant flow rate of 50 ml/min to eliminate the residual air in the reactor. The reactor pressure was then increased to the required H_2-pressure (7 MPa H_2-

pressure), heated to the desired reaction temperature (180 ^{o}C) and maintained at that condition for the given reaction period (3 h) to allow the hydrogenation reaction of glycerol to proceed.

4. After the reaction period, the pressure and temperature of the reactor were decreased slowly. The liquid product was analyzed by HPLC and products were confirmed by GC-mass spectrometry (MS).

5. To confirm the precision, all above steps were repeated two times at the same operating condition.

6. The investigated parameters were listed as the following

   - Reduced temperature: 350 and 600 ^{o}C

   - Types of supported catalyst: Co-, Mo-, CoMo/Al_2O_3

        Co-, Mo-, CoMo/HZSM5

        Co-, Mo-, CoMo/AlMCM-41

   - Weight ratio of supported catalysts to glycerol: 15-35 mg/g glycerol

   - Metal loading: 2.5-20 wt.%

   - Reaction time: 3-9 h

   - Reaction temperature: 100-220 ^{o}C

   - Reaction pressure: 3-9 MPa H_2-pressure

3.2.5 Re-usability of catalyst

To study the stability of an as-prepared catalyst, the re-usability of catalyst was investigated. After the typical run for glycerol hydrogenolysis under the optimum operating condition obtained from previous studies, the catalyst was carried out to test the re-usability by these following steps.

1. The catalyst was separated from the liquid product by filtration, washed with acetone and de-ionized water and dried at 110 ^{o}C in hot air oven overnight.

2. Prior to evaluate the catalytic activity, the used catalyst was reduced under a H_2 atmosphere at constant flow rate of 50 ml/min in a fixed-bed reactor at 600 $^{\circ}$C for 4 h.

3. The catalytic activity for glycerol hydrogenolysis was run on the above following steps as shown in Figure 3.4 under the same optimum operating condition.

```
┌─────────────────────────┐     ┌─────────────────────────────┐
│ Reduced catalyst under H₂│  +  │ Prepared 20 wt.% glycerol   │
│   atmosphere for 4 h     │     │         solution            │
└─────────────────────────┘     └─────────────────────────────┘
                                 ┌─────────────────────────────┐
                                 │ Mixed the reduced catalyst  │
                                 │ with glycerol solution in   │
                                 │        PARR reactor         │
                                 └─────────────────────────────┘
┌──────────────────────────────────────────────────────────────┐
│ Purged with pure H₂ several times and pressed up to the       │
│              required H₂-pressure                              │
└──────────────────────────────────────────────────────────────┘
        ┌─────────────────────────────────────────────┐
        │ Heated up to the desired reaction temperature│
        └─────────────────────────────────────────────┘
┌──────────────────────────────────────────────────────────────┐
│    Maintained at this condition for the given reaction period │
└──────────────────────────────────────────────────────────────┘
┌──────────────────────────────────────────────────────────────┐
│      The liquid product was analyzed by HPLC and GC-MS        │
└──────────────────────────────────────────────────────────────┘
```

Figure 3.4 Schematic diagram of glycerol hydrogenolysis.

3.2.6 Products characterization

3.2.6.1 Identification of product distribution in liquid product

The generated compounds from the hydrogenolysis of glycerol were characterized by gas chromatograph and mass spectrometry (Agilent, GC 7890A, Mass 5975C) equipped with a flame ionization detector. Hewlett-Packard Chemstation software was used to collect and analyze the data. A DB-5ms GC-column (30 m x 250 μm x 0.25 μm) was used to analyze the product formation.

3.2.6.2 Concentration of glycerol and generated products

The concentration of glycerol and generated products was analyzed at particular time by high performance liquid chromatography (Agilent 1100 Series) equipped with a Pinnacle II C-18 5µm (250 x 4.6 mm) column and refractive index detector (RID). The mobile phase was a 99:1 (v/v) ratio of 10 mM H_2SO_4 with pure methanol at flow rate of 0.5 ml/min. The column temperature was controlled at 40 °C. The net glycerol conversion, the product selectivity and the product yield of selected products were calculated on the basis of Eqs. (3.1), (3.2) and (3.3), respectively, and the example of calculation was shown in Appendix A:

$$\text{Glycerol conversion}\,(\%) = \frac{\text{amount of glycerol converted}\,(C\text{-based mole})}{\text{total amount of glycerol in reactant}\,(C\text{-based mole})} \times 100 \tag{3.1}$$

$$\text{Product selectivity}\,(\%) = \frac{\text{amount of glycerol converted to each product}\,(C\text{-based mole})}{\text{amount of glycerol converted}\,(C\text{-based mole})} \times 100 \tag{3.2}$$

$$\text{Product yield}\,(\%) = \frac{\text{amount of glycerol converted to each product}\,(C\text{-based mole})}{\text{total amount of glycerol in reactant}\,(C\text{-based mole})} \times 100 \tag{3.3}$$

CHAPTER IV

RESULTS AND DISCUSSION

This chapter presents the effect of parameters on the morphology of supported Co-, Mo-, and CoMo catalysts and their activities on glycerol hydrogenolysis including glycerol conversion and selectivity to the desired products including acrolein, 1,2-PDO and 1,3-PDO. The mechanism of glycerol hydrogenolysis over these non-precious catalysts was proposed and the re-usability was finally examined.

4.1 Catalytic performance of the catalysts for glycerol hydrogenolysis

4.1.1 Effect of reduced temperature

Theoretically, the reduction of catalyst in the presence of hydrogen resulted the generation of catalyst in metallic form, which helped to increase its catalytic activity. This reduction temperature was selected from the temperature programmed reduction (TPR)-profiles.

Figure 4.1 shows the TPR patterns of Al_2O_3-supported catalysts. It can be seen that the reduction of Co_2O_3 on the Co/Al_2O_3 catalyst started at a temperature about 350 ^oC and proceeded by two steps observed in the temperature of 350-428 ^oC and 428-570 ^oC for Co_2O_3 to CoO (Co^{3+} to Co^{2+}) and then CoO to Co (Co^{2+} to Co), respectively [103-105]. The similar result was collected for the reduction of MoO_3 on the Mo/Al_2O_3 catalysts. The reduction temperature was started at a temperature of 340 ^oC, with two reduction regions at 340-550 ^oC and 550-670 ^oC for MoO_3 to MoO_2 (Mo^{6+} to Mo^{4+}) and then MoO_2 to Mo (Mo^{4+} to Mo), respectively [103, 106, 107, 108]. The maximal hydrogen consumption for the Co/Al_2O_3 and Mo/Al_2O_3 catalysts occurred at 461 and 507 ^oC, respectively. This demonstrates that, the CoO phase was reduced to Co metal form (Co^{2+} to Co) more than that of the Co_2O_3 phase to CoO phase form (Co^{3+} to Co^{2+}) in the case of Co/Al_2O_3 catalyst and the MoO_3 phase was reduced to MoO_2 phase form (Mo^{6+} to Mo^{4+}) more than that of the MoO_2 to Mo metal form (Mo^{4+} to Mo) in the case of Mo/Al_2O_3 catalyst.
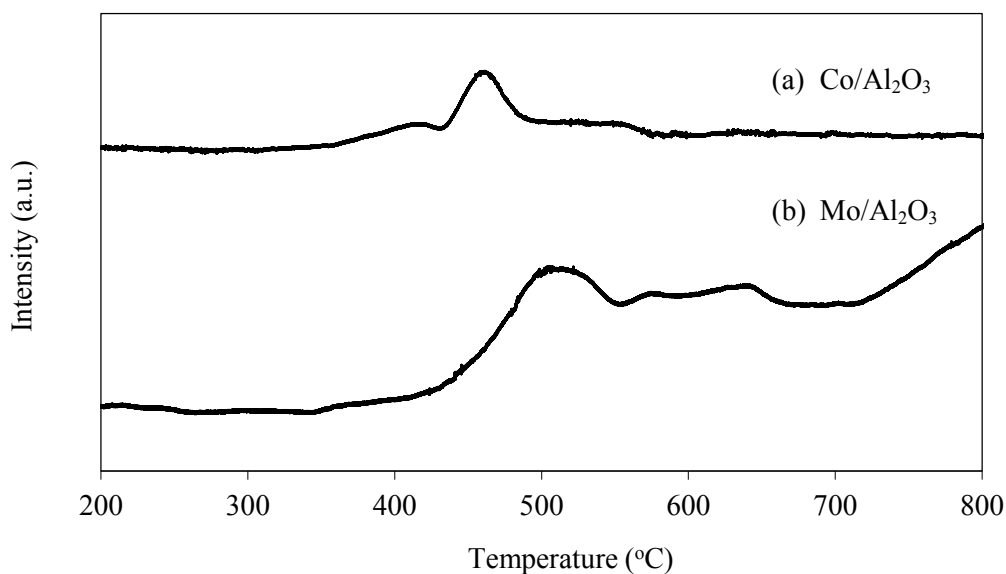
Figure 4.1 TPR-profiles of (a) Co/Al_2O_3 and (b) Mo/Al_2O_3 catalysts.

From the literatures, it was found that the two main reduction peaks for the Co/HZSM5 catalyst exhibited at 300 and 430 ^oC for the Co^{2+} and Co forms, respectively, and the maximal hydrogen consumption was 430 ^oC [105]. On the other hand, the TPR-profile for the Co/AlMCM-41 catalyst was not found in the literatures. From the TPR-profile of the impregnated 6% Mo/HZSM5 catalyst, its exhibited the maximal hydrogen consumption peaks at 511 ^oC and at 672 ^oC for Mo^{4+} and Mo forms, respectively, as claimed by previous literatures [106, 107]. The three main peaks of the TPR-profile for the Ni-Mo/AlMCM-41 catalyst exhibited at 431, 523, and 734 ^oC [108], the maximal hydrogen consumption was 523 ^oC, suggesting that the temperature of 431 ^oC showed the reduction temperature of Ni metal, as confirmed by previous literature [109]. Thus, the reduction temperatures of 350 and 600 ^oC that were selected to investigate the effect of the reduction temperature on the catalytic performance for glycerol hydrogenolysis, covered the maximal hydrogen consumption for both metals.

Figure 4.2 shows the XRD patterns of the reduced Co/Al_2O_3 catalysts under the reduced temperature of 350 and 600 °C, denoted by Co/Al_2O_3 (350°C) and Co/Al_2O_3 (600°C), respectively, it exhibited characteristic peaks of Al_2O_3, Co_2O_3,

CoO and Co^o phase. For the Co/Al$_2$O$_3$ (350°C) catalyst, the XRD diffraction peak of Co$_2$O$_3$ phase was sharper but the intensity of Co^o peak was weaker and broader than that of Co/Al$_2$O$_3$ (600°C) catalyst. This might be due to the Co$_2$O$_3$ phase was not reduced completely to CoO and Co^o phase at lower reduced temperature as above mentioned.
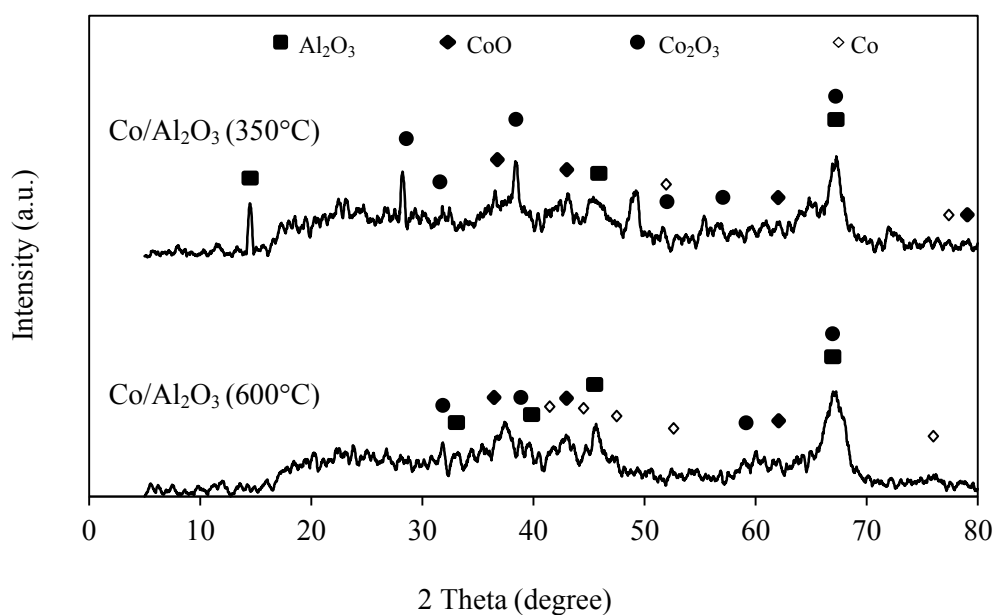
Figure 4.2 XRD patterns of the reduced Co/Al$_2$O$_3$ catalysts at wide angle.

Figure 4.3 shows the hydrogenolysis of glycerol which was carried out in Parr reactor under the conditions of 180 °C reaction temperature, 7 MPa H$_2$-pressure and 3 h reaction time using 20 wt.% initial glycerol concentration in the presence of 5 wt.% Co/Al$_2$O$_3$ catalysts. The utilized catalyst was reduced at 350 and 600 °C for 4 h in H$_2$ stream, and the weight ratio of catalyst to glycerol was fixed at 15 mg/g. It can be seen that the catalyst reduced at 600 °C gave the glycerol conversion (X$_G$, 18.7%) and production yield (Y) of acrolein (3.5%), 1,2-PDO (2.6%), and 1,3-PDO (1.8%) greater than that reduced at 350 °C. In addition, no acrolein, an intermediate for forming 1,3-PDO, was obtained from the catalytic hydrogenolysis of glycerol using a lower reduced temperature. This result supports the fact that lower reduced temperature cannot facilitate complete a reduction of

oxidic to metallic Co form, which leads to the decrease in catalytic activity of catalysts. At the reduced temperature of 600 $^{\circ}$C, the Co species for all types of support was in metallic Co form and the Mo species for Al_2O_3 support was in metallic Mo form while for HZSM5 and AlMCM-41 supports were Mo^{4+} form. Hence, the reduced temperature used in glycerol hydrogenolysis over Co-based catalysts is 600 $^{\circ}$C.
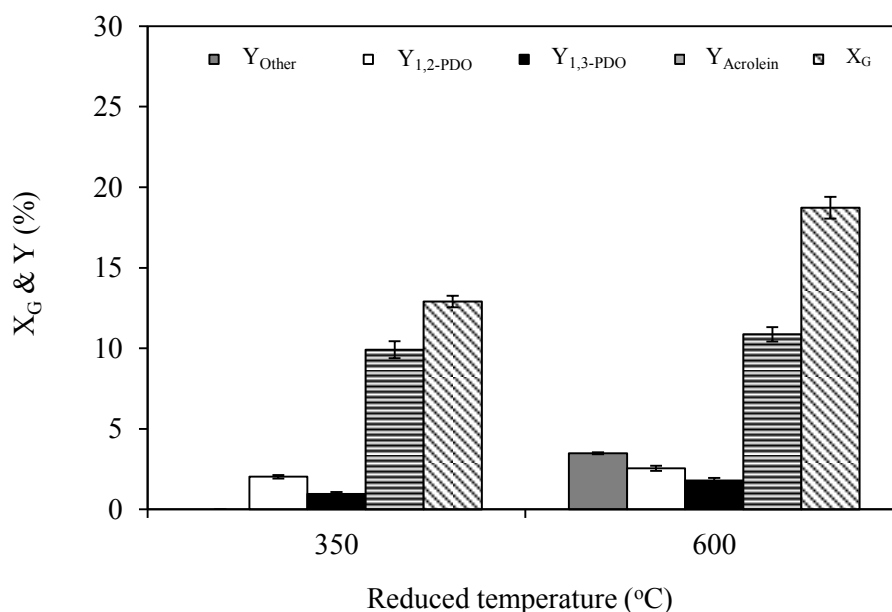
Figure 4.3 Effect of reduced temperature on glycerol conversion and production yield from glycerol hydrogenolysis at 180 $^{\circ}$C reaction temperature, 7 MPa H_2-pressure, 3 h reaction time and 20 wt.% initial glycerol concentration, weight ratio of 5 wt.% Co/Al_2O_3 catalyst to glycerol of 15 mg/g.

4.1.2 Effect of catalyst types

The glycerol hydrogenolysis requires a bifunctional catalyst containing both acid and metal functionalities. In this work, non-precious metal including Co, Mo, and CoMo were impregnated on acidic supports as Al_2O_3, HZSM5, and AlMCM-41. All of these acid catalysts were characterized by BET, XRD, SEM-EDX, TEM and TPD.

The BET specific surface area and pore volume of the different types of supported Co, Mo, and CoMo catalysts were all decreased significantly compared to the bare supports as shown in Table 4.1. That is, the BET specific surface area of the calcined Co-, Mo-, and CoMo/Al_2O_3, Co-, Mo-, and CoMo/HZSM5, and Co-, Mo-, and CoMo/AlMCM-41 catalysts were 1.28-, 1.87-, 2.47-, 1.02-, 1.47-, 1.63-, 1.37-, 2.77-, and 3.45-fold lower, respectively, than their supports. The pore volumes were reduced slightly from 0.23 to 0.19, 0.16 and 0.13 cm^3/g for Co/Al_2O_3, Mo/Al_2O_3 and CoMo/Al_2O_3, respectively, 0.27 to 0.10, 0.07 and 0.06 cm^3/g for Co/HZSM5, Mo/HZSM5, and CoMo/HZSM5, respectively and 1.64 to 1.28, 0.64, and 0.60 cm^3/g for Co/AlMCM-41, Mo/AlMCM-41, and CoMo/AlMCM-41, respectively. This might be attributed to the deposition of these metals on the external grains of supports and some pore blockage or partial destruction of the porous structure cannot be excluded [88].

Table 4.1 Textural properties of the utilized supports and their corresponding supported catalysts at a nominal 5 wt.% loading.

Support / supported catalyst	Specific surface area (m^2/g)	Pore volume (cm^3/g)	Average pore diameter (nm)
Al_2O_3	131	0.23	5.0
Co/Al_2O_3	102	0.19	5.0
Mo/Al_2O_3	70	0.16	4.1
CoMo/Al_2O_3	53	0.13	4.1
HZSM5	270	0.27	1.8
Co/HZSM5	264	0.10	1.4
Mo/HZSM5	184	0.07	1.4
CoMo/HZSM5	166	0.06	1.4
AlMCM-41	1250	1.64	5.1
Co/AlMCM-41	915	1.28	2.9
Mo/AlMCM-41	451	0.64	2.4
CoMo/AlMCM-41	362	0.60	2.4

* BET method for surface area and SF method for pore size distribution

Moreover, it can be seen that the BET specific surface area and pore volume of Co supported catalysts exhibited higher than that of Mo and CoMo supported catalysts for all types of support due to the larger shape of Mo crystalline structure, which can be confirmed by XRD and TEM images. In addition, some partial destruction and laceration of the porous structure resulted to the slight change of the average pore diameter of supported catalysts compared with their supports.

The crystalline phases formed in all supported catalysts were evaluated by XRD analysis as shown in Figures 4.4, 4.5, and 4.6. The XRD pattern of the calcined Co-, Mo-, and CoMo/Al$_2$O$_3$ exhibited peaks at 2θ of 37.8^o ,45.8^o, and 66.8^o which are the main characteristics peaks of Al$_2$O$_3$ (Figure 4.4). Similarly, the XRD pattern of Co-, Mo-, and CoMo/HZSM5 exhibited peaks at 2θ of 7.8^o, 8.7^o, 23.1^o, 23.3^o, 23.6^o, 23.8^o, and 24.3^o, which are the main characteristics peaks of HZSM5 (Figure 4.5). For Co/Al$_2$O$_3$ and Co/HZSM5 catalysts, Co was presented as fine particle and highly dispersed on the support surface resulted to no diffraction peaks of metallic Co phase in XRD pattern, as claimed by previous literatures [9, 17, 85, 110]. Because the XRD diffraction peaks of Co species in all Co supported catalysts were weak and broad, the average crystal sizes of Co^o phase or Co$_2$O$_3$ phase could not be calculated by Scherrer equation [9]. This indicates that the impregnation of Co metals at 5 wt.% loading onto either Al$_2$O$_3$ or HZSM5 had no significant effect on the structure of their support. On the other hand, the diffraction peaks of MoO$_3$ were detected, which was the crystalline structure of Mo. The presence of Mo and CoMo on Al$_2$O$_3$ and HZSM5 supportes reduced the intensity of the main characteristics peaks of their supports, implying that the surface support was covered by the impregnated Mo and CoMo particles [100]. This result related to the reduction of BET surface area and pore size of both metals.
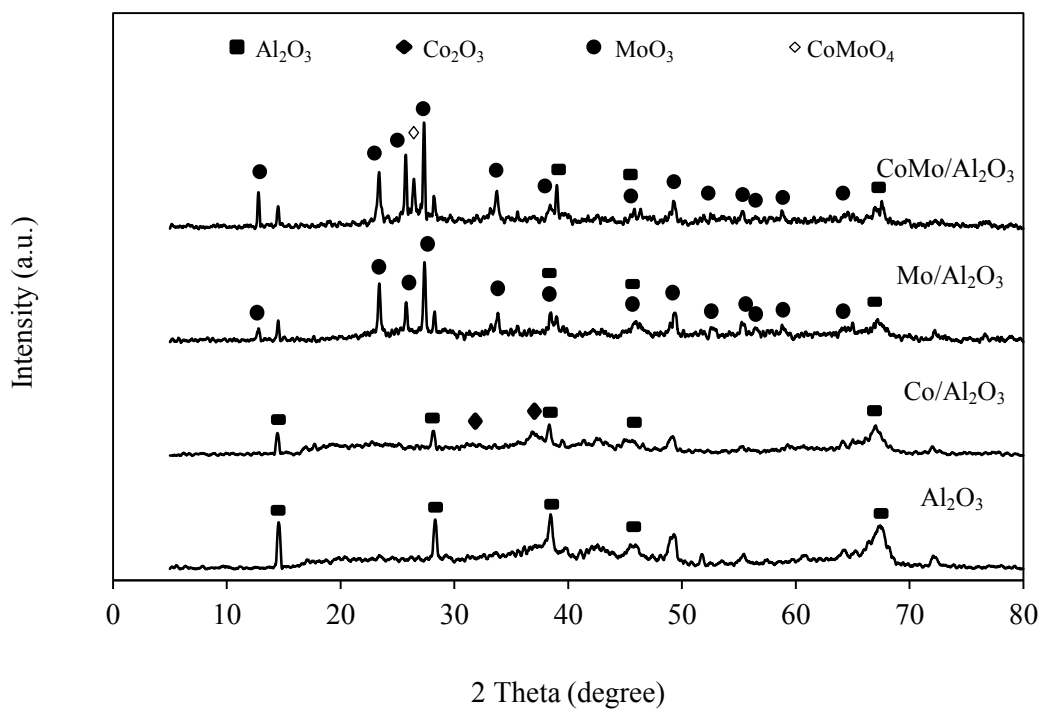
Figure 4.4 XRD patterns of the Co-, Mo-, and CoMo/Al$_2$O$_3$ catalysts and their
supports at wide angle.
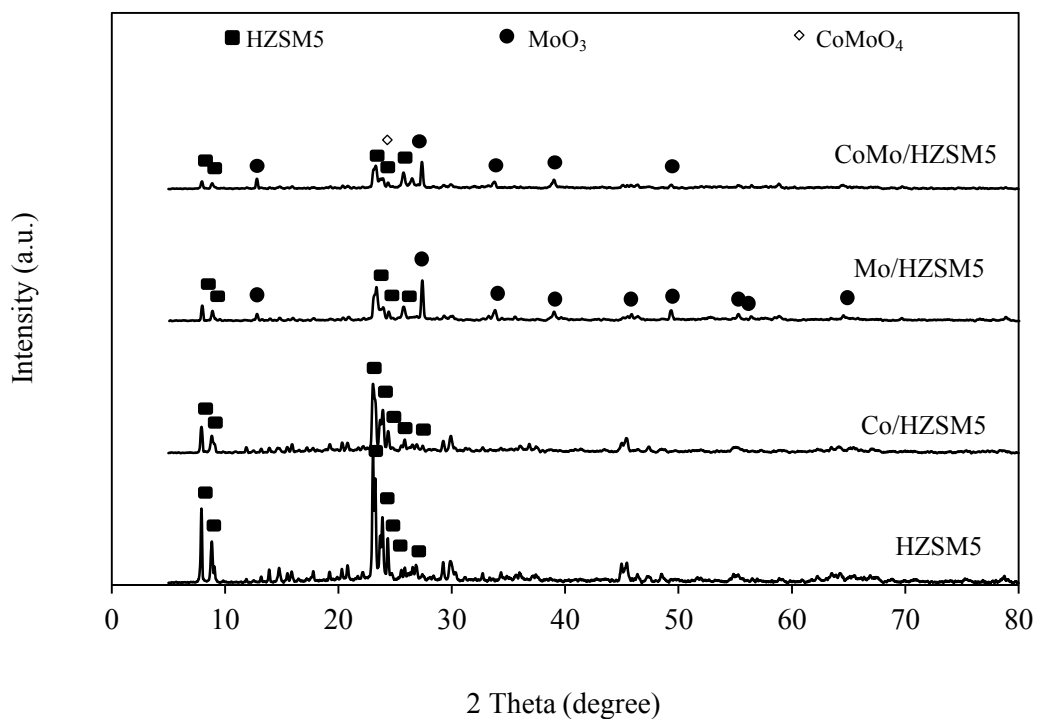

Figure 4.5 XRD patterns of the Co-, Mo-, and CoMo/HZSM5 catalysts and their
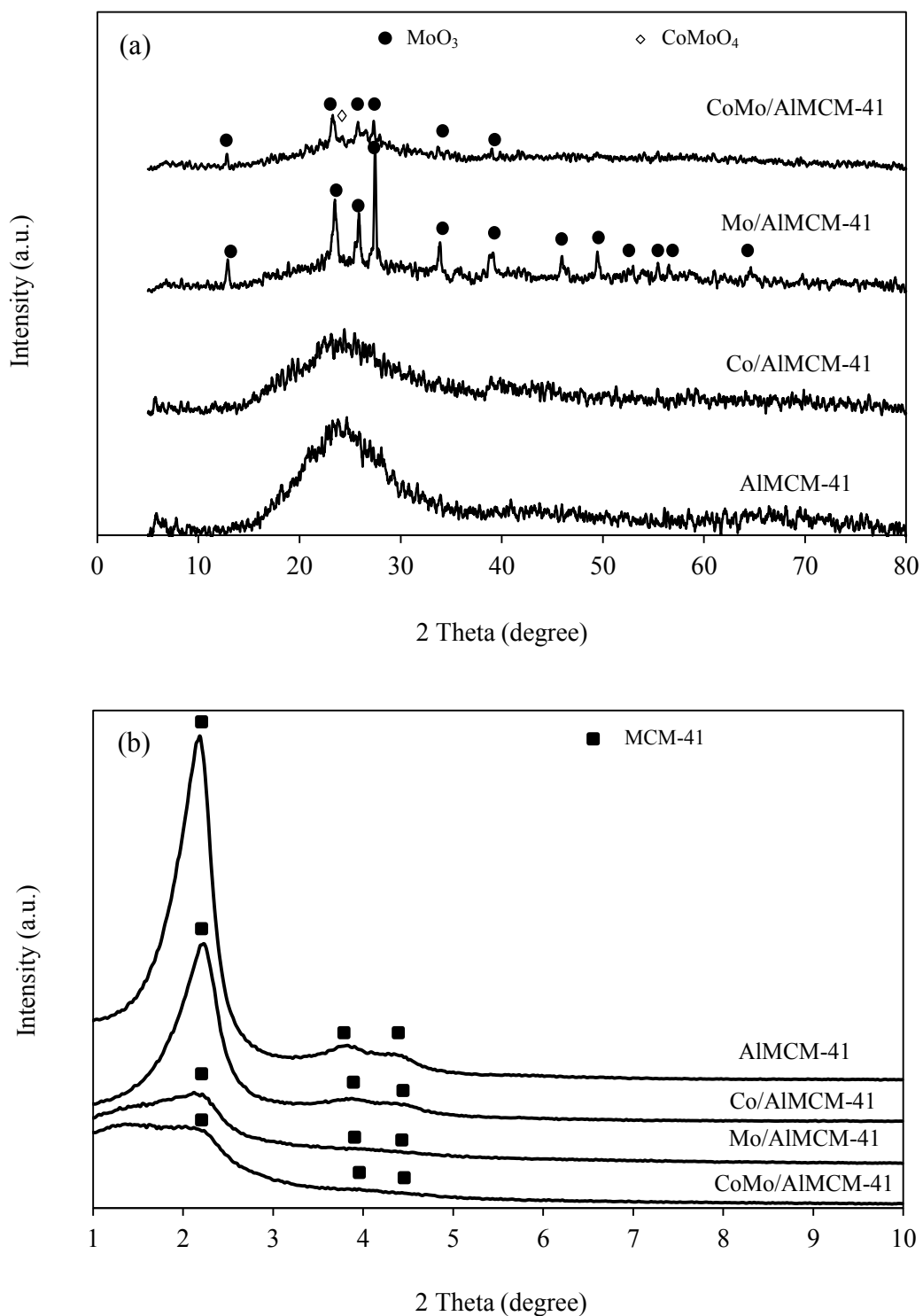supports at wide angle.

Figure 4.6 XRD patterns of the Co-, Mo-, and CoMo/AlMCM-41 catalysts and their supports at (a) wide angle and (b) low angle.

For Co-, Mo-, and CoMo/AlMCM-41, no characteristic peaks of Co or AlMCM-41 were observed during the wide angle scan but the presence of Mo and CoMo on AlMCM-41 supported exhibited the intensity of the main characteristics peaks of MoO_3 (Figure 4.6 (a)). However, the typical diffraction pattern of AlMCM-41 appeared at a low angle at 2θ of 2.2^o, 3.9^o and 4.3^o, indicating the presence of the support in a hexagonal mesophase [111, 112]. No new peaks, except the typical diffraction peaks of AlMCM-41, were formed in Co/AlMCM-41 catalyst as shown in Figure 4.6 (b), suggesting that the impregnated Co metal also has no effect on the structure of its support but the presence of Mo and CoMo on AlMCM-41 reduced the intensity of hexagonal peak due to the large crystalline structure of Mo and CoMo [100, 111], resulting to the decrease of the BET surface area and pore size of catalysts.

The existence of Co, Mo, and CoMo elements on each types of support was confirmed by SEM-EDX analysis. The SEM micrographs and the corresponding results of the X-ray images and EDX spectras of the Al_2O_3, HZSM5, and AlMCM-41 supported catalysts are shown in Figures 4.7, 4.8, and 4.9, respectively. The typical external particle morphologies of the calcined Co-, Mo-, and CoMo/Al_2O_3 catalysts are represented by SEM micrographs as shown in Figure 4.7 (b). The lighter area represents the Al_2O_3 support with their metals. It can be seen that the morphology of Mo on Al_2O_3 support was clearly observed than that of Co because Mo is represented in crystalline structure while Co is represented in the fine spherical particles. However, it can be seen that the catalyst structure resulted from the binding together of catalyst particles into aggregates or clumps of vary sizes and shapes. For the X-ray images, the elemental distribution of the calcined Co-, Mo-, and CoMo/Al_2O_3 catalysts are shown in Figure 4.7 (c). The white or light spots on the external surfaces represent high concentration of Co and Mo metals which were dispersed very well on the surface of support, and the dark area represents the Al_2O_3 support, which was confirmed the existence of both metal species by EDX spectra as shown in Figure 4.7 (a).

Figure 4.7 (a) EDX spectra of elements in catalyst particles, (b) SEM micrographs of
crystalline particles and (c) X-ray images of catalysts dispersion of all Al_2O_3
supported catalysts.

Figure 4.8 (a) EDX spectra of elements in catalyst particles, (b) SEM micrographs of crystalline particles and (c) X-ray images of catalysts dispersion of all HZSM5 supported catalysts.

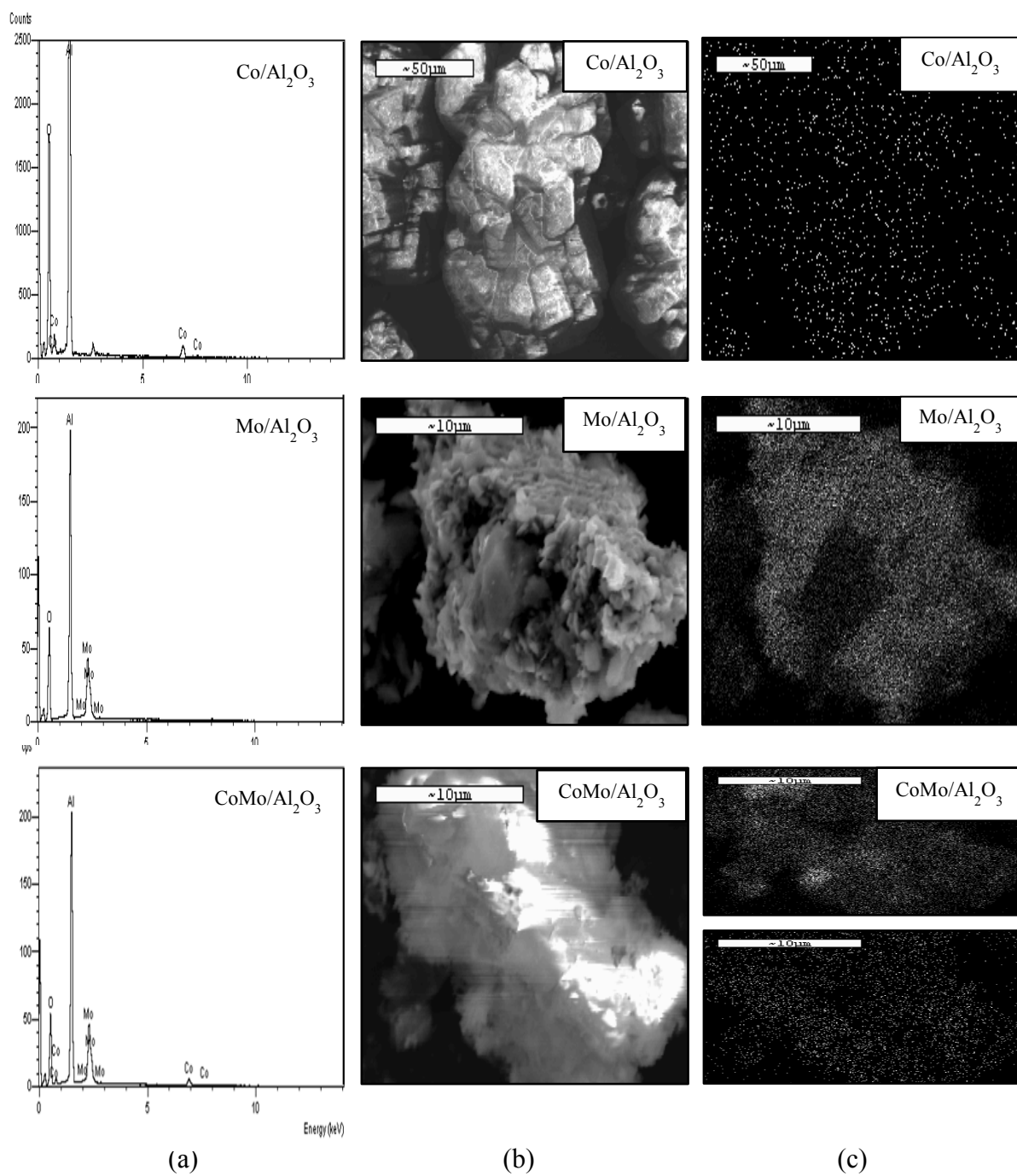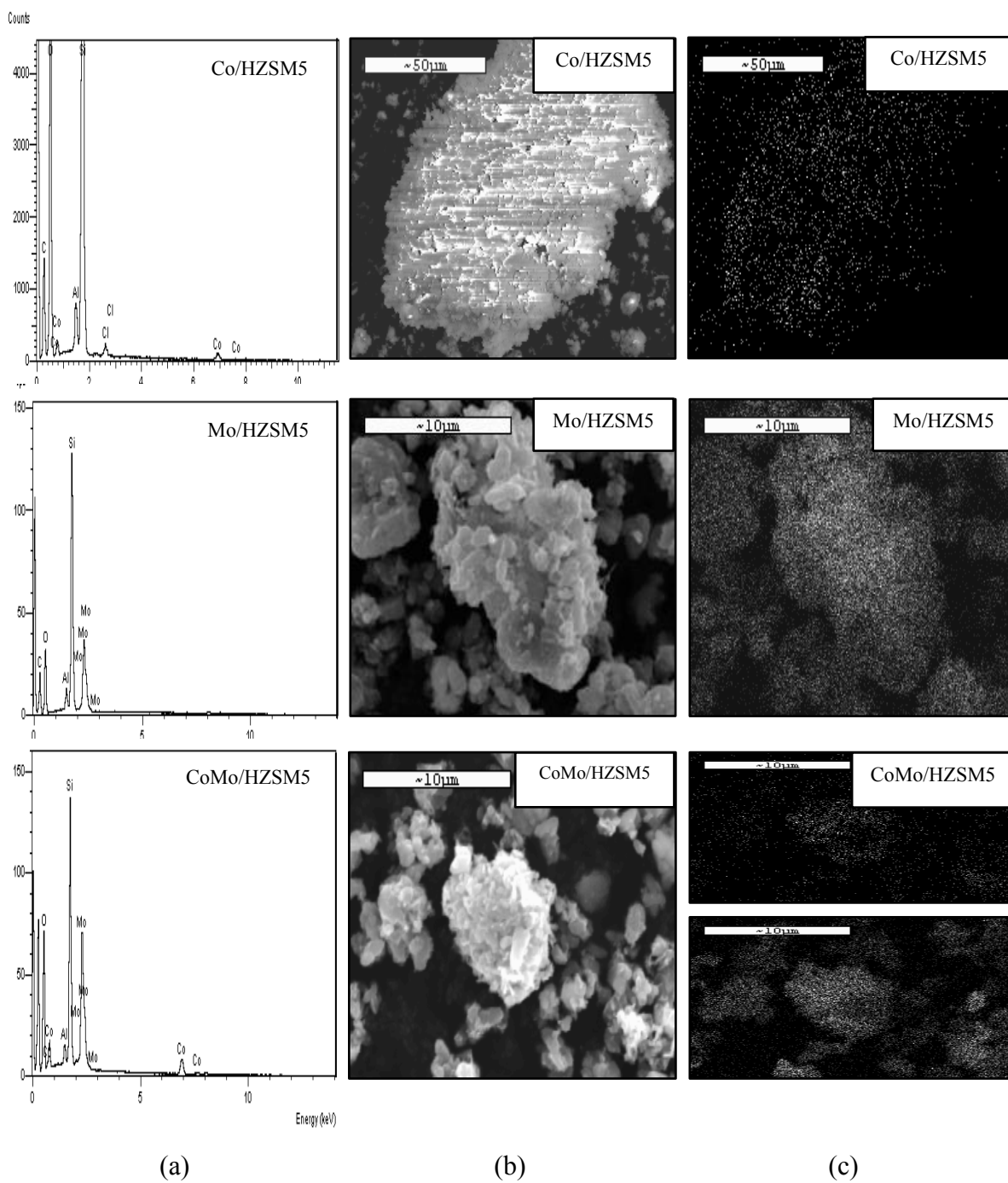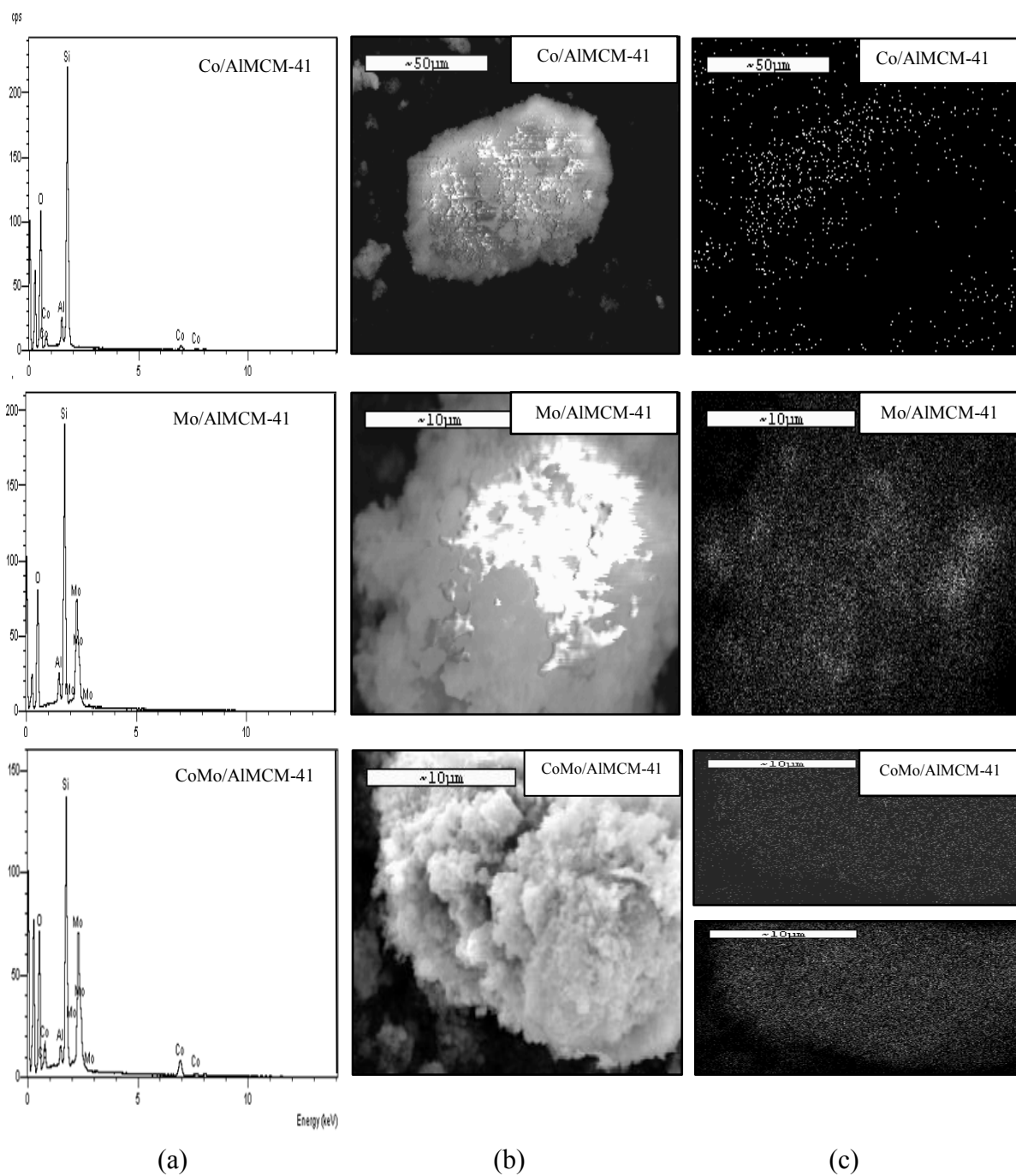Figure 4.9 (a) EDX spectra of elements in catalyst particles, (b) SEM micrographs of crystalline particles and (c) X-ray images of catalysts dispersion of all AlMCM-41 supported catalysts.

The amount of all metal species is tabulated in Table 4.2, it is visualized that the amount of each element for monometallic catalysts, as Co- and Mo- on all supports, was similar to 5 wt.%, while the amount of Co element on CoMo supported catalysts was about 1% which less than that of Mo element on all supports. This might be attributed to the effect of the catalyst loading sequence. That is, Mo is added first on support and then Co. According to this procedure, Mo crystals may cover almost fully on the support surface, resulting to the presence of small surface of support available for Co coverage. In the case of the calcined Co-, Mo- and CoMo over HZSM5 and AlMCM-41 supports as respectively shown in Figures 4.8 and 4.9, it could be explained similar to all above-explanation of Al_2O_3 supported catalyst.

Table 4.2 Amount of elements in the nominal 5 wt.% Co-based catalyst particles.

Catalysts	Amount of metal elements (%)	
	Co	Mo
Co/Al_2O_3	4.91 ± 0.47	-
Mo/Al_2O_3	-	4.38 ± 0.03
$CoMo/Al_2O_3$	1.24 ± 0.07	5.19 ± 0.63
Co/HZSM5	4.89 ± 0.28	-
Mo/HZSM5	-	5.58 ± 0.76
CoMo/HZSM5	1.55 ± 0.17	5.35 ± 0.57
Co/AlMCM-41	4.74 ± 0.52	-
Mo/AlMCM-41	-	4.89 ± 0.56
CoMo/AlMCM-41	1.31 ± 0.19	6.15 ± 0.18

TEM images of the calcined Co, Mo, and CoMo catalysts supported on three different supports are presented in Figure 4.10. The shapes of Co particles on all supports were approximately spherical particles. For Co/AlMCM-41 catalyst, the boundary of Co particles could be clearly observed, while Co on the surface of Al_2O_3 and HZSM5 were fine sphere in stick-shaped particles and the boundary of Co particles was very unclear. The existence of Co particles on these supports was confirmed by the SEM-EDX images. For Mo, some large Mo particles were observed

on the exterior of the Al_2O_3, HZSM5, and AlMCM-41. This could be due to their shapes were the crystalline particles, their morphology and microstructure were bigger than that of Co particles. For CoMo catalysts, it was found that the shapes of catalyst particle were mixed between the spherical shape of Co and crystalline structure of Mo and some stick-shaped particles, which could be observed on the exterior of the three types of support in their TEM images as shown in Figure 4.10.
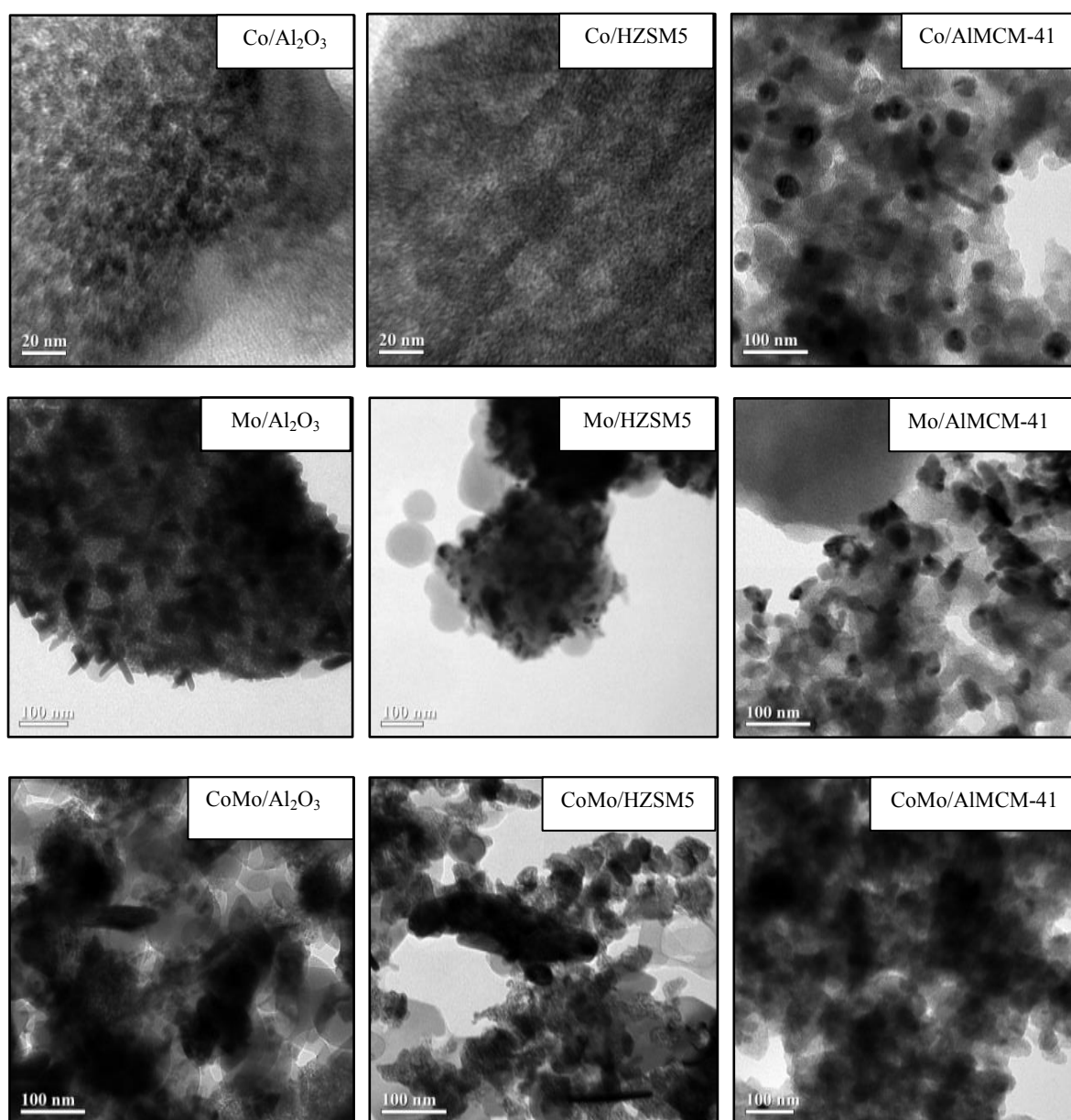

Figure 4.10 TEM images of all prepared supported catalysts.

The surface acidity of the supported catalysts was quantitatively determined by the integration of the desorption curve for NH_3-TPD analysis as shown in Figures 4.11 (a), (b), and (c) for the calcined Al_2O_3, HZSM5, and AlMCM-41 supported catalysts, respectively. The area under the curves, the amount of NH_3 desorbed, was proportional to the number of moles of acidic sites. Then, the number of moles of acidic sites per weight of active phase could be determined. Theoretically, according to the NH_3 desorption temperature, the strength of acid sites are usually classified into three types, weak- (150-300 ^{o}C), medium- (300-500 ^{o}C), and strong- (500-650 ^{o}C) strength [85]. As shown in Figure 4.11 (a), all of the catalysts over Al_2O_3 support exhibited a centering NH_3 desorption peak at around 230, 245, and 228 ^{o}C for Co/Al_2O_3, Mo/Al_2O_3 and $CoMo/Al_2O_3$, respectively, indicating the presence of a weak acidity site. In the case of the HZSM5 support, two main peaks and a weak shoulder were observed, the NH_3 desorption peaks of Co/HZSM5 catalyst exhibited around 268, 364 and 520 ^{o}C. For Mo/HZSM5 catalyst, the NH_3 desorption peaks exhibited around 275, 421 and 604 ^{o}C, and the NH_3 desorption peaks of CoMo/HZSM5 catalyst exhibited around 282, 387, and 505 ^{o}C, indicating that the HZSM5 supported catalysts had weak-, medium-, and strong-strength, respectively as shown in Figure 4.11 (b). The NH_3-desorption peaks of the as-prepared AlMCM-41 support catalysts are exhibited as an overlapping of two peaks at weak- and medium-strength of the acid sites. The centering NH_3 desorption peaks of Co/AlMCM-41 catalyst was observed at around 235 and 387 ^{o}C, respectively. For Mo/AlMCM-41 catalyst, the centering NH_3 desorption peaks exhibited around 229 and 376 ^{o}C, respectively. Finally, the centering NH_3 desorption peaks of CoMo/AlMCM-41 catalyst exhibited around 291 and 435 ^{o}C, respectively as shown in Figure 4.11 (c). The NH_3-TPD profiles of Al_2O_3 support catalysts showed poorer desorption peaks than the HZSM5 supports and AlMCM-41 supported catalysts and the maximum desorption peaks were observed in the HZSM5 support catalysts.
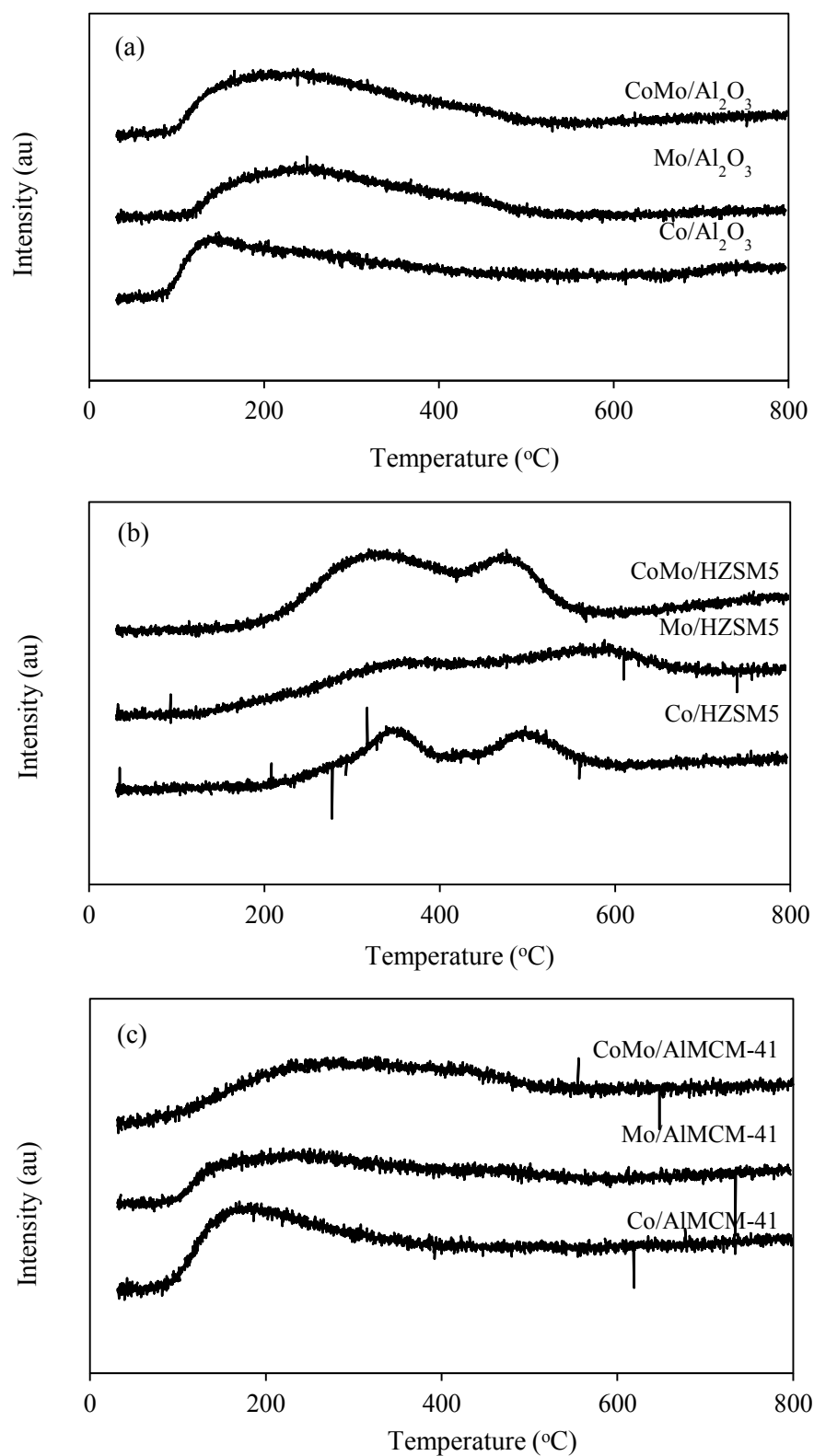
Figure 4.11 NH$_3$-TPD analysis all prepared supported Co-based catalysts.

The acidity of the supported Co-based catalysts was tabulated in Table 4.3. For the same type of support, the Co metal exhibited higher total acidity than that of the Mo and CoMo metals. The Co/HZSM5 catalyst showed the maximum total acidity (1.37 mmol/g), which was higher than that of Co/AlMCM-41 (1.31 mmol/g) and Co/ γ-Al$_2$O$_3$ (1.30 mmol/g), respectively. Among the same metal, all of the HZSM5 supported catalysts exhibited higher total acidity than that of the others supported catalysts.

Table 4.3 Acidity of the supported Co-based catalysts.

Catalysts	Acid site distribution (mmol/g)			
	Weak acid	Medium acid	Strong acid	Total acid
Co/Al$_2$O$_3$	1.30	-	-	1.30
Mo/Al$_2$O$_3$	0.97	-	-	0.97
CoMo/Al$_2$O$_3$	0.94	-	-	0.94
Co/HZSM5	0.60	0.41	0.36	1.37
Mo/HZSM5	0.49	0.44	0.31	1.24
CoMo/HZSM5	0.06	0.54	0.44	1.04
Co/AlMCM-41	0.83	0.48	-	1.31
Mo/AlMCM-41	0.32	0.63	-	0.95
CoMo/AlMCM-41	0.51	0.43	-	0.94

Figures 4.12 and 4.13 show the glycerol conversion, the production yield, and the selectivity of glycerol hydrogenolysis in Parr reactor under the conditions of 180 ^{o}C reaction temperature, 7 MPa H$_2$-pressure, 3 h reaction time and 20 wt.% initial glycerol concentration with the weight ratio of catalyst to glycerol of 15 mg/g in the presence of all prepared supported Co-based catalysts. The conversion of glycerol and production yield from glycerol hydrogenolysis in the presence of the supported Co-based catalysts with a constant loading of 5 wt.% could be identified. Different types of catalyst provided different glycerol conversions under the same operating condition. Particularly, the Co/HZSM5 catalyst can promote the maximum glycerol conversion (20.8%) compared with other types of catalyst. Figure 4.14

demonstrated that the glycerol conversion of glycerol hydrogenolysis decreased with the decrease of the total acidity and pore volume of all prepared supported catalysts, suggesting that the total acidity and pore volume affected the glycerol conversion but the average pore diameter was not. For the same type of support, the presence of Co species exhibited higher glycerol conversion than that of Mo and CoMo species, which was coincidence with the trend of the BET surface area as in the order of Co > Mo > CoMo.

Figure 4.11 and Table 4.3 exhibited that the Co/HZSM5 catalyst has a more acidic sites compared with other types of catalyst. The maximum total acidic sites were observed in case of Co/HZSM5 catalysts (1.37 mmol/g) and the total acidic sites of Co/AlMCM-41 were similar to Co/Al_2O_3 catalysts (1.31 and 1.30 mmol/g, respectively). This result related to the glycerol conversion as 20.8, 19.4, and 18.7% for Co/HZSM5, Co/AlMCM-41, and Co/Al_2O_3, respectively. For HZSM5 supported catalysts, the glycerol conversion of around 20.8, 15.7, and 14.2% for Co-, Mo-, and CoMo/HZSM5, respectively, was obtained with the formation of three desired products; acrolein, 1,2-PDO, and 1,3-PDO as shown in Figure 4.12. Similarly, the glycerol conversion obtained from using Co-, Mo-, and CoMo/Al_2O_3 catalysts were 18.7, 11.6, and 10.3%, respectively and Co-, Mo-, and CoMo/AlMCM-41 catalysts were 19.4, 13.1, and 11.4%, respectively. It seems that the supported Co catalyst can promote higher glycerol conversion than that of supported Mo-, and CoMo catalysts. Thus, it can be conclude that, for Mo species, both of Mo^{4+} and Mo phase were not effective for glycerol hydrogenolysis. This might be due to the Mo acidic catalyst generated a large amount of by-products as claimed by previous literature [3]. These results related with their BET specific surface area and pore volumes as shown in Table 4.1. The production yield of acrolein, 1,2-PDO, and 1,3-PDO for Co/HZSM5 catalyst were 4.9, 3.3, and 1.8%, respectively, for Mo/HZSM5 catalyst were 2.7, 1.6, and 1.5%, respectively and for CoMo/HZSM5 catalyst were 2.3, 1.5, and 1.4%, respectively, the yield of some desired products was still too low. However, the high production of 1,2-PDO was observed in the presence of Al_2O_3 and HZSM5 supports, for all types of catalyst, while more generation of 1,3-PDO was obtained in the case of AlMCM-41. This might be attributed to AlMCM-41 has the more specific surface area and pore volume compared to other two catalysts. The large pore volume of

AlMCM-41 induces the steric effect and selectively bonds with the 1st-OH group of glycerol, resulting to the formation of 1,3-PDO [11]. The formation of acrolein varied directly with the glycerol conversion but inverted with the formation of 1,3-PDO as shown in Figure 4.13. It might be due to the fact that acrolein is an intermediate of alternative path for forming 1,3-PDO. According to the literature [113], the propanediols formation proceeds via glycerol dehydration to acetol or 3-hydroxypropanal on acid catalyst and in order hydrogenation to 1,2-PDO and 1,3-PDO over metal catalysts, respectively. The acetol and 3-hydroxypropanal were not detected in any experiment, suggesting that acetol can hydrogenate fastly to 1,2-PDO, while 3-hydroxypropanal can dehydrate into acrolein or hydrogenate to 1,3-PDO. Additionally, the selectivity to acrolein was related to the selectivity of 1,3-PDO. The formation of acrolein decreased when the formation of 1,3-PDO increased.
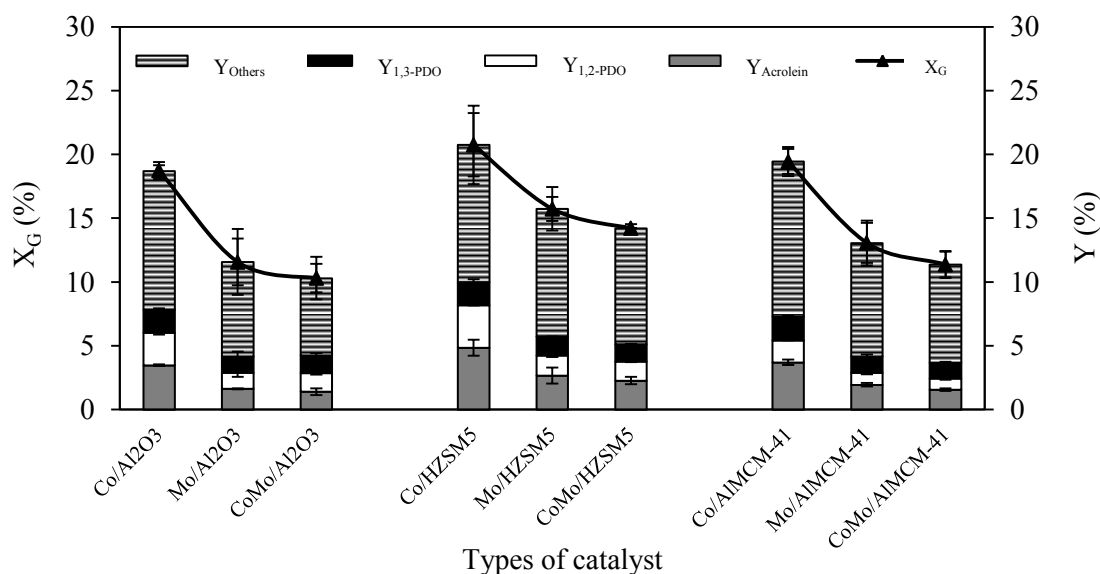
Figure 4.12 Effect of catalyst types on glycerol conversion and production yield from glycerol hydrogenolysis at 180 °C reaction temperature, 7 MPa H_2-pressure, 3 h reaction time and 20 wt.% initial glycerol concentration, weight of 5 wt.% metal loading to glycerol of 15 mg/g.
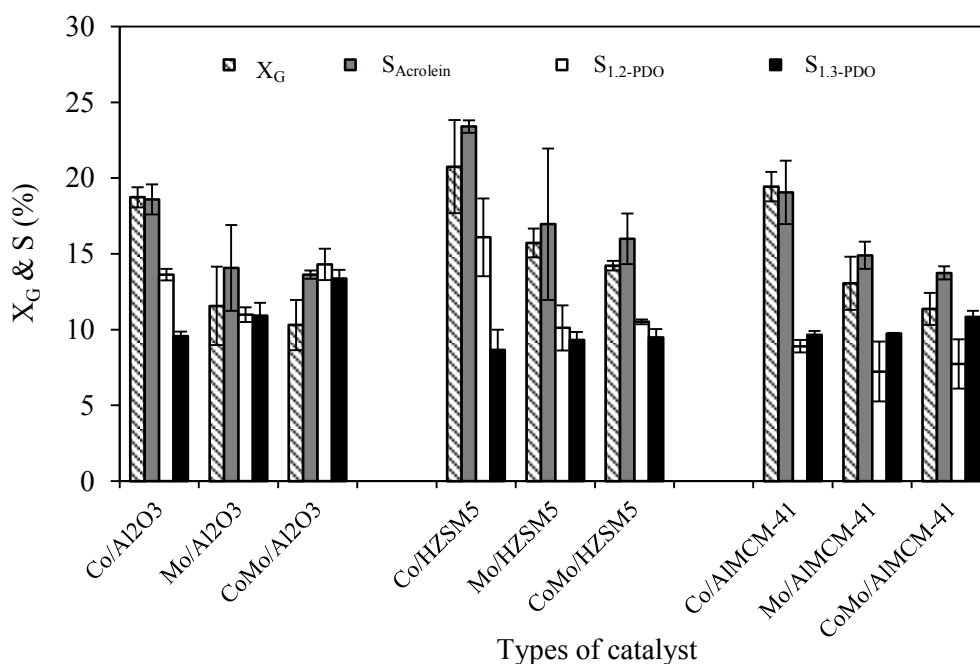
Figure 4.13 Effect of catalyst types on glycerol conversion and selectivity of desired products from glycerol hydrogenolysis at 180 $^{\circ}$C reaction temperature, 7 MPa H_2-pressure, 3 h reaction time and 20 wt.% initial glycerol concentration, weight of 5 wt.% metal loading to glycerol of 15 mg/g.
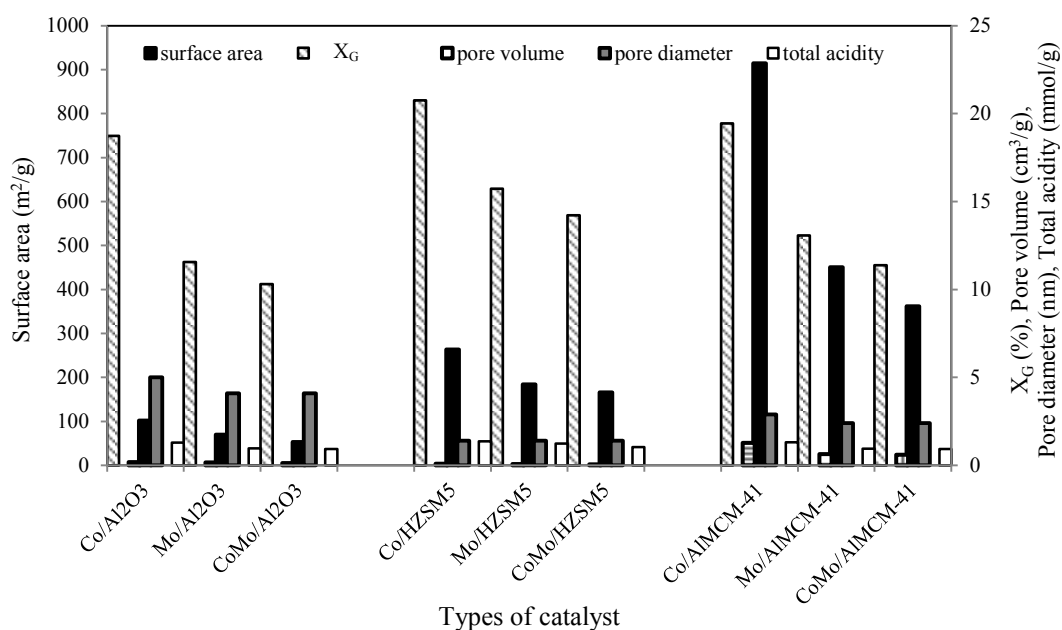
Figure 4.14 Trend of the glycerol conversion related to the BET surface area, pore volume, pore diameter, and total acidity of all prepared supported Co-based catalysts.

According to the morphological characterization and the catalytic activity of the different types of as-prepared supported catalyst, it seems that the support acidity affected directly and stronger than the textural properties on the net glycerol conversion, as claimed by previous literatures [10, 81, 84, 85]. Hence, the optimum catalyst selected for further study in glycerol hydrogenolysis was the Co-based catalysts over HZSM5 support.

4.1.3 Effect of weight ratio of supported catalysts to glycerol

In order to minimize the cost of catalyst replacement, a minimum amount of fresh catalyst could be used in each batch. The glycerol hydrogenolysis was carried out to investigate the minimum weight ratio of supported catalysts to glycerol required to achieve the maximum glycerol conversion and production yield. The weight ratio of supported catalysts to glycerol on glycerol hydrogenolysis was explored in the range of 15 to 35 mg/g glycerol at a constant catalyst loading of 5 wt.%, 180 ^{o}C reaction temperature, 7 MPa H_2-pressure for 3 h in the presence of Co-, Mo-, and CoMo/HZSM5 catalysts. As demonstrated in Figure 4.15 (a), it seems that the glycerol conversion remained constant, while the production yield of the desired products as 1,2-PDO, and 1,3-PDO increased when the weight ratio of supported catalyst to glycerol increased from 15 to 20 mg/g. As the weight ratio of supported catalysts to glycerol increased, more active metal and surface area available for the glycerol hydrogenolysis resulted to the production yield of the desired products increased. The production yield of acrolein changed slightly and related with the formation of 1,3-PDO, the formation of acrolein decreased when the formation of 1,3-PDO increased. The high glycerol conversion, as 21.1%, and production yield of acrolein, 1,2-PDO, and 1,3-PDO, as 2.7, 6.3, and 4.2%, respectively, were obtained at the weight ratio of supported catalysts to glycerol of 20 mg/g. Any further increase the weight ratio of supported catalysts to glycerol changed the production yield slightly, while the glycerol conversion decreased with further increase the weight ratio. This might be due to the aggregation of supported catalyst, resulting to the decrease in active surface area.
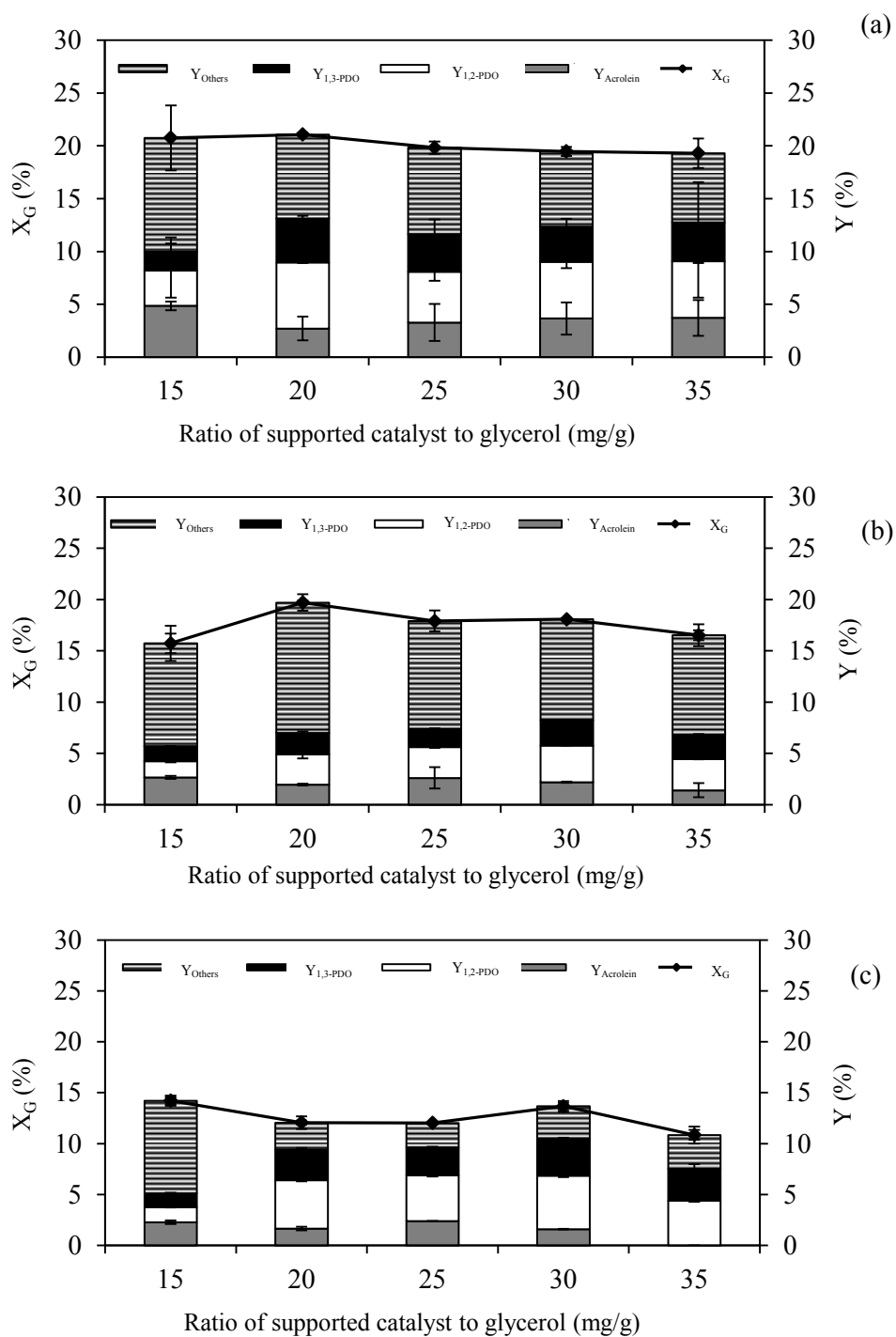
Figure 4.15 Effect of supported catalyst to glycerol ratio on glycerol conversion and production yield from glycerol hydrogenolysis over reduced (a) Co/HZSM5, (b) Mo/HZSM5 and (c) CoMo/HZSM5 catalysts at 180 ^{o}C reaction temperature, 7 MPa H_2-pressure, 3 h reaction time, and 20wt.% initial glycerol concentration.

Similarly, for Mo/HZSM5 catalyst, the glycerol conversion increased with the weight ratio of supported catalyst to glycerol increased from 15 to 20 mg/g. Further increase the weight ratio of supported catalysts to glycerol could not increase the catalytic activity of Mo/HZSM5 as shown in Figure 4.15 (b). The production yield of 1,2-PDO, and 1,3-PDO increased slightly with the increase of the weight ratio of supported catalysts to glycerol from 15 to 30 mg/g. At this condition, the glycerol conversion was 18.1% and production yield of acrolein, 1,2-PDO and 1,3-PDO were 2.2, 3.6, and 2.5%, respectively. However, the glycerol conversion and production yield of all desired products for Mo/HZSM5 catalyst was still lower than that of Co/HZSM5 catalyst. For the CoMo/HZSM5 catalyst, it gave the lowest yield of the other products. However, its glycerol conversion was still lower than that of the other catalysts as shown in Figure 4.15 (c), suggesting that the active surface area of the catalyst was concealed with more both metals. Hence, the optimum catalyst selected for further study in glycerol hydrogenolysis was the Co/HZSM5 catalyst at the weight ratio of supported catalysts to glycerol of 20 mg/g.

4.1.4 Effect of metal loading

To get more hydrogenation products, the increase in metal loading on the support was performed. The BET specific surface areas, pore volumes, and pore diameters of Co/HZSM5 catalyst at different metal loadings in the range of 2.5 to 20 wt.%, compared with their supports, are tabulated in Table 4.4. The increase of Co metal loading impregnated on HZSM5 supports, from 2.5 to 20 wt.%, led to the decrease in the BET specific surface area from 302 to 165 m^2/g. This result supported the above mention that the increase of Co metal loading resulted to the deposition of Co metal on the external grains of supports and some pore blockage or partial destruction of the porous structure cannot be excluded [88]. However, the BET specific surface area of 2.5 wt.% Co/HZSM5 catalyst increased from 270 to 302 m^2/g, compared to bare support. It might be attributed to the optimum amount and well dispersion of Co particles on its support. The pore volume of different Co loadings decreased from 0.27 to 0.06 cm^3/g with the increase of Co loading from 0 to 20 wt.%. This might be due to some pore blockage of the Co particles. Similarly, the slight change of the average pore diameter of supported catalysts compared to bare support,

probably due to the partial destruction and laceration of the porous structure in the presence of high Co loading.

Table 4.4 Textural properties of the Co/HZSM5 catalysts at different metal loadings and its support.

Support / supported catalyst	Specific surface area (m^2/g)	Pore volume (cm^3/g)	Average pore diameter (nm)
HZSM5	270	0.27	1.8
2.5 wt.% Co/HZSM5	302	0.11	1.4
5 wt.% Co/HZSM5	264	0.10	1.4
10 wt.% Co/HZSM5	204	0.08	1.4
15 wt.% Co/HZSM5	189	0.07	1.4
20 wt.% Co/HZSM5	165	0.06	1.3

The effect of Co metal loading on the glycerol conversion and production yield from glycerol hydrogenolysis, was evaluated at 180 ^{o}C reaction temperature, 7 MPa H_2-pressure for 3 h reaction time in the presence of 20 mg Co/HZSM5/g glycerol. As shown in Figure 4.16, the 2.5 wt.% Co metal loading performed highly in the catalytic glycerol hydrogenolysis with 25.3% of glycerol conversion. Further increase the Co metal loading from 2.5 to 20.0 wt.% resulted to the decrease of glycerol conversion from 25.3 to 14.9% which related to the decrease of their BET specific surface area and pore volume. This might be attributed to the fact that the Co metal loading of 2.5 wt.% had more active surface area available for the reactions but the amount of metal was still too low for hydrogenation activity resulted to the low production of desired products. At the same time, the production yield of acrolein, 1,2-PDO, and 1,3-PDO increased when the Co metal loading was increased from 2.5 to 5.0 wt.%. Further raising the Co metal loading greater than 5.0 wt.% led to the slight decrease of the production yield of acrolein, 1,2-PDO and 1,3-PDO. This might be due to the formation of large catalyst particle on the support surface in the presence of high metal loading, which led to the reduction of catalyst activity, as reported by previous literature [17]. The high production yield of acrolein,

1,2-PDO, and 1,3-PDO were 2.7, 6.3, and 4.2%, respectively. Hence, the appropriate Co metal loading chosen for further study in glycerol hydrogenolysis was 5.0 wt.%.
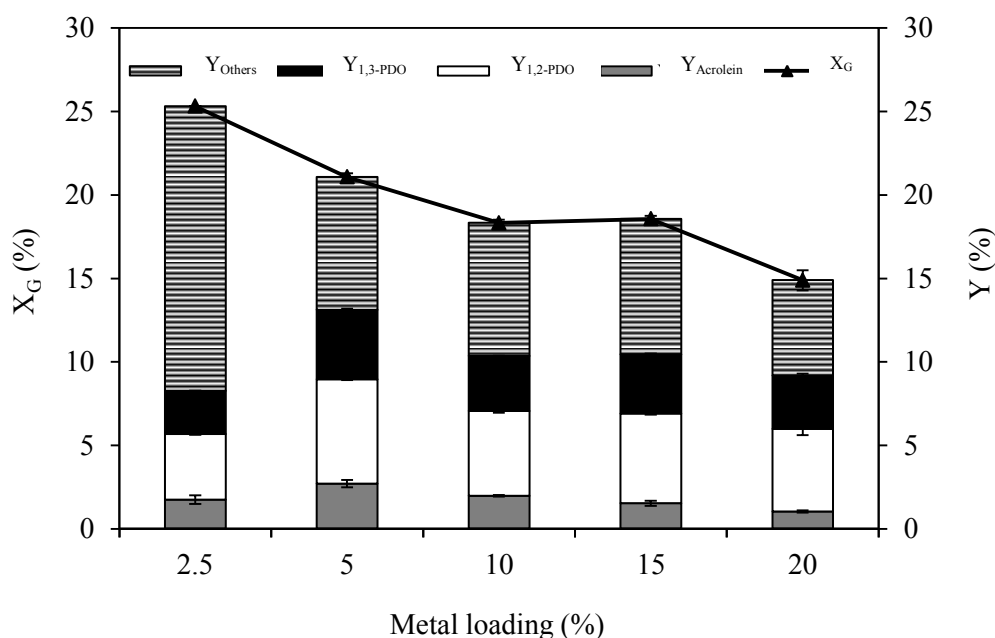

Figure 4.16 Effect of metal loading on glycerol conversion and production yield from glycerol hydrogenolysis over reduced Co/HZSM5 catalysts at 180 ^{o}C reaction temperature, 7 MPa H$_2$-pressure, 3 h reaction time, and 20 wt.% initial glycerol concentration with weight ratio of supported catalysts to glycerol of 20 mg/g.

4.1.5 Effect of reaction time

The influence of the reaction time on the glycerol hydrogenolysis was explored from 3 to 9 h over a 20 mg of 5 wt.% Co/HZSM5/g glycerol at 180 ^{o}C reaction temperature and 7 MPa H$_2$-pressure. As displayed in Figure 4.17, the glycerol conversion gradually increased from 21.1 to 42.5% as the reaction time was increased from 3 to 9 h. It seems that the reaction time has a positive effect on glycerol conversion, as claimed by previous literatures [9, 10, 17, 82, 84, 85]. The reaction time at 3 h provided the production yield of the desired products as acrolein, 1,2-PDO, and 1,3-PDO of 2.7, 6.3, and 4.2%, respectively. These production yields changed slightly when the reaction time was further increased and remained constant

at 6 h. High glycerol conversion, about 42%, and the production yield of acrolein, 1,2-PDO, and 1,3-PDO as about 1.0, 8.0, and 5.2%, respectively, were reached within 6 h and remained constant with further increasing the reaction time. The prolonged reaction time promoted an excess cleavage of C-C bonds to small products and/or the condensation and acetalization of glycerol and acrolein/3-hydroxypropanal to cyclic acetals, resulting to the increase of the other by-products. Hence, the reaction time for 6 h was determined as the optimum operating time for the glycerol hydrogenolysis.
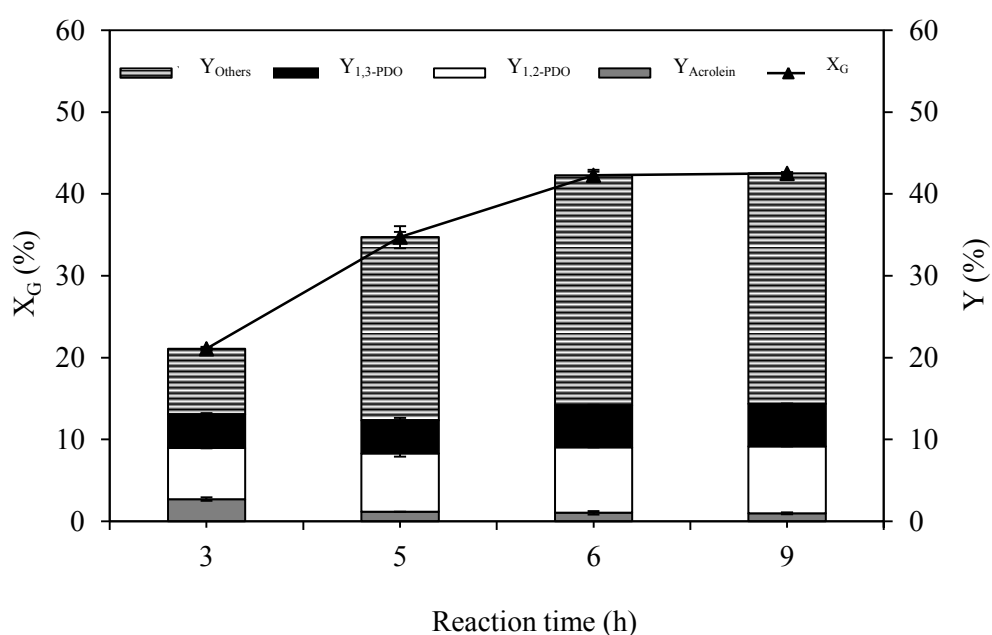

Figure 4.17 Effect of reaction time on glycerol conversion and the production yield from glycerol hydrogenolysis over 20 mg of 5 wt.% Co/HZSM5/g glycerol at 180 $^{\circ}$C reaction temperature, 7 MPa H_2-pressure.

4.1.6 Effect of reaction temperature

Besides the reaction time, the reaction temperature was investigated for catalytic performance of glycerol hydrogenolysis over 20 mg of 5 wt.% Co/HZSM5/g glycerol under the condition of 7 MPa H_2-pressure, 6 h reaction time in the range of 100 to 220 ^{o}C reaction temperature. As demonstrated in Figure 4.18, the glycerol conversion increased continuously from 33.1 to 55.3% as the reaction temperature was increased from 100 to 220 ^{o}C. The formation of 1,2-PDO and 1,3-PDO was observed during the operating temperature of 100 to 220 ^{o}C, providing the maximum yield of 8.0 and 5.2%, respectively at 180 ^{o}C. Further increasing of the operating temperature from 180 to 220 ^{o}C dropped their production yield. This causes by the fact that propanediols can undergo further hydrogenolysis to generate lower alcohol molecules and forming the polymerization products at high temperature, as reported by previous literatures [10, 17, 84, 85, 114]. However, low acrolein yield was formed during the investigated temperature range, its maximum yield was observed at 100 ^{o}C of 1.9% which might be due to this operating temperature still too low for the catalytic performance to 1,3-PDO. In addition, no acrolein was observed at the operating temperature of 140 and 220 ^{o}C which was caused by the further hydrogenolysis of acrolein to 1,3-PDO and/or degrade to lower alcohols. This demonstrated that higher reaction temperature can enhance a more dehydration of glycerol but lowered the production yield of acrolein, 1,2-PDO, and 1,3-PDO due to the formation of other by-products. Hence, to get a good glycerol conversion and high selectivity to the desired products, the reaction temperature of 180 ^{o}C should be used for further studies.
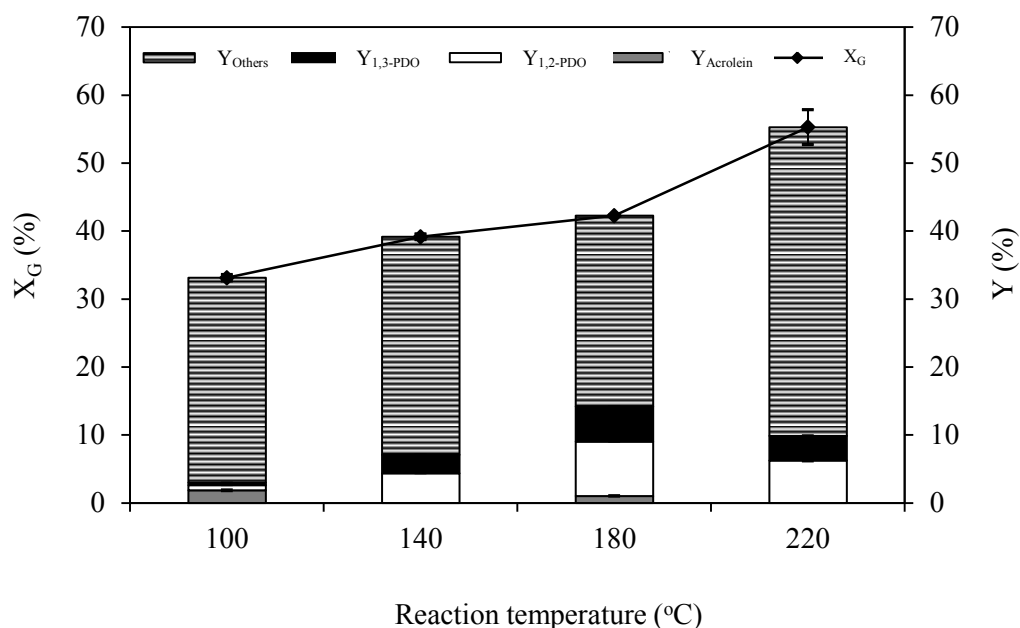
Figure 4.18 Effect of reaction temperature on glycerol conversion and the production yield from glycerol hydrogenolysis over 20 mg of 5 wt.% Co/HZSM5/g glycerol at 7 MPa H_2-pressure for 6 h.

4.1.7 Effect of reaction pressure

The effect of the H_2-pressure on the glycerol conversion and product distribution from glycerol hydrogenolysis was evaluated at 180 ^{o}C reaction temperature for 8 h in the range of 3 to 9 MPa H_2-pressure over the 20 mg of 5 wt.% Co/HZSM5/g glycerol. Figure 4.19 demonstrates that the glycerol conversion increased greatly from 8.7 to 42.3% with the increasing H_2-pressure from 3 to 7 MPa and increased gradually to 44.6% with further increase the operating pressure to 9 MPa. This is attributed to an increase in the dehydration rate in the presence of a high H_2-pressure. The production yield of 1,2-PDO was increased continuously from 3.0 to 8.0%. Similar to the case of 1,3-PDO, it increased from 1.9 to 5.2% when the H_2-pressure was increased from 3 to 7 MPa. Further increase of H_2-pressure from 7 to 9 MPa resulted to the decrease of the production yield of the desired products or the increase of the other by-products. This might be due to the hydrogenation of the desired products to lower carbon molecules (ex. C_2H_5OH) or hydrogenolysis to 1-propanol at high H_2-pressure [10, 115]. Increasing the H_2-pressure can facilitate the

acrolein hydrogenation to form 1,3-PDO and/or degradation to lower alcohols, resulting to the low production yield of acrolein. Hence, the optimum operating pressure for glycerol hydrogenolysis over Co/HZSM5 catalyst was 7 MPa H_2-pressure.
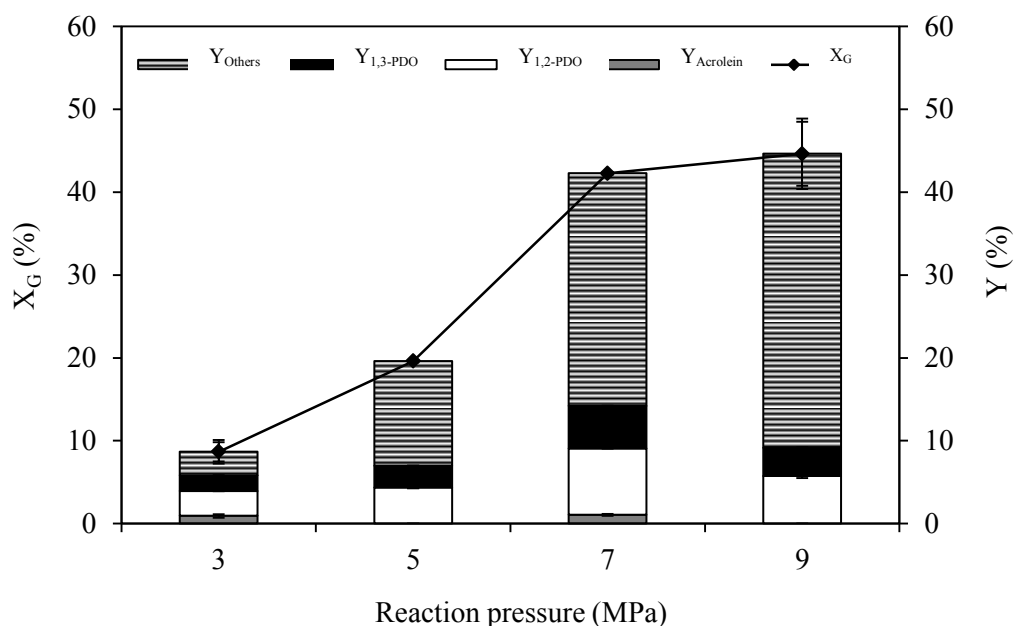
Figure 4.19 Effect of reaction pressure on glycerol conversion and the production yield from glycerol hydrogenolysis over 20 mg of 5 wt.% Co/HZSM5/g glycerol at 180 ^{o}C reaction temperature for 6 h.

4.2 Re-usability of utilized catalyst

After the typical run under the condition of 180 ^{o}C reaction temperature, 7 MPa H_2-pressure for 6 h reaction time, the 5 wt.% Co/HZSM5 catalysts was separated from the liquid product by filtration, washed with acetone and de-ionized water and dried at 110 ^{o}C in hot air oven overnight. Prior the reaction, a used catalyst was reduced again at 600 ^{o}C for 4 h and the hydrogenation reaction was then carried out with fresh glycerol feed under the same conditions. The first (1st) recovered Co/HZSM5 catalyst achieved 43.6% glycerol conversion with the production yield of acrolein, 1,2-PDO, and 1,3-PDO of 7.4, 5.9, and 6.3%, respectively, similar to that of

fresh catalyst as shown in Figure 4.20. This result demonstrated that the first used catalyst had the similar activity compared with the fresh catalyst. Afterward, another reaction was carried out over the used catalyst. For the second and third re-usability, it was found that the glycerol conversion dropped continuously from 43.6 to 29.9%. The production yield of 1,2-PDO and 1,3-PDO were still the same as the fresh catalyst, but no acrolein was produced. It might be due to the crystalline structure of the used Co/HZSM5 catalyst was transformed, as shown in Figure 4.21.
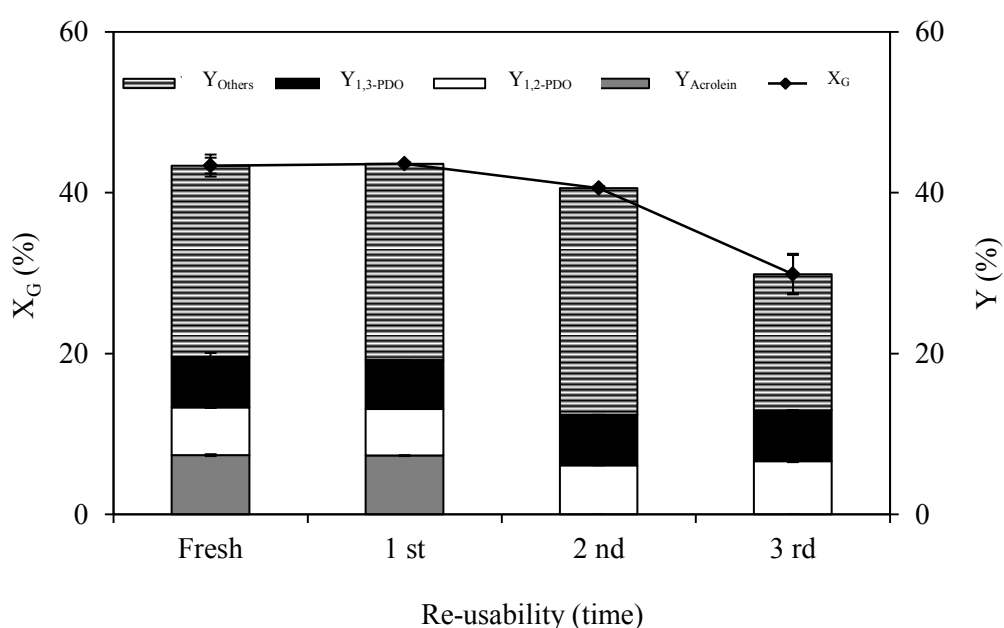
Figure 4.20 Glycerol conversion and the production yield of desired products from glycerol hydrogenolysis over reused catalyst with 20 mg of 5 wt.% Co/HZSM5/g glycerol at 180 $^{\circ}$C reaction temperature and 7 MPa H_2-pressures for 6 h.

It seems to be that the crystalline patterns of the used Co/HZSM5 catalyst showed the main characteristics peaks of HZSM5 and Co_2O_3 but the intensity of these peaks was lower and broader than that of the fresh catalyst, suggesting that partial porous structure of the used catalyst was destruction due to the moisture or pre-heat treatment. Some residue organic matters or pore blockage cannot be excluded, resulting to the limitation of glycerol dehydration to acrolein. This result suggested that the catalytic performance of the used catalyst was not effective for the glycerol

hydrogenolysis in the second re-use due to the limitation of acrolein production, and the increase of the other by-products.
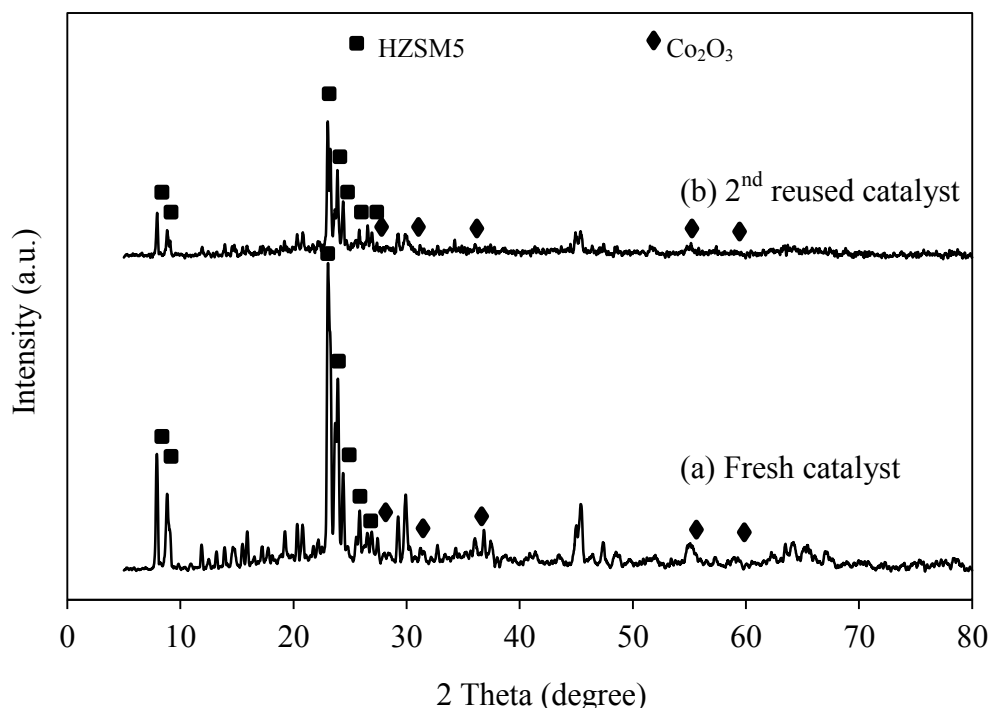
Figure 4.21 XRD patterns of the 5 wt.% Co/HZSM5 catalyst (a) fresh and (b) 2nd used catalyst at wide angle.

4.3 Mechanism of glycerol hydrogenolysis

As annotated in the GC-MS spectra, the GC-MS spectra of the liquid products obtained from glycerol hydrogenolysis over the Co/Al$_2$O$_3$, Co/HZSM5, and Co/AlMCM-41 catalysts as demonstrated in Figure 4.22 (a), (b), and (c), respectively. An about half of the products that were separated by GC-MS could be identified. Of these, largely similar species were found between the reactions mediated by the three different types of supported Co catalyst, such as 1-hydroxyl-2-propanone or acetol, ethylene glycol (EG), 1,2-PDO and 1,3-PDO, and larger molecules, such as 1,3-dioxolane-2-ethyl-4-hydroxymethyl and 1,3-dioxolane-2-ethyl-4-methyl. However, there was no signal of acrolein, suggesting that it might be vaporized on the dry process because its boiling point of 53 ^{o}C [116] was lower than the dried temperature. Some of these compounds have a higher market value compared with crude glycerol

(0.05 USD/lbs) as listed in Table C.1 (Appendix C) that are focused upon hereafter, and also have a high market capacity and application in various industries.

Figure 4.23 demonstrates a simplified schematic diagram showing the possible major reaction pathways to form the products detected over supported Co-based catalysts. Compared to glycerol, all of these generated compounds have many hydrogen and oxygen substitutions with C_2 to C_6 carbon compounds. Previously, the mechanism of glycerol hydrogenolysis to either 1,2-PDO or 1,3-PDO has already been proposed, and consists of the two principal steps of glycerol dehydration and hydrogenation [117]. In the presence of an appropriate catalyst, the -OH group at the C_1 or C_2 position of the glycerol molecule is dehydrated to the two enol intermediate species, 2,3-dihydroxypropene and 3-hydroxypropanal, respectively. Both intermediate species are rapidly rearranged to 1-hydroxyl-2-propanone (or acetol) and acrylaldehyde (or acrolein), which are themselves very reactive and can further react with hydrogen to form 1,2-PDO and 1,3-PDO by catalytic hydrogenation with water as a by-product. In addition, glycerol can be hydrogenated at the C_1-C_2 bond and then cleaved by the addition of H_2 to form EG and methanol in the presence of Co/Al$_2$O$_3$ catalyst. Besides, the in-situ generation of aldols, aldol condensation and acetalization are possible alternative pathways to produce higher alcohols and cyclic acetals.
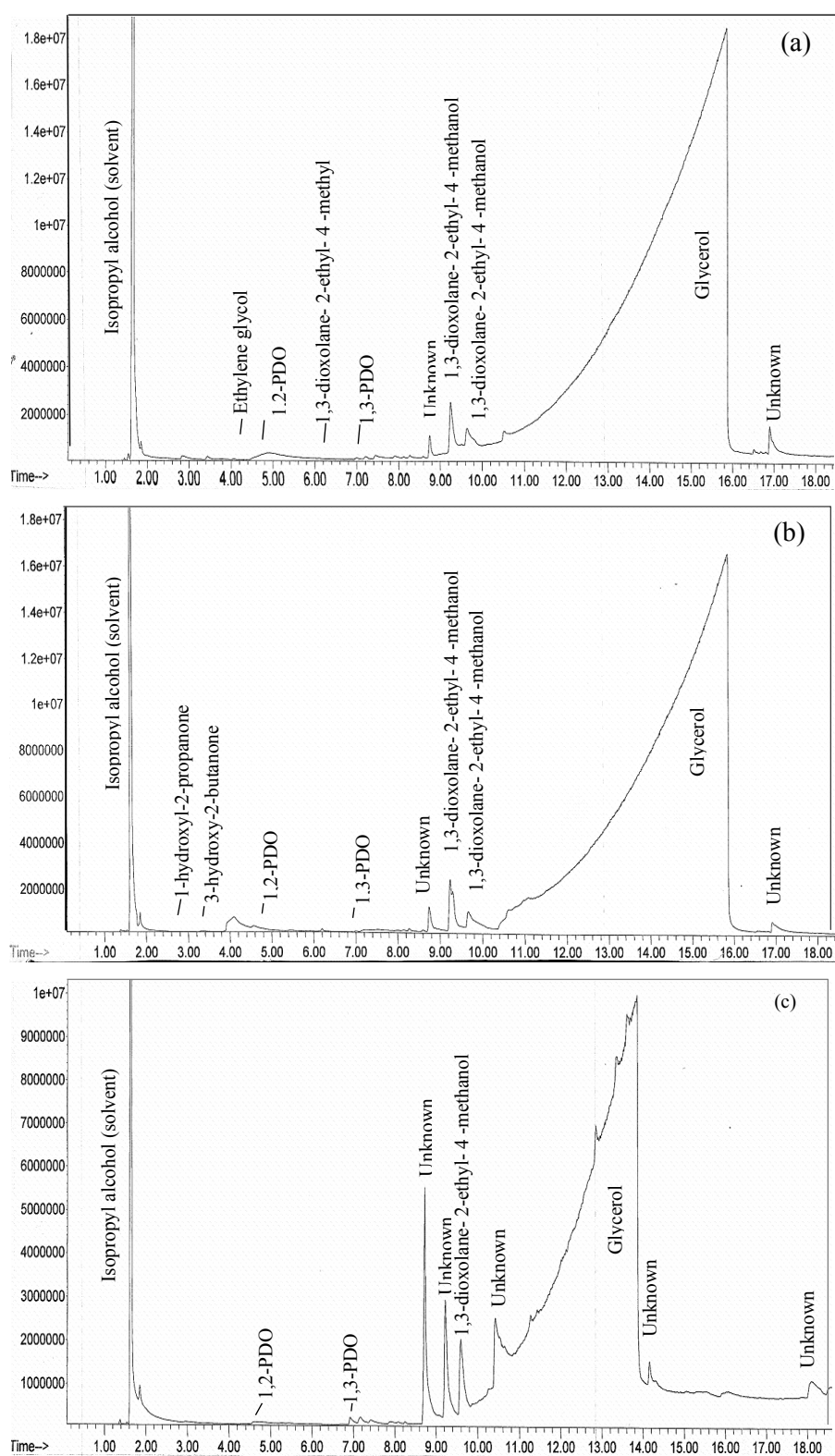
Fig 4.22 GC-MS chromatogram of sample solutions obtained from glycerol hydrogenolysis by (a) Co/Al₂O₃, (b) Co/HZSM5, and (c) Co/AlMCM-41 catalysts.
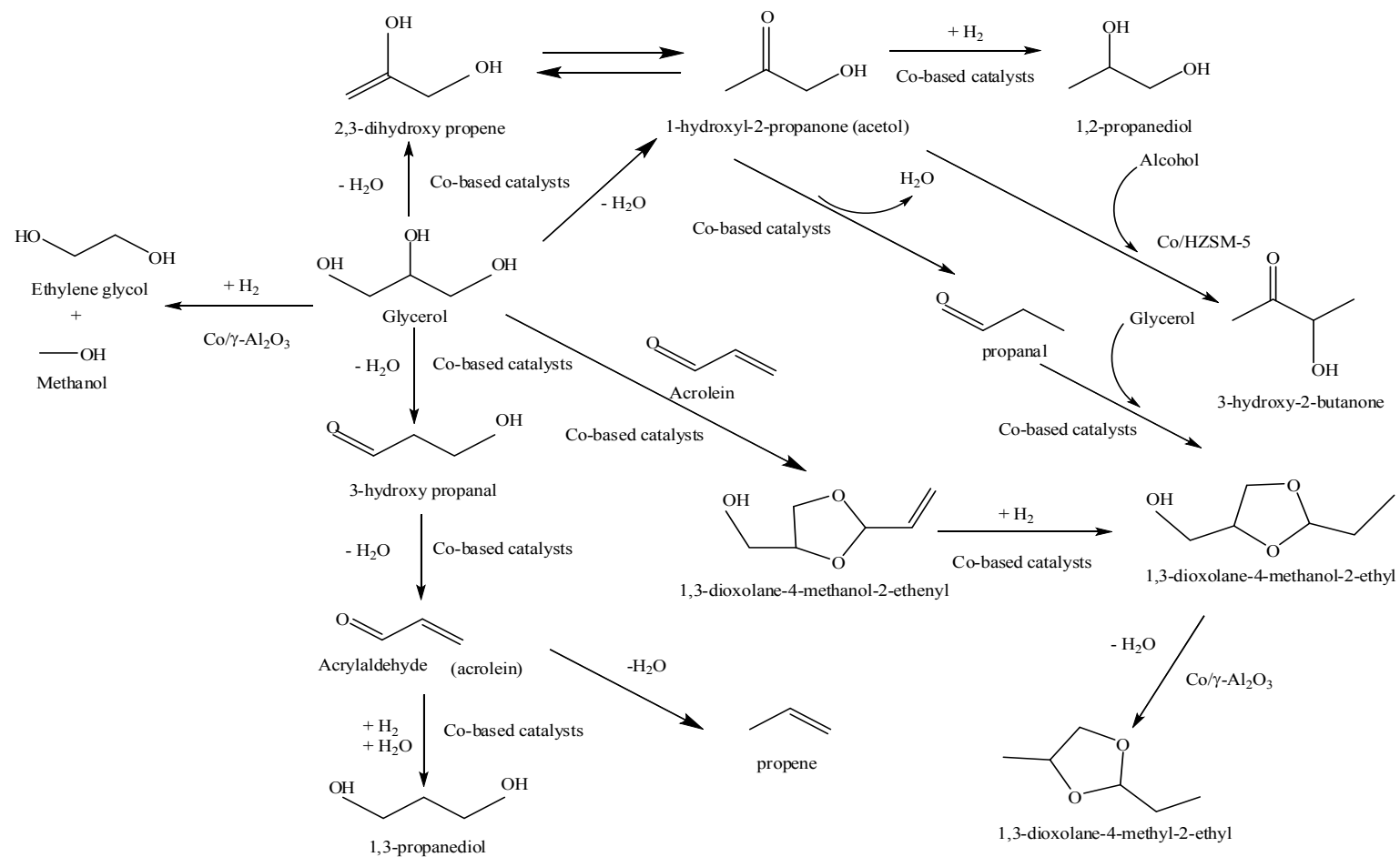
Figure 4.23 Schematic diagram of the possible major reaction pathways of glycerol hydrogenolysis over supported Co-based catalysts.

CHAPTER V

CONCLUSIONS AND RECOMMENDATIONS

5.1 Conclusions

This work was carried out to investigate the effect of parameters and the optimum operating conditions for glycerol hydrogenolysis to desired products including acrolein, 1,2-PDO and 1,3-PDO over Co-based catalysts in an aqueous phase. The results of this work can be concluded as the following:

1. The main products generated in all types of supported Co-based catalysts were acrolein, 1,2-PDO and 1,3-PDO.

2. The activity of glycerol hydrogenolysis depended significantly on the acidity of the utilized catalyst, specific surface area, pore volume and morphology and microstructure of metal.

3. Strong-strength acid catalyst exhibited a better activity for glycerol hydrogenolysis to acrolein and propanediols.

4. The Co/HZSM5 exhibited a better activity for glycerol hydrogenolysis compared with Al_2O_3 and AlMCM-41 supported catalysts.

5. Glycerol hydrogenolysis was dependent upon the weight ratio of catalyst to glycerol, metal loading, reaction temperature, H_2-pressure and reaction time.

6. The maximum conversion of glycerol was 42% and the maximum yield of the desired products including acrolein, 1,2-PDO and 1,3-PDO were 1, 8 and 5%, respectively in the presence of 5 wt.% Co/HZSM5 at the ratio of supported catalysts to glycerol of 20 mg/g at 180 $^\circ$C reaction temperature, 7 MPa H_2-pressure and 6 h reaction time.

7. The catalytic performance of the 2nd -reused catalyst was not effective for the glycerol hydrogenolysis due to the limitation of acrolein production, and the increase of the other by-products.

8. The mechanism of glycerol hydrogenolysis to the desired products as acrolein, 1,2-PDO or 1,3-PDO has already been proposed, consisting of the two principal steps of glycerol dehydration and hydrogenation.

5.2 Recommendations

1. To enhance more glycerol conversion and improve the yield for desired hydrogenolysis products over supported Co-based catalyst in an aqueous phase, the addition of the second metal in the appropriate ratio and the influence of initial glycerol concentration were suggested for further study.

2. The costs of energy consumption for the glycerol hydrogenolysis to product distribution need to be evaluated.

REFERENCES

[1] Cavani, F., Guidetti, S., Marinelli, L., Piccinini, M., Ghedini, E., and Signoretto, M. The control of selectivity in gas-phase glycerol dehydration to acrolein catalysed by sulfated zirconia. Applied Catalysis B: Environmental 100 (October 2010) : 197–204.

[2] Deleplanque, J., Dubois, J.-L., Devaux, J.-F., and Ueda, W. Production of acrolein and acrylic acid through dehydration and oxydehydration of glycerol with mixed oxide catalysts. Catalysis Today 157 (November 2010) : 351-358.

[3] Suprun, W., Lutecki, M., Haber, T., and Papp, H. Acidic catalysts for the dehydration of glycerol: Activity and deactivation. Journal of Molecular Catalysis A: Chemical 309 (August 2009) : 71-78.

[4] Frusteri, F., Arena, F., Bonura, G., Cannilla, C., Spadaro, L., and Di Blasi, O. Catalytic etherification of glycerol by *tert*-butyl alcohol to produce oxygenated additives for diesel fuel. Applied Catalysis A: General 367 (October 2009) : 77–83.

[5] Demirel-Gülen, S., Lucas, M., and Claus, P. Liquid phase oxidation of glycerol over carbon supported gold catalysts, Catalysis Today 102-103 (May 2005) : 166–172.

[6] Kurosaka, T., Maruyama, H., Naribayashi, I., and Sasaki, Y. Production of 1,3-propanediol by hydrogenolysis of glycerol catalyzed by $Pt/WO_3/ZrO_2$. Catalysis Communications 9 (March 2008) : 1360–1363.

[7] Kusunoki, Y., Miyazawa, T., Kunimori, K., and Tomishige, K. Highly active metal-acid bifunctional catalyst system for hydrogenolysis of glycerol under mild reaction conditions. Catalysis Communications 6 (October 2005) : 645-649.

[8] Dasari, M.A., Kiatsimkul, P., Sutterlin, W.R., and Suppes, G.J. Low-pressure hydrogenolysis of glycerol to propylene glycol. Applied Catalysis A: General 281 (January 2005) : 225–231.

[9] Ma, L., He, D., and Li, Z. Promoting effect of rhenium on catalytic performance of Ru catalysts in hydrogenolysis of glycerol to propanediol. Catalysis Communications 9 (September 2008) : 2489-2495.

[10] Balaraju, M., Rekha, V., Sai Prasad, P.S., Prabhavathi Devi, B.L.A., Prasad, R.B.N., and Lingaiah, N. Influence of solid acids as co-catalysts on glycerol hydrogenolysis to propylene glycol over Ru/C catalysts. Applied Catalysis A: General 354 (February 2009) : 82-87.

[11] Nakagawa, Y., Shinmi, Y., Koso, S., and Tomishige, K. Direct hydrogenolysis of glycerol 1,3-propanediol over rhenium-modified iridium catalyst. Journal of Catalysis 272 (June 2010) : 191-194.

[12] Chaminand, J., Djakovitch, L.aurent, Gallezot, P., Marion, P., Pinel, C., and Rosier, C. Glycerol hydrogenolysis on heterogeneous catalysts. Green Chemistry Journals 6 (August 2004) : 359-361.

[13] Guo, X., Li, Y., Shi, R., Liu, Q., Zhan, E., and Shen, W. Co/MgO catalysts for hydrogenolysis of glycerol to 1,2-propanediol. Applied Catalysis A: General 371 (December 2009) : 108–113.

[14] Szajewski, J. Propylene glycol (PIM 443). IPCS INChem [online]. August, 1991. Available from: http://www.inchem.org/documents/pims/chemical/pim443.htm. [2001, August 25].

[15] Yazdani, S.S., and Gonzalez, R. Anaerobic fermentation of glycerol: a path to economic viability for the biofuels industry. Current Opinion in Biotechnology 18 (May 2007) : 213-219.

[16] Connor, R., and Adkins, H. Hydrogenolysis of oxygenated organic compounds. Journal of the American Chemical Society 54 (December 1932) : 4678-4690.

[17] Guo, L., Zhou, J., Mao, J., Guo, X., and Zhang, S. Supported Cu catalysts for the selective hydrogenolysis of glycerol to propanediols. Applied Catalysis A: General 367 (August 2009) : 93-98.

[18] Garcia, A.P., Ramos, E.R., Angel, G.del, Navarrete, J., and Contreras, C.A. Catalytic activity of supported cobalt catalyst, in the crotonaldehyde hydrogenation reaction. AZojomo: Journal of Materials Online 3 (December 2007) : 1-9.

[19] Wikipedia the free encyclopedia. Glycerol. Wikimedia Foundation, Inc [online]. Available from: http://en.wikipedia.org/wiki/Glycerol. [2012, August 2].

[20] Bibra. Toxicity profile for glycerol. Bibra toxicology advice and consulting [online]. 1993. Available from: http://www.bibra-information.co.uk/profile-109.html [2013, March 13].

[21] Perry, R.H., Green, D.W., and Maloney, J.O. Perry's chemical engineers' handbook. 7th edition. New York: McGraw-Hill, 1997.

[22] Brady, J.E. General chemistry principal and structure. 5th edition. Wiley, John & Sons, 2007.

[23] Rahmat, N., Abdullah, A.Z., and Mohamed, A.R. Recent progress on innovative and potential technologies for glycerol transformation into fuel additives: A critical review. Renewable and Sustainable Energy Reviews 14 (April 2010) : 987-1000.

[24] Striūgas, N. Analysis of acrolein production during glycerol combustion. Laboratory of combustion processes [online]. 2010. Available from: http://cost.ensic.univlorraine.fr/cost/fileadmin/utilisateurs/COST_Documents/20100128-MC/20100915-Meeting/WG2/L1830-Striugas.pdf [2013, March 15].

[25] Kiatkittipong, W., Intaracharoen, P., Laosiripojana, N., Chaisuk, C., Praserthdam, P., and Assabumrungrat, S. Glycerol ethers synthesis from glycerol etherification with tert-butyl alcohol in reactive distillation. Computers & Chemical Engineering 35 (October 2011) : 2034‑2043.

[26] Pagliaro, M., and Rossi, M. The future of glycerol: new uses of a versatile raw material. In the royal society of chemistry, RSC Green Chemistry, 8, 2nd edition, pp.1-28. Cambridge : RSC publishing, 2008.

[27] Muhammad, A., and Ahmad, Z.A. Critical review on the current scenario and significance of crude glycerol resulting from biodiesel industry towards more sustainable renewable energy industry. Renewable and Sustainable Energy Reviews 16 (June 2012) : 2671‑2686.

[28] Clomburg, J.M., and Gonzalez R. Anaerobic fermentation of glycerol: a platform for renewable fuels and chemicals. Trends in Biotechnology 31 (January 2013) : 20-28.

[29] Yan, S., Salley, S.O., and Simon Ng., K.Y. Simultaneous transesterification and esterification of unrefined or waste oils over ZnO-La$_2$O$_3$ catalysts. Applied Catalysis A: General 353 (February 2009) : 203–212.

[30] Noweck, K. Production, Technologies and Applications of Fatty Alcohols. In *abiosus* e.V. Conferences, the 4th Workshop on Fats and Oils as Renewable Feedstock for the Chemical Industry, pp. 20. Karlsruhe, Germany, 2011.

[31] Sevas educational society. Manufacturing processes. Glycerol [online]. 2007. Available from: http://www.sbioinformatics.com/design_thesis/Glycerol/ Glycerol_Methods-2520of-2520Production.pdf [2013, March 16].

[32] Wang, Z.X., Zhuge, J., Fang, H., and Prior, B.A. Glycerol production by microbial fermentation: A review. Biotechnol Advances 19 (June 2001) : 201-223.

[33] Léon, R., and Galván, F. Glycerol photoproduction by free and Ca-alginate entrapped cells of *Chlamydomonas reinhardtii*. Journal of Biotechnology 42 (August 1995) : 61−67.

[34] Yazdani, S.S., and Gonzalez, R. Anaerobic fermentation of glycerol: a path to economic viability for the biofuels industry. Current Opinion in Biotechnology 18 (May 2007) : 213–219.

[35] Wolfson, A., Litvak, G., Dlugy, C., Shotland, Y., and Tavor, D. Employing crude glycerol from biodiesel production as an alternative green reaction medium. Industrial Crops and Products 30 (July 2009) : 78-81.

[36] National Biodiesel Board. US biodiesel demand. Biodiesel America's Advanced Biofuel [online]. 2008. Available from: http://www.biodiesel.org/pdf files/fuelfactsheets/ProductionGraphSlide.pdf [2012, January 10].

[37] Petrosil Group. U.S. glycerine production soars in 2009. Petrosil Glycerine Report digital market intelligence [online]. 2009. Available from: http://www.glycerinereport.com/20091911/us-glycerine-production-soars-2009 [2012, January 10].

[38] ABG Inc. Company. Glycerin market analysis. U.S. Soybean Export Council Inc. [online]. 2007. Available from: http://www.asasea.com/downloaddoc.php [2012, January 10].

[39] Omni Tech International Ltd. The potential impact of rising petrochemical prices on soy use for industrial applications. A Survey of Recent Chemical Price Trends [online]. 2008. Available from: http://soynewuses.org/wp-content/uploads/pdf/2010_PriceTrendUpdate.pdf. [2012, January 10].

[40] Bogaart, V. Glycerin Marke Brief. Croda Oleochemicals – new ideas in natural Ingredients [online]. 2009. Available from: http://www.npt.nl/vereniging/images/stories/Verslagen/PresentatieBogaartCroda 15042010.pdf [2012, January 10].

[41] Yang, F., Hanna, M.A., and Sun, R. Value-added uses for crude glycerol--a byproduct of biodiesel production. Biotechnology for Biofuels 5 (March 2012) : 13.

[42] Guerrero-Pérez, M.O., Rosas, J.M., Bedia, J., Rodríguez-Mirasol, J., and Cordero, T. Recent Inventions in Glycerol Transformations and Processing. Recent Patents on Chemical Engineering 2 (2009) : 11-21.

[43] Pachauri, N., and He, B. Value-added Utilization of Crude Glycerol from Biodiesel Production: A Survey of Current Research Activities. In American Society of Agricultural and Biological Engineers, The 2006 ASABE Annual International Meeting, 066223. Oregon: ASABE Oregon Convention Center, 2006.

[44] Slinn, M., Kendall, K., Mallon, C., and Andres, J. Steam reforming of biodiesel by-product to make renewable hydrogen. Bioresource Technology 99 (September 2008) : 5851-5858.

[45] Pairojpiriyakul, T., Croiset, E., Kiatkittipong, W., Kiatkittipong, K., Arpornwichanop, A., Assabumrungrat, S. Hydrogen production from catalytic supercritical water reforming of glycerol with cobalt-based catalysts. International journal of hydrogen energy 38 (April 2013) : 4368-4379.

[46] Adhikari, S., Fernando, S.D., and Haryanto, A. Hydrogen production from glycerin by steam reforming over nickel catalysts. Renewable Energy 33 (May 2008) : 1097-1100.

[47] Iriondo, A., et al. Hydrogen production from glycerol over nickel catalysts supported on Al_2O_3 modified by Mg, Zr, Ce or La. <u>Topics in Catalysis</u> 49 (July 2008) : 46-58.

[48] Kondarides, D.I., Daskalaki, V.M., Patsoura, A., and Verykios, X.E. Hydrogen production by photo induced reforming of biomass components and derivatives at ambient conditions. <u>Catalysis Letters</u> 122 (April 2008) : 26-32.

[49] Kamonsuangkasem, K., Therdthianwong, S., and Therdthianwong, A. Hydrogen production from yellow glycerol via catalytic oxidative steam reforming. <u>Fuel Processing Technology</u> 106 (February 2013) : 695–703.

[50] Valliyappan, T., Bakhshi, N.N., and Dalai, A.K. Pyrolysis of glycerol for the production of hydrogen or syn gas. <u>Bioresource Technology</u> 99 (July 2008) : 4476-4483.

[51] Fernández, Y., Arenillas, A., Díez, M.A., Pis, J.J., and Menéndez, J.A. Pyrolysis of glycerol over activated carbons for syngas production. <u>Journal of Analytical and Applied Pyrolysis</u> 84 (March 2009) : 145-150.

[52] Xiu, S., Shahbazi, A., Shirley, V., Mims, M.R., and Wallace, C.W. Effectiveness and mechanisms of crude glycerol on the biofuel production from swine manure through hydrothermal pyrolysis. <u>Journal of Analytical and Applied Pyrolysis</u> 87 (March 2010) : 194-198.

[53] Skoulou, V.K., Manara, P., and Zabaniotou, A.A. H_2 enriched fuels from co-pyrolysis of crude glycerol with biomass. <u>Journal of Analytical and Applied Pyrolysis</u> 97 (September 2012) : 198-204.

[54] May, A., Salvadó, J., Torras, C., and Montané, D. Catalytic gasification of glycerol in supercritical water. <u>Chemical Engineering Journal</u> 160 (June 2010) : 751-759.

[55] Guo, S., Guo, L., Cao, C., Yin, J., Lu, Y., and Zhang, X. Hydrogen production from glycerol by supercritical water gasification in a continuous flow tubular reactor. <u>International Journal of Hydrogen Energy</u> 37 (April 2012) : 5559-5568.

[56] Atong, D., Pechyen, C., Aht-Ong, D., and Sricharoenchaikul, V. Synthetic olivine supported nickel catalysts for gasification of glycerol. <u>Applied Clay Science</u> 53 (August 2011) : 244-253.

[57] Wei, L., Pordesimo, L.O., Haryanto, A., and Wooten, J. Co-gasification of hardwood chips and crude glycerol in a pilot scale downdraft gasifier. Bioresource Technology 102 (March 2011) : 6266-6272.

[58] Wua, K.J., Lin, Y.H., Lo, Y.C., Chen, C.Y., Chen, W.M., and Chang, J.S. Converting glycerol into hydrogen, ethanol, and diols with a *Klebsiella* sp. HE1 strain via anaerobic fermentation. Journal of the Taiwan Institute of Chemical Engineers 42 (January 2011) : 20‑25.

[59] Metsoviti, M., Paraskevaidi, K., Koutinas, A., Zeng, A., and Papanikolaou, S. Production of 1,3-propanediol, 2,3-butanediol and ethanol by a newly isolated *Klebsiella oxytoca* strain growing on biodiesel-derived glycerol based media. Process Biochemistry 47 (December 2012) : 1872-1882.

[60] Moon, C., Lee, C.H., Sang, B.I., and Uma, Y. Optimization of medium compositions favoring butanol and 1,3-propanediol production from glycerol by Clostridium pasteurianum. Bioresource Technology 102 (November 2011) : 10561‑10568.

[61] Kao, W.C., Lin, D.S., Cheng, C.L., Chen, B.Y., Lin, C.Y., and Chang, J.S. Enhancing butanol production with Clostridium pasteurianum CH4 using sequential glucose‑glycerol addition and simultaneous dual-substrate cultivation strategies. Bioresource Technology 135 (May 2013) : 324‑330.

[62] Chai, S.H., Wang, H.P., Liang, Y., and Xu, B.Q. Sustainable production of acrolein: Gas-phase dehydration of glycerol over Nb_2O_5 catalyst. Journal of Catalysis 250 (September 2007) : 342-349.

[63] Chai, S.H., Wang, H.P., Liang, Y., and Xu, B.Q. Sustainable production of acrolein: Investigation of solid acid-base catalysts for gas-phase dehydration of glycerol. Green Chemistry (June 2007) : 1130-1136.

[64] Atia, H., Armbruster, U., and Martin, A. Dehydration of glycerol in gas phase using heteropolyacid catalysts as active compounds. Journal of Catalysis 258 (August 2008) : 71-82.

[65] Tsukuda, E., Sato, S., Takahashi, R., and Sodesawa, T. Production of acrolein from glycerol over silica-supported heteropolyacids. Catalysis Communications 8 (September 2007) : 1349-1353.

[66] Witsuthammakul, A., and Sooknoi, T. Direct conversion of glycerol to acrylic acid via integrated dehydration‑oxidation bed system. Applied Catalysis A: General 413– 414 (January 2012) : 109– 116.

[67] Rodrigues, E.G., Pereira, M.F.R., Delgado, J.J., Chen, X., and Órfão, J.J.M. Enhancement of the selectivity to dihydroxyacetone in glycerol oxidation using gold nanoparticles supported on carbon nanotubes. Catalysis Communications 16 (November 2011) : 64-69.

[68] Pollington, S.D., et al. Enhanced selective glycerol oxidation in multiphase structured reactors. Catalysis Today 145 (July 2009) :169‑175.

[69] Lu, L., Wei, L., Zhu, K., Wei, D., and Hua, Q. Combining metabolic engineering and adaptive evolution to enhance the production of dihydroxyacetone from glycerol by *Gluconobacter oxydans* in a low-cost way. Bioresource Technology 117 (August 2012) : 317-324.

[70] Gil, S., Marchena, M., Sánchez-Silva, L., Romero, A., Sánchez, P., and Valverde, J.L. Effect of the operation conditions on the selective oxidation of glycerol with catalysts based on Au supported on carbonaceous materials. Chemical Engineering Journal 178 (December 2011) : 423-435.

[71] Liang, D., Gao, J., Sun, H., Chen, P., Hou, Z., and Zheng, X. Selective oxidation of glycerol with oxygen in a base-free aqueous solution over MWNTs supported Pt catalysts. Applied Catalysis B: Environmental 106 (August 2011) : 423-432.

[72] Anuar, M.R., Abdullah, A.Z., and Othman, M.R. Etherification of glycerol to polyglycerols over hydrotalcite catalyst prepared using a combustion method. Catalysis Communications 32 (February 2013) : 67–70.

[73] Cristina, G.S., Ramon, M.T., Josefa, M.M.R., Jose, S.G., Antonio, J.L., and Pedro, M.T. Etherification of glycerol to polyglycerols over MgAl mixed oxides. Catalysis Today 167 (June 2011) : 84–90.

[74] Gholami, Z., Abdullah, A.Z., and Lee, K.T. Glycerol etherification to polyglycerols using $Ca_{1+x} Al_{1\_x} La_xO_3$ composite catalysts in a solventless

medium. <u>Journal of the Taiwan Institute of Chemical Engineers</u> 44 (2013) : 117‒122.

[75] van Heerden, C.D., and Nicol, W. Continuous succinic acid fermentation by *Actinobacillus succinogenes*. <u>Biochemical Engineering Journal</u> 73 (April 2013) : 5-11.

[76] Song, H., and Lee, S.Y. Production of succinic acid by bacterial fermentation. <u>Enzyme and Microbial Technology</u> 39 (July 2006) : 352-361.

[77] Vlysidis, A., Binns, M., Webb, C., and Theodoropoulos, C. Glycerol utilisation for the production of chemicals: Conversion to succinic acid, a combined experimental and computational study. <u>Biochemical Engineering Journal</u> 58–59 (December 2011) : 1-11.

[78] Moralejo-Gárate, H., Kleerebezem, R., Mosquera-Corral, A., and van Loosdrecht, M.C.M. Impact of oxygen limitation on glycerol-based biopolymer production by bacterial enrichments. <u>Water Research</u> 47 (March 2013) : 1209-1217.

[79] Besson, M., Gallezot, P., Pigamo, A., and Reifsnyder, S. Development of an improved continuous hydrogenation process for the production of 1,3-propanediol using titania supported ruthenium catalysts. <u>Applied Catalysis A: General</u> 250 (September 2003) : 117–124.

[80] Feng, J., Fu, H., Wang, J., Li, R., Chen, H., and Li, X. Hydrogenolysis of glycerol to glycols over ruthenium catalysts: Effect of support and catalyst reduction temperature. <u>Catalysis Communications</u> 9 (March 2008) : 1458-1464.

[81] Roy, D., Subramaniam, B., and Chaudhari, R.V. Aqueous phase hydrogenolysis of glycerol to 1,2-propanediol without external hydrogen addition. <u>Catalysis Today</u> 156 (October 2010) : 31‒37.

[82] Gong, L., et al. Selective hydrogenolysis of glycerol to 1,3-propanediol over a $Pt/WO_3/TiO_2/SiO_2$ catalyst in aqueous media. <u>Applied Catalysis A: General</u> 390 (December 2010) : 119–126.

[83] Ma, L., and He, D. Influence of catalyst pretreatment on catalytic properties and performances of $Ru–Re/SiO_2$ in glycerol hydrogenolysis to propanediols. <u>Catalysis Today</u> 149 (January 2010) : 148–156.

[84] Hamzah, N., Nordin, N.M., Nadzri, A.H.A., Nik, Y.A., Kassim, M.B., and Yarmo, M.A. Enhanced activity of Ru/TiO$_2$ catalyst using bisupport, bentonite-TiO$_2$ for hydrogenolysis of glycerol in aqueous media. Applied Catalysis A: General 419– 420 (March 2012) : 133– 141.

[85] Zhu, S., Qiu, Y., Zhu, Y., Hao, S., Zheng, H., and Li, Y. Hydrogenolysis of glycerol to 1,3-propanediol over bifunctional catalysts containing Pt and heteropolyacids. Catalysis Today 212 (September 2012) : 120–126.

[86] Gandarias, I., Arias, P.L., Fernandez, S.G., Requies, J., Doukkali, M.E., and Guemez, M.B. Hydrogenolysis through catalytic transfer hydrogenation: Glycerol conversion to 1,2-propanediol. Catalysis Today 195 (November 2012) : 22– 31.

[87] Liu, L., Zhang, Y., Wang, A., and Zhang, T. Mesoporous WO$_3$ supported Pt catalyst for hydrogenolysis of glycerol to 1,3-propanediol. Chinese Journal of Catalysis 33 (July-August 2012) : 1257-1261.

[88] Vasiliadou, E.S., Eggenhuisen, T.M., Munnik, P., de Jongh, P.E., de Jong, K.P., and Lemonidou, A.A. Synthesis and performance of highly dispersed Cu/SiO$_2$ catalysts for the hydrogenolysis of glycerol. Applied Catalysis B: Environmental In Press (January 2013).

[89] Bolado, S., Treviño, R.E., García-Cubero, M.T., and González-Benito, G. Glycerol hydrogenolysis to 1, 2 propanediol over Ru/C catalyst. Catalysis Communications 12 (November 2010) : 122–126.

[90] Lee, S.H., and Moon, D.J. Studies on the conversion of glycerol to 1,2-propanediol over Ru-based catalyst under mild conditions. Catalysis Today 174 (October 2011) : 10– 16.

[91] Masel, R.I. Catalysis by metals. Chemical kinetics and catalysis, pp. 879. New York : John Wiley & Sons, Inc., 2001.

[92] Llorca, J., Homs, N., Sales, J., and de la Piscina, P.R. Efficient production of hydrogen over supported cobalt catalysts from ethanol steam reforming. Journal of Catalysis 209 (July 2002) : 306-317.

[93] Song, H., Zhang, L.Z., Watson, R.B., Braden, D., and Ozkan, U.S. Investigation of bio-ethanol steam reforming over cobalt-based catalysts. Catalysis Today 129 (December 2007) : 346-354.

[94] Moura, J.S., et al. Ethanol steam reforming over rhodium and cobalt-based catalysts: Effect of the support. International Journal of Hydrogen Energy 37 (February 2012) : 3213-3224.

[95] Zhu, S., Zhu, Y., Gao, X., Mo, T., Zhu, Y., and Li, Y. Production of bioadditives from glycerol esterification over zirconia supported heteropolyacids. Bioresource Technology 130 (February 2013) : 45-51.

[96] Trejda, M., Stawicka, K., Dubinska, A., and Ziolek, M. Development of niobium containing acidic catalysts for glycerol esterification. Catalysis Today 187 (June 2012) : 129– 134.

[97] Zhou, L., Al-Zaini, E., and Adesina, A.A. Catalytic characteristics and parameters optimization of the glycerol acetylation over solid acid catalysts. Fuel 103 (January 2013) : 617‑625.

[98] Melero, J.A., Vicente, G., Paniagua, M., Morales, G., and Muñoz, P. Etherification of biodiesel-derived glycerol with ethanol for fuel formulation over sulfonic modified catalysts. Bioresource Technology 103 (January 2012) : 142-151.

[99] Alhanash, A., Kozhevnikova, E.F., and Kozhevnikov, I.V. Hydrogenolysis of glycerol to propanediol over Ru: Polyoxometalate bifunctional catalyst. Catalysis Letters 120 (January 2008) : 307-311.

[100] Ferrari, M., Delmon, B., and Grange, P. Influence of the impregnation order of molybdenum and cobalt in carbon-supported catalysts for hydrodeoxygenation reactions. Carbon 40 (April 2002) : 497–511.

[101] Bhagiyalakshmi, M., Yun, L.J., Anuradha, R., and Jang, H.T. Utilization of rice husk ash as silica source for the synthesis of mesoporous silicas and their application to CO_2 adsorption through TREN/TEPA grafting. Journal of Hazardous Materials 175 (March 2010) : 928-938.

[102] Fischer, A., Maciejewski, M., Bürgi, T., Mallat, T., and Baiker, A. Cobalt-catalyzed amination of 1,3-propanediol: Effects of catalyst promotion and use of supercritical ammonia as solvent and reactant. Journal of Catalysis 183 (April 1999) : 373-383.

[103] Antoniak, K., Kowalik, P., Prochniak, W., Konkol, M., Wach, A., Kuśtrowski, P., and Ryczkowski, J. Effect of flash calcined alumina support and potassium doping on the activity of Co–Mo catalysts in sour gas shift process. Applied Catalysis A: General 423– 424 (May 2012) : 114– 120.

[104] Jongsomjit, B., Panpranot, J., and Goodwin, J.G. Effect of zirconia-modified alumina on the properties of Co/γ-Al$_2$O$_3$ catalysts. Journal of Catalysis 215 (April 2003) : 66–77.

[105] Wang, S., Yin, Q., Guo, J., Ru, B., and Zhu, L. Improved Fischer–Tropsch synthesis for gasoline over Ru, Ni promoted Co/HZSM-5 catalysts. Fuel 108 (June 2013) : 597–603.

[106] Hongmei, L., and Yide, X. H$_2$-TPR study on Mo/HZSM-5 catalyst for CH4 dehydroaromatization. Chinese Journal of Catalysis 27 (April 2006) : 319–323.

[107] Han, Y., Lu, C., Xu, D., Zhang, Y., Hu, Y., and Huang, H. Molybdenum oxide modified HZSM-5 catalyst: Surface acidity and catalytic performance for the dehydration of aqueous ethanol. Applied Catalysis A: General 396 (April 2011) : 8–13.

[108] Deepa, G., Sankaranarayanan, T.M., Shanthi, K., and Viswanathan, B. Hydrodenitrogenation of model N-compounds over NiO-MoO$_3$ supported on mesoporous materials. Catalysis Today 198 (December 2012) : 252– 262.

[109] Zhang, Y, Liu, B., Tu, B., Dong, Y., and Cheng, M. Redox cycling of Ni–YSZ anode investigated by TPR technique. Solid State Ionics 176 (September 2005) : 2193 – 2199.

[110] Shinmi, Y., Koso, S., Kubota, T., Nakagawa, Y., and Tomishige, K. Modification of Rh/SiO$_2$ catalyst for the hydrogenolysis of glycerol in water. Applied Catalysis B: Environmental 94 (February 2010) : 318–326.

[111] Souza, M.J.B., Marinkovic, B.A., Jardim, P.M., Araujo, A.S., Pedrosa, A.M.G., Souza, R.R. HDS of thiophene over CoMo/AlMCM-41 with different Si/Al ratios. Applied Catalysis A: General 316 (January 2007) : 212–218.

[112] Kim, J.H., Tanabe, M., and Niwa, M. Characterization and catalytic activity of the AlMCM-41 prepared by a method of gel equilibrium adjustment. Microporous Materials 10 (June 1997) : 85-93.

[113] Gandarias, I., Arias, P.L., Requies, J., Guemez, M.B., and Fierro, J.L.G. Hydrogenolysis of glycerol to propanediols over a Pt/ASA catalyst: The role of acid and metal sites on product selectivity and the reaction mechanism. Applied Catalysis B: Environmental 97 (June 2010) : 248–256.

[114] Zheng, Y., Chen, X., and Shen, Y. Commodity chemicals derived from glycerol, an important biorefinery feedstock. Chemical Reviews 108 (December 2008) : 5253–5277.

[115] Miyazawa, T., Kusunoki, Y., Kunimori, K., and Tomishige, K. Glycerol conversion in the aqueous solution under hydrogen over Ru/C + an ion-exchange resin and its reaction mechanism. Journal of Catalysis 240 (June 2006) : 213–221.

[116] Wikipedia the free encyclopedia. Acrolein. Wikimedia Foundation, Inc [online]. Available from: http://en.wikipedia.org/wiki/Acrolein. [2013, August 7].

[117] Nakagawa, Y., Ning, X., Amada, Y., and Tomishige, K. Solid acid co-catalyst for the hydrogenolysis of glycerol to 1,3-propanediol over Ir-ReO$_x$/SiO$_2$. Applied Catalysis A: General 433-434 (August 2012) : 128-134.

APPENDICES

APPENDIX A

CALCULATION EXAMPLE

A.1 Calculation of metal loading

Example 1: The calculation for 5 wt.% Co/Al_2O_3 catalyst.

Given,

The amount of water adsorption for 1.00 g Al_2O_3 support		0.5 ml
Molecular weight of $CoCl_2 \cdot 6H_2O$		238 g/mol
Molecular weight of Co		59 g/mol
Al_2O_3 support 100 g would have been Co on Al_2O_3		5 g

If Al_2O_3 support 1.00 g would have been Co on Al_2O_3 0.05 g

So,   Co metal   0.05 g would be obtained from $CoCl_2 \cdot 6H_2O$

$$\frac{g\ CoCl2 \cdot 6H2O\ x\ g\ Co(Al2O3)}{g\ Co} = \frac{238\ x\ 0.05}{59} =\ 0.2017\ g$$

And $CoCl_2$ solution 0.5 ml would have been $CoCl_2 \cdot 6H_2O$ 0.2017 g

So, $CoCl_2$ solution 10 ml would have been $CoCl_2 \cdot 6H_2O$ 4.034 g

Example 2: The calculation for 5 wt.% Mo/HZSM5 catalyst:

Given,

The amount of water adsorption for 1.00 g HZSM5 support		1.0 ml
Molecular weight of $(NH_4)_6 \cdot Mo_7O_{24} \cdot 4H_2O$		1,236 g/mol
Molecular weight of Mo		96 g/mol
HZSM5 support 100 g would have been Mo on HZSM5		5 g

If   HZSM5 support 1.00 g would have been Mo on HZSM5   0.05 g

So,   Mo metal   0.05 g would be obtained from $(NH_4)_6 \cdot Mo_7O_{24} \cdot 4H_2O$

$$\frac{g\ (NH4)6 \cdot Mo7O24 \cdot 4H2O\ x\ g\ Mo(HZSM5)}{g\ Mo} = \frac{1236\ x\ 0.05}{96} =\ 0.6438\ g$$

And $(NH_4)_6 \cdot Mo_7O_{24}$ solution 1.0 ml would have been $(NH_4)_6 \cdot Mo_7O_{24} \cdot 4H_2O$

$$= 0.6438\ g$$

So, $(NH_4)_6 \cdot Mo_7O_{24}$ solution 10 ml would have been $(NH_4)_6 \cdot Mo_7O_{24} \cdot 4H_2O$

$$= 6.438\ g$$

A.2 Calculation of glycerol conversion, product selectivity and product yield

The net glycerol conversion, the product selectivity and the product yield of three selected products were calculated on the basis of Eqs. (1), (2) and (3), respectively:

$$\text{Glycerol conversion}\,(\%) \;=\; \frac{\text{amount of glycerol converted (C - based mole)}}{\text{total amount of glycerol in reactant (C - based mole)}} \times 100$$

(A.1)

$$\text{Product selectivity}\,(\%) \;=\; \frac{\text{amount of glycerol converted to each product (C - based mole)}}{\text{amount of glycerol converted (C - based mole)}} \times 100$$

(A.2)

$$\text{Product yield}\,(\%) \;=\; \frac{\text{amount of glycerol converted to each product (C - based mole)}}{\text{total amount of glycerol in reactant (C - based mole)}} \times 100$$

(A.3)

Example: The calculation of the glycerol conversion, the product selectivity and the production yield of acrolein for glycerol hydrogenolysis over 5 wt.% Co/Al_2O_3 catalyst under the condition of 180 $^{\circ}$C, 7 MPa H_2-pressure and 3 h reaction time with the weight ratio of catalyst to glycerol of 15 mg/g.

Given, Molecular weight of glycerol ($C_3H_8O_3$)   92 g/mol

      Molecular weight of acrolein (C_3H_4O)   56 g/mol

For glycerol concentration (wt.%):

From the Eq. of calibration curve as shown in appendix B:

      $y = 1{,}604{,}233.15x$

Given,

    $y = \text{area peak} = 1713669.6$

    $x = \text{glycerol concentration (wt.\%)}$

      $x = \dfrac{1713669.6}{1604233.15} = 21.36 \ \text{wt.\%}$

So,   initial glycerol concentration $= 21.36 \ \text{wt.\%}$

For glycerol concentration (C-based mol) $= \dfrac{glycerol\ concentration\ (wt.\%)}{MW\ of\ glycerol} \; x \; C\ mol$

$$= \dfrac{21.36}{92} \; x \; 3 = 0.70 \text{ (C-based mol)}$$

So, initial glycerol concentration = 0.70 C-based mol

And glycerol concentration obtained from glycerol hydrogenolysis is 0.57 (C-based mol)

For the glycerol conversion (%) as calculated by Eq. (A.1)

$$\text{Glycerol conversion} = \dfrac{(0.70-0.57)}{0.70} \; x \; 100 = 18.57\ \%$$

For the product selectivity (%) as calculated by Eq. (A.2)

The acrolein concentration generated from glycerol hydrogenolysis is 0.03 (C-based mol)

$$\text{Product selectivity} = \dfrac{0.03}{(0.70-0.57)} \; x \; 100 = 23.08\ \%$$

For the product yield (%) as calculated by Eq. (A.3)

$$\text{Product yield} = \dfrac{0.03}{0.70} \; x \; 100 = 4.29\ \%$$

APPENDIX B

CALIBRATION CURVE

B.1 Calibration curve of glycerol solution

Table B.1 Data of different glycerol concentration for calibration curve

Glycerol concentration (wt.%)	Peak area			
	1	2	Average	Average (dilute 1:20)
10	778773.4	76892.6	427833	8556660
20	1549001.1	1550001	1549501.1	30990021
30	2337628	2334177.2	2335902.6	46718052
40	3260532.3	3260469	3260500.7	65210013
50	4106534.5	4109412	4107973.3	82159465
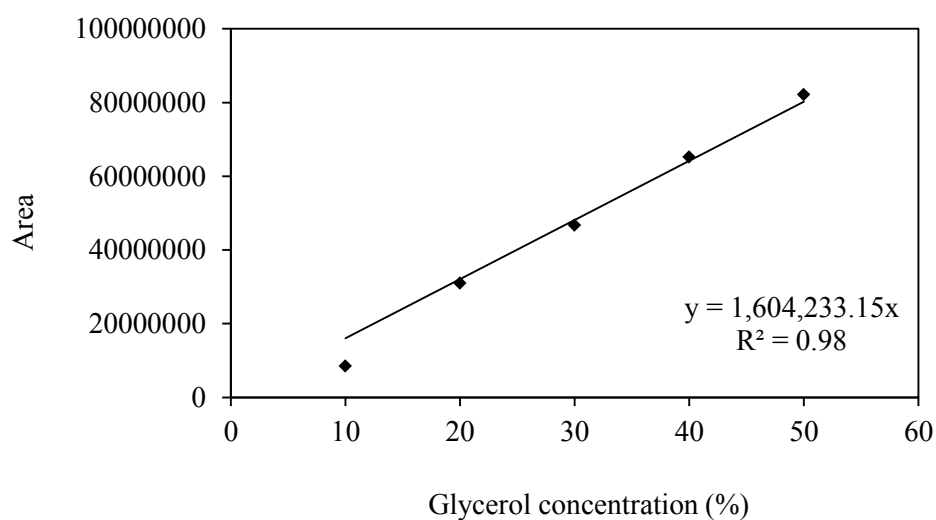
Figure B.1 Calibration curve of glycerol solution.

B.2 Calibration curve of acrolein solution

Table B.2 Data of different acrolein concentration for calibration curve

Acrolein concentration (wt.%)	Peak area			
	1	2	Average	Average (dilute 1:5)
0.5	16993.7	16616.4	16805.05	84025.25
1.0	28457.5	25065.3	26761.4	133807
1.5	34391.6	33288.9	33840.25	169201.25
2.0	52338.3	52182.6	52260.45	261302.25
2.5	71154.4	70865.7	71010.05	355050.25
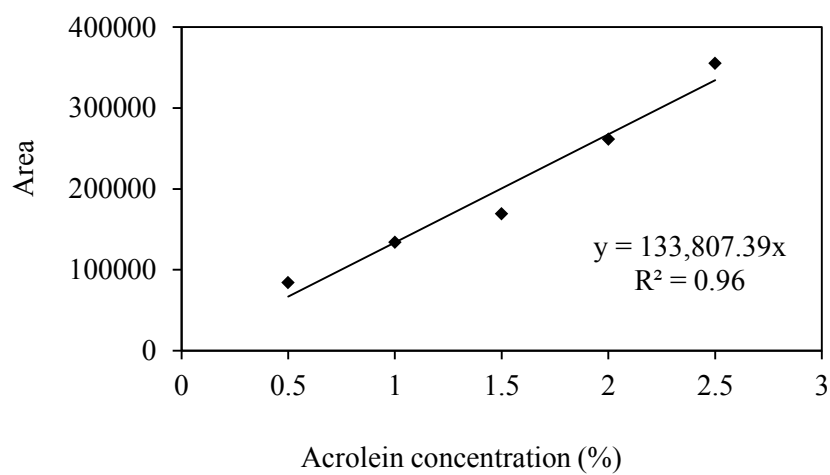
Figure B.2 Calibration curve of acrolein solution.

B.3 Calibration curve of 1,2-PDO solution

Table B.3 Data of different 1,2-PDO concentration for calibration curve

1,2-PDO concentration (wt.%)	Peak area			
	1	2	Average	Average (dilute 1:5)
0.5	126719.2	125740.3	126229.75	631148.75
1.0	237915.6	237705	237810.3	1189051.5
1.5	373547.2	374283.4	373915.3	1869576.5
2.0	492627.1	492381.7	492504.4	2462522
2.5	623971.6	623531.7	623751.65	3118758.3
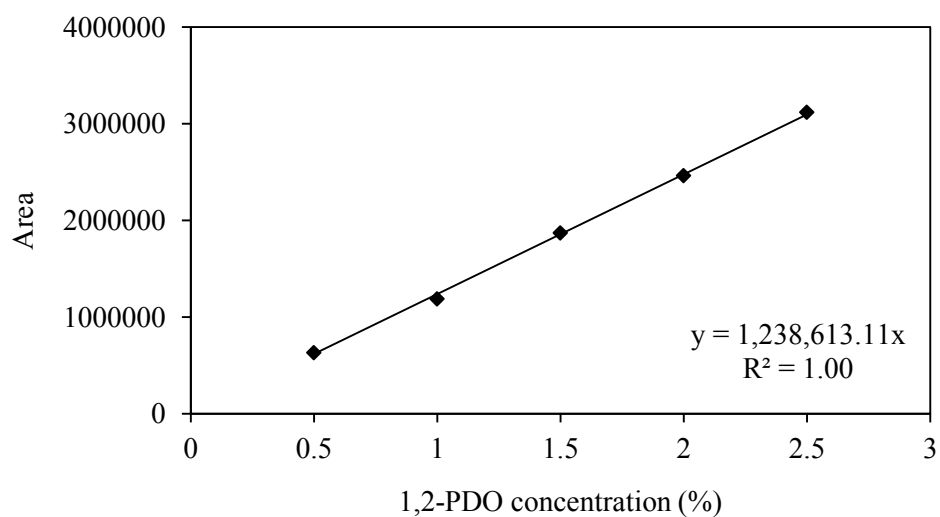
Figure B.3 Calibration curve of 1,2-PDO solution.

B.4 Calibration curve of 1,3-PDO solution

Table B.4 Data of different 1,3-PDO concentration for calibration curve

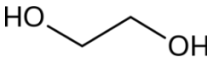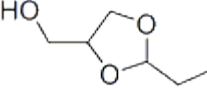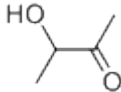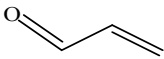| 1,3-PDO concentration (wt.%)	Peak area			
	1	2	Average	Average (dilute 1:5)
0.5	124970.5	123077.9	124024.2	620121
1.0	244950.3	238894.4	241922.35	1209611.8
1.5	370658.5	370653.4	370655.95	1853279.8
2.0	499168.4	500100.3	499634.35	2498171.8
2.5	618783.7	620393.7	619588.7	3097943.5
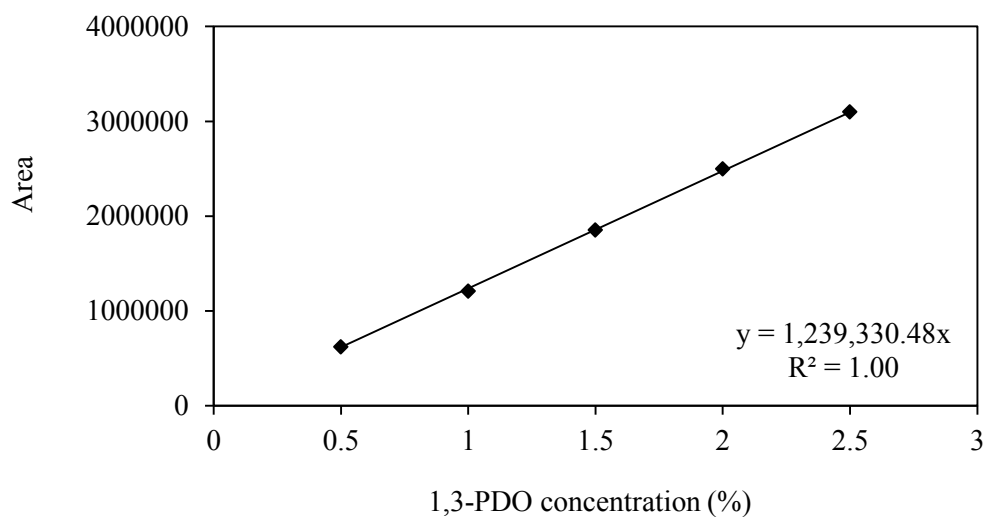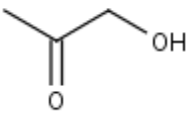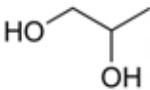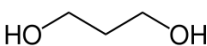
Figure B.4 Calibration curve of 1,3-PDO solution.

APPENDIX C

PRODUCTS IDENTIFICATION

Table C.1 List of identifiable products generated from glycerol hydrogenolysis over supported Co-based catalyst.

IUPAC name (Molecular formula)	Other names	Chemical structure	USD/lb (Purity, %)[a] [CAS No.]
1-Hydroxypropan-2-one ($C_3H_6O_2$)	1-Hydroxyl-2-propanone; Acetol		N/A [111-09-6]
Propane-1,2-diol ($C_3H_8O_2$)	1,2-Propanediol; Propylene glycol		4.77(>99.5 %) 0.52 (99.5%) [57-55-6]
Propane-1,3-diol ($C_3H_8O_2$)	Trimethylene glycol; 1,3-propanediol		102.34 (>98%) [504-63-2]
Ethane-1,2-diol ($C_2H_6O_2$)	Ethylene glycol; 1,2-Ethanediol glycol; Hypodicarbonous acid; Monoethylene glycol		0.84 (99.9%) 2.96 (99%) [107-21-1]
2-Ethyl-1,3-Dioxolane-4-Methanol ($C_6H_{12}O_3$)	1,3-Dioxolane- 2-ethyl- 4 -methanol or 1,3-dioxolane- 2-ethyl- 4-		N/A [53951-44-3]

IUPAC name (Molecular formula)	Other names	Chemical structure	USD/lb (Purity, %)[a] [CAS No.]
	hydroxymethyl		
3-Hydroxybutan-2-one ($C_4H_8O_2$)	3-Hydroxy-2-butanone		703.81 [513-86-0]
2-Propenal (C_3H_4O)	Acrolein; Acrylaldehyde; Acrylic aldehyde		68.18 (97%) [107-02-8]

[a] Reagent grade

BIOGRAPHY

Miss Supattra Raksaphort was born on November 14th 1979 in Chanthaburi province, Thailand. She received the Bachelor Degree of Chemistry from Faculty of Science, Chiangmai University in 2002. Then, she resumed studying in 2002 and graduated the Master's Degree of Science in Chemical Technology from Faculty of Science, Chulalongkorn University in 2005. After that, she became to assistant researcher in Materials Innovation Department, The Thailand Institute of Scientific and Technological Research and received the vacancy of researcher in the Institute of Research and Development, Rambhai Barni Rajabhat University at Chanthaburi province in 2006. In 2009, she attended in the Doctoral Degree at the same Department. She has received the Faculty Development Scholarships fund from the Office of the Higher Education Commission.